A NUMERICAL STUDY

OF TROPICAL CONVECTIVE BANDS

by

Jimy Dudhia

Atmospheric Physics Group
Physics Department
Imperial College

January 1984

A thesis submitted in part fulfilment of the degree
of Ph.D of the University of London.

ABSTRACT

This thesis is based on meteorological data obtained during the GARP Atlantic Tropical Experiment. An attempt is made to determine the primary mechanisms responsible for the formation, growth and persistence of quasi-stationary bands of cumulonimbus clouds with lengths of up to 250 km. These are commonly observed features in the region of the Inter Tropical Convergence Zone and thus play an important part in the vertical transport of energy.

In this work, a numerical model is employed in order to study in detail the way in which cumulonimbus clouds are organised in such systems by simulating a typical observed case. The model used has been developed by the Imperial College Atmospheric Physics Group since 1979 and is three-dimensional with a parameterisation of cloud and rain processes. Several results were obtained in both the numerical convection modelling and meteorological aspects of this work. It was found that the vertical resolution of the numerical domain is important to the way simulated clouds behave and this research gives an indication as to the resolution requirements or modifications of the numerical scheme in order to achieve a realistic simulation.

The primary theme of this thesis is the effect of a large scale forced vertical motion on cloud development. It is found that even a small ascent rate applied over the whole domain can significantly aid the growth of model clouds producing a long-lived convective system in environmental conditions where the absence of forcing cannot. These simulation results can be interpreted in terms of real meteorological effects which probably contribute to the growth of observed convective bands. Possible large scale mechanisms for this forcing are discussed and its imposition in the numerical model is justified in terms of GATE observations.

The modelling results are used to determine the flow associated with these bands and their overall transport properties with the aims of obtaining a dynamical description of the band itself and finding the effect of the band's transports on the large scale environment.

CONTENTS

TITLE 1

ABSTRACT 2

CONTENTS 3

LIST OF FIGURES 6

CHAPTER 1: INTRODUCTION
1.1 Tropical Convection over Oceans 9
1.2 The Macroscale Structure of Cumulonimbi 12
1.3 Supercell and Multicell Storms 15
1.4 Directional Shear and Cell Motion 16
1.5 Richardson Number and Storm Type 17
1.6 Squall Lines in the Tropics 17
1.7 Squall Lines and Stationary Bands 19

CHAPTER 2: OBSERVATIONAL SURVEY
2.1 The GATE Array 21
2.2 GATE Radar Observations 23
2.3 General Features of Convection Observed 23
2.4 The Case of 3rd September, 1974 25
2.5 Conditions Prior to 3rd Sept. Band 28
2.5.1 Temperature and Moisture Profile 28
2.5.2 Wind Profile 32

CHAPTER 3: NUMERICAL SIMULATION OF BAND CONVECTION: PART I
3.1 The Numerical Model 35
3.2 Simulation with a 100 mb Vertical Resolution 40
3.2.1 Introduction 40
3.2.2 Domain and Sounding 40
3.2.3 Simulated Structure and Development 42
3.2.4 The Effects of Vertical Resolution 46
3.3 Mixing 47
3.3.1 Introduction 47
3.3.2 Saturation Point Analysis 49
3.3.3 Effects of Vertical Resolution on the Surface Layer 52
3.4 Dispersion 53
3.4.1 Introduction 53
3.4.2 Dispersion in the Low Resolution Simulation 55
3.4.3 Resolution and Dispersion 57
3.4.4 Diffusion and Dispersion 60
3.5 Simulations with 50 mb Resolution 61
3.5.1 Introduction 61
3.5.2 Comparison with 9-Level Results 63
3.5.3 Dependence of Development on Initialisation 64
3.5.4 Dependence of Development on Jet Strength 65

CHAPTER 4: LARGE SCALE INFLUENCES ON CONVECTION
4.1 Introduction 67
4.2 Evidence for Large Scale Ascent on 3 Sept. 67
4.3 Easterly Waves 70
4.3.1 Easterly Waves in GATE 70
4.3.2 The Origin of Easterly Waves 71
4.3.3 Flow Associated with Easterly Waves 75
4.3.4 Energetics of Easterly Waves in the Eastern Atlantic 77
4.4 The Inter Tropical Convergence Zone 81

CHAPTER 5: NUMERICAL SIMULATION OF BAND CONVECTION: PART II - INCLUDING LARGE SCALE INFLUENCES
5.1 Introduction 85
5.2 Large Scale Ascent in Numerical Models 85
5.2.1 Review of Methods of Imposing Large Scale Motion 85
5.2.2 Review of Results of Past Models 89
5.3 Numerical Simulation with Imposed Ascent 90
5.3.1 Method of Imposing Ascent in Band Simulations 90
5.3.2 Imposed Ascent and Momentum 92
5.3.3 Imposed Ascent and Boundary Conditions 93
5.3.4 Modified Boundary Conditions 96
5.4 Magnitude of Imposed Ascent 98
5.5 Effect of Ascent on the Thermodynamic Sounding 102
5.6 Comparative Simulations with and without Imposed Ascent 104
5.6.1 Simulations 104
5.6.2 Results and Discussion 106
5.7 Sensitivity of Development to Forced Convergence Profile 108
5.7.1 Simulations 108
5.7.2 Results and Discussion 110
5.8 Mechanisms of Forced Convection 112
5.8.1 Simulations 112
5.8.2 Results and Discussion 113
5.9 Simulation with Ascent as an Initial Condition 115
5.9.1 Simulation 115
5.9.2 Results and Discussion 116

CHAPTER 6: SIMULATED BAND DEVELOPMENT, STRUCTURE AND TRANSPORT PROPERTIES

6.1 Introduction 118
6.2 Convective Band Development 118
6.2.1 Initial Growth Stage 118
6.2.2 Band Development Stage 123
6.2.3 Mature Stage 127
6.3 The Flow Structure of the Band 134
6.3.1 Model Trajectories 134
6.3.2 Updraught Trajectories and Structure 135
6.3.3 Downdraught Trajectories and Structure 139
6.4 Comparison with Observed Convection 143
6.4.1 Comparison with GATE Observations 143
6.4.2 Comparison with 14 September Band Study 145
6.4.3 Comparison with Large Scale Convective Behaviour 151
6.5 Mean Behaviour and Vertical Transport Properties of the Band 152
6.5.1 Introduction 152
6.5.2 Mean Temperature Changes 152
6.5.3 Mean Moisture Content Changes 157
6.5.4 Latent Heating Profile 158
6.6 Vertical Transport Properties and Apparent Heat and Moisture Sources 160
6.6.1 Apparent Heat and Moisture Sources 160
6.6.2 Mean Transports in the Mature Stage 162
6.6.3 Heat Transport Properties 163
6.6.4 Moisture Transport Properties 163
6.7 Time Development of Mean Heating and Moistening Profiles 165
6.8 Moist Static Energy 168
6.9 Summary of Mean Transport Properties 169

CHAPTER 7: CONCLUSION

7.1 Large Scale Ascent and Tropical Band Convection 174
7.2 Summary of Simulated Band Structure 176
7.3 Environmental Conditions Favourable for Stationary Band Development 178
7.4 Conclusion and Further Work 179

REFERENCES 182

ACKNOWLEDGEMENTS 185

FIGURES

2.1 The GATE array. Phase III

2.2 Radar development at Oceanographer, 1700-2400 GMT 3 Sept 1974. Range 250 km. R marks position of Researcher at 2100.

2.3a Thermodynamic sounding at Researcher, 1800.

2.3b As 2.3a for Oceanographer, 1800.

2.4 Wind profile at Oceanographer, 1800.

3.1 Model grid box showing points at which variables are defined

3.2 Thermodynamic sounding at Researcher, 2100.

3.3 9-level model clouds at 120 min. Horizontal sections at 650, 750, 850 mb.

3.4 9-level model 950 mb air less than environmental temperature by more than 1 K.

3.5 Saturation Points of mixtures of distinct air types.

3.6 Vertical velocity and temperature deviation. Max. and min. point values in the 800-900 mb layer.

3.7 Thermodynamic sounding used in the 18-level simulations.

4.1 Vertical velocity in GATE area (μb/sec) at 900 mb and radar echoes. (Ogura et al., 1979)

4.2 Time series of 700 mb vertical velocity (dashed) and precipitation rate. (Reeves et al., 1977)

4.3 Composite vertical velocity (mb/day) in relation to convective events. Stages 00 and 0 before convective growth. (Frank, 1978)

4.4a Absolute vorticity ($x10^{-5}$/sec) versus latitude at 5°E, 700 mb. (Rennick, 1976)

4.4b GATE Phase III mean absolute vorticity ($x10^{-5}$) for 10°E-31°W. (Reed et al., 1977)

4.5 Easterly wave composite temperature deviation. (Thompson et al., 1979)

4.6 As 4.5 for vertical velocity (mb/day).

4.7 Mean Phase III vertical velocity profile in B-scale area compared to W. Pacific. (Thompson et al., 1979)

4.8 Meridional wind component at (a) surface and (b) 700 mb for easterly wave composite. (Chen and Ogura, 1982)

4.9 ITCZ composite height anomalies. (Frank, 1983)

5.1 Divergence profile during convectively active periods in GATE. (McBride and Gray, 1978)

5.2 (a) Vertical velocity from fig. 5.1 profile. (b) 1 cm/sec imposed ascent employed in simulation BD45.

5.3 Rate of change of (a) temperature and (b) moisture content with ascent as in fig. 5.2a.

5.4 Rainfall in 20 min. intervals for simulations BD47, BD44, BD39, BD40.

5.5 Area with temperature 1 K cooler than environment at 975 mb in BD47, BD39, BD44, BD40.

5.6 Mean temperature at 975 mb for simulations BD44 (0), BD45 (1), BD43 (2).

5.7 Rainfall in 20 min. intervals for simulations BD44, BD45, BD43

5.8 Mean temperature at 975 mb in simulations BD40T, BD40Q, BD35, BD40.

5.9 As fig. 5.8 but for total domain cloud volume.

5.10 Rainfall in 20 min. intervals for simulations BD45, BD51.

5.11 As 5.10 but for area with temperature 1 K cooler than environment.

6.1 Vertical velocity at 24 min. E-W section. NB all figs. have linear pressure scale from 100-1000 mb.

6.2 As fig. 6.1 for height (pressure) deviation.

6.3a Vertical velocity at 80 min. E-W slab mean (average taken over 10 km in N-S direction).

6.3b As fig. 6.3a for cloud water content.

6.4a Pressure-time plot of domain mean vertical velocity (0-2 hrs).

6.4b As fig. 6.4a but 1-3 hrs.

6.5a Vertical velocity at 160 min. E-W slab.

6.5b As 6.5a but for cloud water content

6.6 675mb wind with vertical velocity contours at 160 min.

6.7 Reverse trajectories from an updraught, 160-124 min. NB all trajectory plots have a log (pressure) vertical scale.

6.8 16 inflow trajectories from 975 mb 124-180 min.

6.9 16 inflow trajectories from 900 mb 124-180 min.

6.10 16 reverse trajectories from cold surface outflow 180-124 min.

6.11 16 trajectories from 975 mb 124-180 min.

6.12a Temperature deviation at 975 mb 180 min.

6.12b As fig. 6.12a for moisture content.

6.13 Velocity at 875 mb 180 min.

6.14a Height (pressure) deviation at 180 min. N-S slab mean over 20 km.

6.14b As fig. 6.14a for temperature deviation.

6.14c As fig. 6.14a for vertical velocity.

6.15 Horizontal mean rate of change of potential temperature (thin) and latent + subgrid scale heating (thick). Time average for 120-180 min.

6.16 As fig. 6.15 for water vapour content and condensational + subgrid scale moistening.

6.17a Pressure-time plot of domain mean temperature deviation (0-3 hrs).

6.17b Pressure-time plot as fig. 6.17a for only cloud-free regions.

6.17c As fig. 6.17a for cloud.

6.18 As fig. 6.17a for moisture content deviation.

6.19 Q_1 (thick) and eddy flux convergence of heat (thin). 120-180 min.

6.20 Q_2 (thick). and eddy flux convergence of moisture (thin). 120-180 min.

6.21 As 6.15 and 6.16 for 60-120 min.

6.22 As 6.19 and 6.20 for 60-120 min.

6.23 Moist static energy profile (environment and cloud at 180 min.).

6.24a Pressure-time plot of domain mean moist static energy deviation (0-2 hrs).

6.24b As fig. 6.24a for 1-3 hrs.

CHAPTER 1
INTRODUCTION

1.1 Tropical Convection over Oceans

In this study an attempt is made to understand some of the mechanisms responsible for the formation and persistence of a particular case of tropical convection. The convective event upon which this study concentrates was observed during the GATE program being an example of a form of convective organisation typical of the eastern tropical Atlantic in the summer months contributing a significant proportion of the total rainfall. In these cases the convection shows on radar pictures as a distinctive band of deep precipitating convection which either moves very slowly or remains stationary having a length of tens to hundreds of kilometres. They maintain their form for typically three hours but may continue much longer becoming an unorganised cluster of weaker clouds and lighter rain.

These quasi-stationary convective bands are distinct in several respects from tropical squall lines which constitute the other main class of mesoscale organisation in the tropics. The primary difference is the motion of the squall line which is perpendicular to its alignment and generally faster than the wind at any level. A stationary or slow-moving band has little mid-level wind transverse to it being usually aligned along the shear direction. As the mid-level shear in the GATE region is generally nearly easterly squall lines tend to align approximately north-south though they have a pronounced arc shape. Convective bands are observed to usually align NE-SW or east-west though exceptions occur such as the case studied by Zipser, Meitin and Lemone (1981) which was aligned N-S along the shear vector at that time. Squall lines tend to occur rather less frequently than bands but modify a considerably larger area as a result of their motion. They also are more convectively active because the relative inflow of moist surface air provides latent energy at a higher rate.

Apart from these organised systems convection can occur as

amorphous clusters of weaker cells. These can exist on scales of several hundred kilometres and persist for typically half a day. They generally occur when the atmosphere is unstable enough for organisation not to be required for persistence. Bands and squall lines, by virtue of their organised structure, can persist in more stable environments than amorphous clusters.

The GATE region also has periods of very suppressed convection when non-precipitating cumulus clouds of 1-2 km in height predominate.These cumulus fields have little effect on the large scale flow with heat and moisture transports confined to low levels.

In the tropics there is a net influx of heat energy which has to be transported from the surface layer to the upper troposphere and thence polewards. The low latitude Hadley circulation provides this transport ascending at the Inter Tropical Convergence Zone (ITCZ) and descending at about 30 degrees latitude. The ascending branch is comprised of hot deep convective towers which provide all of the vertical transport of energy at the ITCZ. Unlike mid-latitudes where large baroclinic systems provide much of the energy transport, in the tropics there is no large scale source of potential energy and vertical transports are confined to the convective clouds' scale. These clouds derive their energy from a boundary layer which is constantly supplied by turbulent transports of heat and moisture from the ocean surface. The ocean temperature itself is maintained by direct solar heating. On the convective time scale the ocean acts like a constant temperature heat bath to the boundary layer helping it to return to its equilibrium state within a few hours of being dried and cooled by deep convective transports.

The large scale Hadley circulation forces a general ascent in the ITCZ at low to mid levels. This type of forcing is becoming recognised as an important factor in cloud development. Large scale ascent is a source of convective available potential energy (CAPE) because it has the effect of both cooling mid-level air and moistening low-level air increasing the buoyancy of ascending saturated parcels. Whether the large scale convergence is driven by the convection or

drives it is not easily determinable from large scale data. It is possible that prior to cloud development large scale convergence exists and hence aids it whereas after the deep convection has started the convergence is more a result of cloud mass fluxes. Thus while some parts of the ITCZ may be producing convergence others may be benefiting from it.

Compared to land, solar heating of the ocean has a much smaller diurnal effect on the surface heat and moisture fluxes, due to the ocean having a higher thermal inertia than the land. As a result of this the stability of the boundary layer changes little from day to night and convection is observed to occur almost independently of the diurnal heating cycle. However, radiative cooling in the atmosphere has been shown to impose a diurnal modulation on the large scale inflow into pre-existing clouds. This produces a vertical velocity maximum at about 7 am local time (McBride and Gray, 1978). In the Eastern Pacific and Western Atlantic this leads immediately to an enhancement of the rainfall rate whereas in the Eastern Atlantic GATE area the enhanced rainfall does not occur until the early afternoon. This time lag between moisture convergence and maximum precipitation is a distinguishing feature of the GATE region and applies equally to convergence produced by differential radiative cooling (McBride and Gray, 1978) and by other mechanisms such as easterly-wave dynamics. It is probably related to the strong mid-level easterly jet in this region which can delay the development of convection. This jet, known as the African Easterly Jet, owes its origin to a south to north temperature gradient between Equatorial Africa and the Sahara Desert. Although this is a tropical region, a thermal wind effect can occur if the time and length scales of the temperature are sufficiently long. During the convection studied in this thesis the mid-level easterly jet was around 20 m/s at 4 km . As the GATE area lies to the south of the main axis of the African Easterly Jet the strength of the jet is modulated by southward momentum transports due to easterly waves which are thought to result from the barotropic instability of the jet. Easterly waves were particularly strong during early September and several studies have shown their importance in connection with tropical convection, e.g. Thompson, Payne, Recker and Reed (1979),

Chen and Ogura (1982).

1.2 The Macroscale Structure of Cumulonimbi

The most severe and long lasting cumulonimbus clouds in mid-latitudes and in the tropics tend to have a scale of organisation larger than the individual cell. Here a cell is defined as a rain producing cloud resulting from a single updraught. Depending on the stage of development, a cell may or may not have an associated rain driven downdraught and cold surface outflow. New cells may just have a strong updraught with little or no downdraught air. Decaying cells, conversely, may have a weak updraught remnant at mid- to upper- levels but a substantial downdraught with heavy rainfall and a cold outflow at the surface. In cases of isolated short-lived showers the downdraught does not cause sufficient surface convergence for the updraught supply to continue nor for a new updraught to form away from the initial updraught. The capacity for sustaining the convective system by surface convergence depends strongly on the environmental conditions at the time of the initial cell. Especially important are the convective available potential energy (CAPE) and wind shear. Together these quantities influence the condensation rate, rainfall, degree of evaporative cooling, temperature and storm relative speed of the downdraught outflow and the storm motion. The importance of CAPE and wind shear in determining these properties is briefly discussed below.

(i) Condensation rate and ascent.

The convective available potential energy gives a measure of the buoyancy achieved by a parcel as it ascends moist adiabatically having risen above its lifting condensation level. The rate of condensation would depend on the updraught speed which in turn depends on both the buoyancy of the updraught and the vertical shear of the wind. The shear has two important effects on the ascent rate. Firstly, a high shear is known to have a dynamical suppressing effect on updraughts which develop through the sheared layer. Energy would be lost by the updraught in counteracting a dynamically induced vertical pressure gradient which results from the fact that upshear of the updraught the

environmental air has to be deviated around the ascending core. Secondly, a high shear would lead to increased entrainment of environmental air. This occurs because the short time scale of renewal of neighbouring environmental air increases the horizontal temperature and moisture gradients. In the case of a weak updraught, dynamical detrainment can occur as the updraught decelerates since this increases its surface area allowing it to mix more easily with surrounding air. After taking the effects of shear into account the ascent rate and hence condensation rate are governed primarily by CAPE. The condensation rate is important for two reasons. It gives both the rate of latent heating of the parcel and hence its rate of change of buoyancy and also the rate of cloud water formation. This is of intrerest because it determines the concentration of cloud water which is a critical parameter in cloud physical processes leading to the production of rain drops.

(ii) Rainfall and evaporation.

In the absence of wind shear all the rain formed in an updraught would fall vertically through saturated ascending air. This would have the effect of imposing a drag force on the updraught equal to the weight of rain which can be comparable to the cloud droplets ascending with the updraught. The net effect of liquid drag is to reduce the buoyancy by a significant factor, typically around one third. Thus the formation of rain can lead to a reduction in strength of an updraught and in some cases can cause its decay. The presence of a shear in the considerably alters the effect of rain on storm development. Instead of being detrimental the rain becomes beneficial, playing an important part in sustaining long lasting storms. It has become recognised (review by Ludlam, 1980) that for a storm to persist it is important to have an environmental wind shear to organise the updraught and downdraught in such a way that they can reinforce each other. In this case rain can fall out of the ascending saturated air and this helps the cell in two ways. First the updraught is less hindered by liquid drag and therefore more able to accelerate giving a higher condensation rate. Secondly, the rain falls into unsaturated environmental air allowing partial evaporation to occur. Hence, downshear of the updraught, large regions of

environmental air can become negatively buoyant through cooling and rain water drag such that an organised descent of this air to the surface is set up. This produces horizontal convergence at the level at which the downdraught originates and thus a downdraught circulation is initiated supported by rain from the updraught, drawing inflow from the mid-level environment. It is advantageous to the strength of the downdraught for this inflow to be fairly dry so that the evaporation rate is high. It is also beneficial for there to be a component of the environmental flow perpendicular to the shear at mid-levels so that the supply of environmental air to the downdraught is continuously renewed. Thus the updraught/downdraught structure of the most organised storms is essentially three dimensional with distinct circulations of ascending and descending air interacting at mid-levels through rainfall and also at the surface through the downdraught's outflow.

(iii) Downdraught outflow and gust front.

The final temperature reached by downdraught air depends on the rate of rainfall from the updraught and the degree of subsaturation of the downdraught inflow. Severe storms often have very cold downdraughts which result from a high evaporation rate at mid-levels caused by a layer of very dry air at the downdraught inflow height. In a typical storm the downdraught air is several degrees cooler than the surface environmental air. On reaching the surface this cold air spreads out at speeds ranging from a few to ten metres per second relative to the surface wind. Its depth is usually between a few hundred metres and a kilometre and unless it is sustained by a continuous supply of cold air it lasts for a few hours before being warmed to the environmental temperature by surface heat fluxes. This outflow forces the ambient air to ascend over the gust front. If the convergence is strong enough this ascent may be sufficient to saturate the rising air which is then unstable with respect to wet adiabatic motion. The amount of convergence produced depends primarily on the depth of the cold outflow and its speed relative to the surface wind. The depth itself depends on the relative position of the front with respect to the source of cold air, since as it spreads out it gets shallower. The relative motion of the front is a function of the depth and

temperature deficit of the cold air but may also depend on the mid-level momentum. An important relative motion to the dynamics of a storm system is that between the outflow front and the updraught core's base which is highly dependent on the low-level shear below about 3 km. The motion of the updraught core is governed by the ambient wind, particularly that at the height of the lower updraught where the upward acceleration occurs, i.e. 2-4 km. In the absence of a low-level shear the relative motion of the gust front to the updraught inflow would be the same as its motion relative to the surface wind. Therefore the region of surface convergence and forced ascent moves away and eventually stops supplying the updraught with surface air of high latent energy. For reasons explained earlier a downdraught's outflow convergence weakens as it moves away from its cold air supply, i.e. the rain area . This usually means that storms which grow in an environment with little or no ambient shear tend not to be long-lived or regenerating types. However topography may sometimes play the same role as low-level shear in slowing down the motion of the gust front relative to the updraught base.

1.3 Supercell and Multicell Storms

Observed long-lived storms can be categorised into two types. Supercells have a steady almost time independent structure. There is a continuous updraught/downdraught interaction resulting from the organised inflow to both. The structure of this type of storm is usually three dimensional and therefore its existence depends on the directional wind profile . The two main requirements of this profile are (i) that the low level shear is sufficient to prevent the gust front from moving away from its cold air supply and the updraught base and (ii) that there is a mid-level wind to supply the rain area with dry environmental air so that evaporative cooling can occur efficiently resulting in a strong downdraught. The first of these conditions is more restrictive because of the high speed of a block of cold air relative to the surface wind and only unusual conditions can support supercell storms.

Multicell storms require less low-level shear and are therefore

more common than supercells. In these cases the surface convergence region moves slowly relative to the active cell but this convergence is strong enough and the boundary layer unstable enough for the ascending air to become saturated and buoyant. Thus a new updraught distinct from that producing the gust front is generated upshear from the latter. After 20-30 minutes this new cell produces enough rain to restrengthen the gust front which has meanwhile moved downshear (upwind relative to the surface air) and another cell may then form on it. Thus multicell storms consist of a number of successive cells generated at a gust front which then move upshear away from the front and gradually decay as they are cut off from their supply of ambient surface air. As with supercell systems the motion of a multicell system depends on both the direction of mid-level winds and the direction of low-level shear since the former determines the motion of developed cells and the latter determines the position of the strongest surface convergence relative to the cell, this being the likeliest place for a new cell to develop. As a whole a multicell system tends to move in a direction different from that of individual cells within it. Similarly the direction of motion of a supercell is governed to some extent by the direction from which its updraught is supplied most by buoyant air.

1.4 Directional Shear and Cell Motion

A generalisation which can be made from observations and numerical modelling studies (e.g. Thorpe and Miller, 1978, Klemp and Wilhelmson, 1978) is that in the presence of a clockwise turning wind with height severe storms or supercells tend to move to the right of the mid-level wind (and to the left for anticlockwise turning). From the arguments of the previous section it can be seen that the region of maximum surface convergence would be to the right of the mid-level wind vector. Under these circumstances the downdraught inflow tends to be from the right in the cell relative frame. This accounts for the fact that in cases of storm splitting the right moving storm is favoured by a clockwise turning. The downdraught inflow to the left moving storm would be impeded by the other cell. For similar reasons multicell storms develop to the right of the mid-level flow.

1.5 Richardson Number and Storm Type

The Richardson number is defined as the ratio of convective available potential energy to the ambient kinetic energy difference between the surface and a typical cloud top height. It is therefore dependent on both the environmental instability and shear which are the two most important factors in determining its development. Low Richardson numbers lead to conditions favourable for supercell type storms whereas higher values are found to be associated with the multicell type (Weisman and Klemp, 1982). Qualitatively this can be accounted for by the fact that a low Richardson number implies either that the shear is strong or the instability is low, i.e. the downdraught is weak. In either case the region of convergence is held almost stationary with respect to the cell. A higher Richardson number results in either a stronger updraught/downdraught circulation through the atmosphere being less stable or a smaller shear both of which would allow the gust front to move producing a multicell type of storm. Weisman and Klemp (1982) attribute a Richardson number of 50 to the boundary between supercell and multicell favouring conditions. I.e. for Ri less than 50 supercell type storms would tend to occur. They find from numerical simulations that low Richardson numbers (less than 8) are detrimental to storms because the shear is too high compared to the updraught strength. At very high Richardson numbers storms tend not to regenerate because the downdraught outflow spreads away from the updraught base too quickly. This is because the shear is of insufficient strength to prevent the density current head from moving rapidly away from the rain area. In these situations isolated showers would be expected to prevail.

1.6 Squall Lines in the Tropics

Tropical squall lines are distinguished from the types of convection described so far by the fact that they are observed to move as a whole faster than the wind at any level. Therefore all the inflow to a squall line is from the front and the outflow is to the rear. Squall lines are not observed as often as slow moving systems but by virtue of their motion can modify large areas of atmosphere.

They are found to be aligned perpendicularly to the direction of low-level shear moving faster than the mid-level jet and have a high relative inflow speed of boundary layer air. Individual cells build at the front of the line and gradually move back towards the rear as they go through their mature and dying stages. During the mature stage the rainfall rate reaches a maximum value and a strong downdraught exists at low levels. Behind the line there is a mesoscale ascent in the upper half of the troposphere consisting of decaying updraughts and producing a uniform lighter rain area. In the lower half of the troposphere there is a mesoscale descent and subsidence warming. This may partly be driven by rain and partly by the spreading of the convective downdraught outflow. There is also the dynamical reason that the boundary layer air has ascended so that some of the air originally above it has to descend to replace it since convective downdraughts tend to be shallower than the boundary layer supply to the updraughts.

Observations indicate that squall lines can only exist in the presence of a mid-tropospheric wind maximum so that there is only significant motion relative to the squall line at lower and upper levels. It is believed that the process of regeneration is very similar to that of multicell systems in which a squall front which may be several hundred kilometres in length is sustained by the line elements' convective downdraughts. The horizontal extent of the convergence line makes it efficient in forcing ascent meaning that squall lines can probably exist in less convectively unstable environments than slow moving and unaligned systems. Confirmation of this comes from GATE radar pictures (Mansfield, 1977) in which squall lines are observed to propagate through stationary convective features which had already modified the boundary layer and stabilised it to some degree.

Dual Doppler radar results over W.Africa (Chong and Testud, 1983) show that ascent at squall fronts often occurs in two stages. Initially a deep layer below the jet is forced to ascend with updraughts reaching 4 km. This air stops ascending as much of it fails to reach a level of free convection. This is partly due to the

dryness of air above the boundary layer and partly due to liquid loading. Squall lines can be seen as systems in which a fast moving front of cold air forces ascent of a deep layer of the lower troposphere producing a gravity wave. The squall line speed is sufficiently great to prevent this wave from moving ahead. The lowest 1-2 km of this layer reaches its level of free convection and thus becomes unstable with respect to ascent through the less buoyant air above. However, this process cannot occur immediately because in order for one layer of air to ascend through another it has to be organised into updraughts. Thus several kilometres behind the line of initial ascent there is a second region with updraught cores reaching the upper troposphere. Between these two regions there is a minor subsidence of air which has failed to become buoyant.

1.7 Squall Lines and Stationary Bands

Tropical convection is frequently organised into linear features as seen on radar images. In these cases individual cumulonimbi have a component of motion perpendicular to the line as they develop. Relative to the line of cells there is usually a strong low-level shear of boundary layer air with the surface air approaching the line at a relative speed of several to ten metres per second. In this respect stationary and squall lines are similar. In both cases mid-level air moves slowly in the direction transverse to the line and this is consistent with the slow relative cell motion required to sustain the surface front.

The difference between the two cases is that since the mid-level air perpendicular to a sqall line is a jet maximum the inflow to the line is all from the front whereas in the stationary case there is no such restriction on the direction of flow and in areas of mid-level convergence it may be from both sides of the line.

A contributory factor to the strength of linear convective features in general is the enhanced efficiency of a quasi-two-dimensional ascent at the gust front. Curvature of the front allows some environmental air to deviate instead of ascending but a

long straight front effectively forces all approaching air to ascend. Since the lower part of the boundary layer is initially stable to vertical motion before becoming saturated, forced ascent is an important part of sustaining a convective system.

Fast moving squall lines differ markedly from convective bands when the direction of low-level shear is considered. In the case of the former the maximum shear vector is in the direction of motion of the line. In the slow moving bands the shear vector varies with height but its magnitude is generally greatest along the band. I.e. the cells develop in a line parallel to the direction of maximum shear. However, in order to sustain this form of convection there has to be at least a component of the shear perpendicular to the band in the boundary layer to supply low level moisture as the band develops. This means that whereas squall lines can exist in unidirectional environmental shears, stationary and slow moving bands usually require a three dimensional profile consisting of a strong mid-level shear to determine the alignment and a perpendicular lower level shear to supply inflow to the updraughts. This latter environmental shear may not be so important in the later stages as the convection provides its own inflow convergence. In general stationary systems have less vigorous convective cells and the downdraught outfow is consequently not as strong as that of squall lines and therefore requires less boundary layer shear to keep it from moving away from the heavy rain area. The primary reason for the relative weakness of convective bands compared to squall lines is the rate of supply of low-level latent energy. By virtue of their rapid motion relative to the boundary layer squall lines have a far higher supply of surface air than bands which rely solely on the low level ambient shear to provide inflow. This has consequences that (i) for a given boundary layer moisture content squall lines can convert latent energy to convective kinetic energy at a higher rate and hence produce more active downdraughts and (ii) squall lines are able to sustain themselves in a less moist boundary layer.

CHAPTER 2
OBSERVATIONAL SURVEY

2.1 The GATE Array

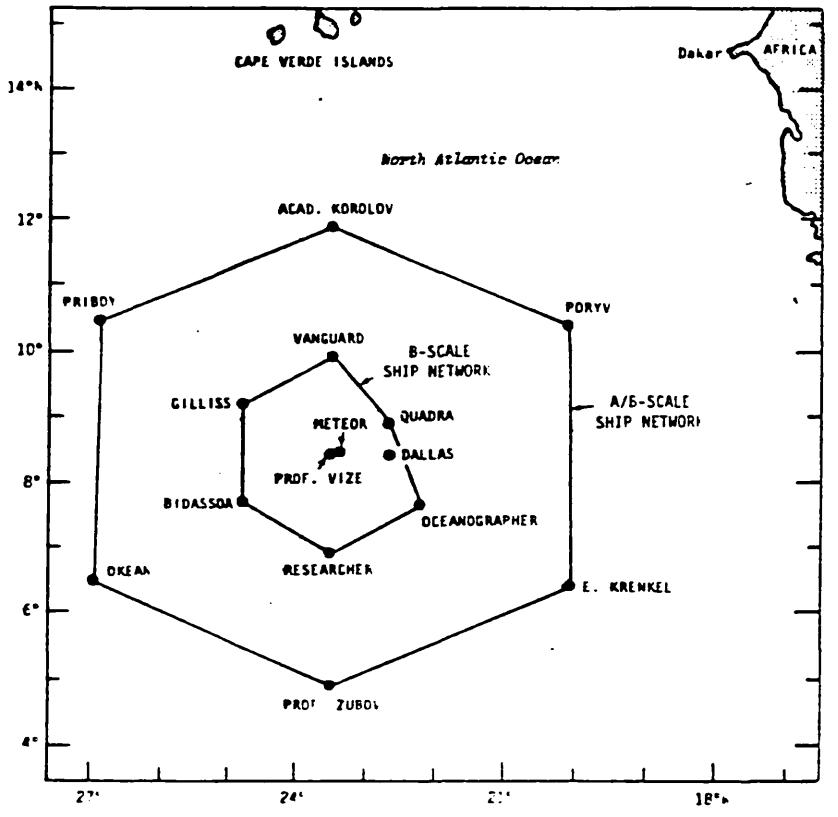
The aim of the GARP Atlantic Tropical Experiment was to provide data on scales ranging from the synoptic to individual cloud scale. These measurements were carried out between late June and mid September, 1974 over an area approximately 700 km across. The centre of this region was at 8N 24W which is in the Eastern Atlantic 1000 km from the African coast (fig. 2.1).

Ships in this network provided temperature, moisture and wind profiles of the atmosphere at 3-hourly intervals and continuous radar coverage of the GATE area.

The area chosen is particularly interesting because it lies on the Inter Tropical Convergence Zone (ITCZ) where convective activity in the tropics is concentrated. The Eastern Atlantic is also a region where easterly waves are well defined and interact with the convective scale. Cumulonimbus updraughts are capable of providing all of the large scale vertical energy transport and play an important part in the earth's general circulation by transporting surface air to the upper troposphere.

GATE data can provide useful information for understanding the formation and organisation of cumulonimbi into mesoscale features. A better knowledge of these processes allows their heat, moisture and momentum transports to be understood and these results used to design convective parameterisation schemes in large scale models.

The ships in the array are spaced less than 200 km apart in two concentric hexagons. As a result of the 3 hour time resolution interesting convective activity observed on the GATE radar can be analysed using data from ships within 100 km of it. Sufficient representative recorded information exists to initialise a numerical simulation because the time and space scales of the data are similar



2.1 The GATE array. Phase III

to those of convective clusters. In contrast wind profiles from certain ships are subject to 'noise' and the choice in practice is more limited.

2.2 GATE Radar Observations

A central part of the GATE program was to obtain a continuous radar record of convective activity. The echoes show the amount of rain per unit volume as the radar is insensitive to small cloud droplets. Thus non-precipitating cumulus and cirrus clouds do not appear and strong cumulonimbus clouds produce intense echoes which can be used to give a measure of their surface rainfall.

Scans every 15 minutes over several elevations provide information on the time development and three-dimensional structure of rain areas from which much dynamical information can be inferred. The 7 ships in the inner hexagon, 167 km in radius provided an overlapping radar network with each having a range of about 200 km. This makes it possible to track even rapidly moving squall lines through much of their lifetime.

In active clusters, the rain areas of several cells may merge into a larger system so that it is not always possible to distinguish an individual cell unless it is active enough to produce a high updraught tower which is more easily resolved than a lower tropospheric echo because of the relative lack of 'background rain'.

2.3 General Features of Convection Observed

Radar sequences show that the overall intensity of convection in the region has a large variability over a few days. There are periods when few or no echoes are present anywhere and others where rain areas are predominant. It is found that the most organised forms of convection i.e. bands and squall lines occur mostly in periods where rain areas account for a small proportion of the total. At these times little other convection exists in the immediate neighbourhood of the organised lines possibly indicating compensating mesoscale descent

on a scale of 100 km.

A commonly observed sequence of events over a few days is as follows: initially there are few rain echoes but isolated clouds develop, some of which are short lived while others develop into lines of clouds and intense rainfall which may persist and grow into mesoscale features. These lines tend to be almost parallel to each other and fairly slow moving, separated by several hundred kilometres when fully developed. Later they tend to broaden and break into amorphous clusters which eventually become part of a large unorganised lightly precipitating feature typical of a highly unstable environment with little shear to organise or suppress convection. Squall lines are rather less common than these slow moving bands but tend to occur during the decaying stage of the bands. Approximately ten bands were observed per week in the GATE region. They have scales ranging from tens to hundreds of kilometres and usually align within 45 deg of NE-SW. Their formation tends to occur in marginally unstable conditions as is proven by the lack of other convection. Isolated clouds in the area have comparatively short life times showing that some mesoscale organisation could be necessary in order to sustain a system.

It is noticeable from radar images that even isolated echoes are elongated parallel to mesoscale bands indicating the presence of a strong shear in the large scale wind field along the bands' axes. It is also found that squall lines align almost perpendicularly to bands in their area, this being consistent with the idea that their motion is parallel to the mid-level jet. These sytems are less frequent than bands, occurring only once or twice per week in the GATE region and have a scale of typically 100 km.

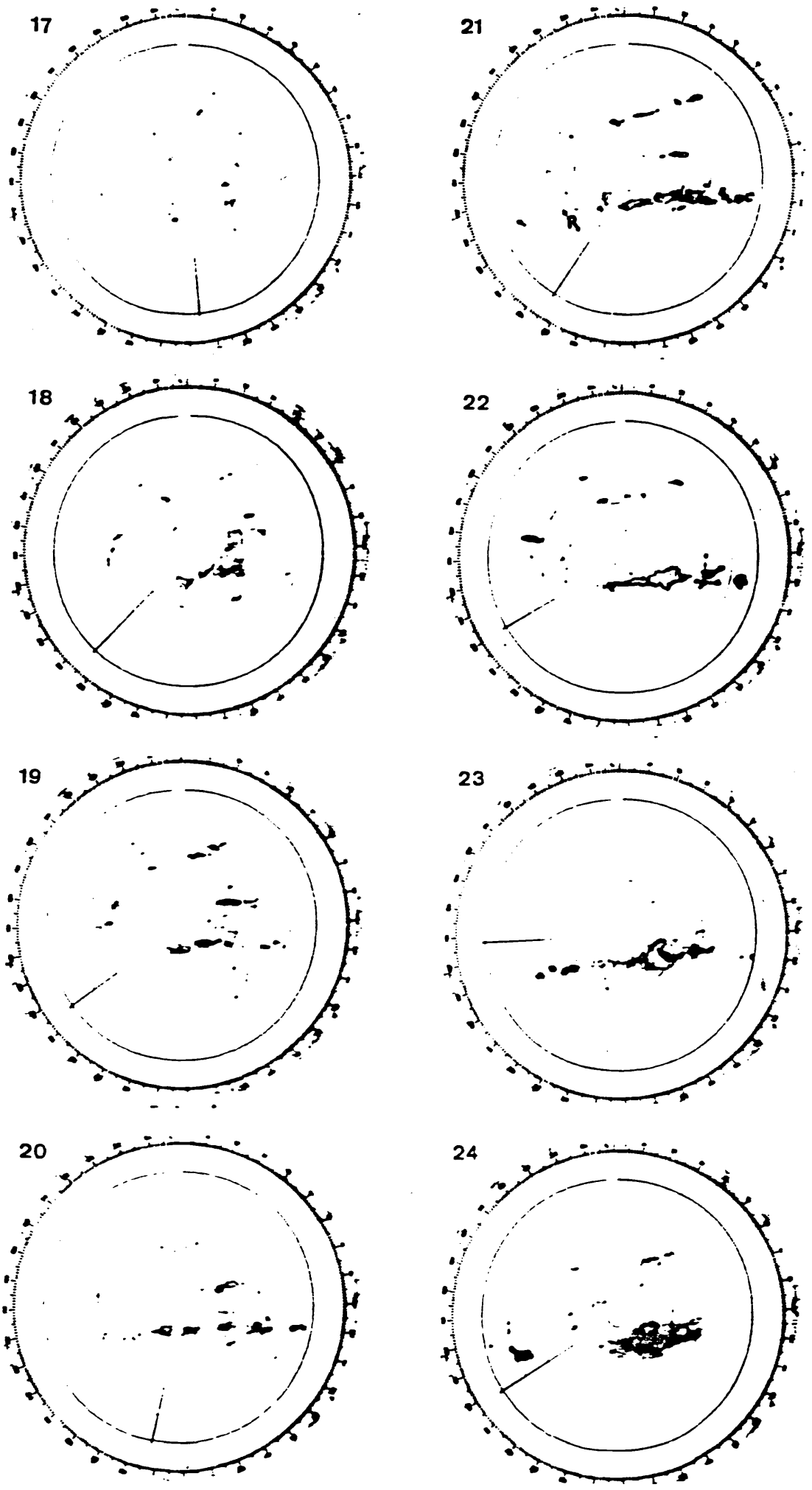
Houze and Cheng (1977) have noted that deep convection in the GATE region is commonly oriented parallel to the low or mid-tropospheric wind direction. In his study of GATE radar echoes 83 per cent show such an alignment. Larger echoes were found to have a stronger correlation with the lower tropospheric wind direction than isolated echoes and in 28 out of the 35 cases considered there was an

agreement to within 25 deg between the echo orientation and the wind at either 850mb or 700mb. The study does not relate the orientation to the lower tropospheric shear which is at least as important as wind direction in determining the alignment of convective features. In the case of isolated echoes the shear is almost certainly a primary cause of elongation since rain produced higher in the cloud is carried further downshear as it falls. As the total shear is of a similar order of magnitude to the rain's fall speed the elongation would be expected to be similar to the cloud height i.e. 10 km. This shows up distinctly on radar images being greater than a typical echo width (5 km).

2.4 The Case of 3rd September, 1974

In the numerical modelling part of this work one particular band observed in GATE was selected as a typical case. By simulating the initial conditions using temperature, moisture and wind profiles recorded at approximately the time and position of band development it was hoped to model part of the observed band so that its properties could be compared with observations. This serves the dual purpose of helping to describe convective bands in more detail and verifying the usefulness of the numerical model used for the study.

The 3rd Sept. was a day in Phase III of GATE, a period in which synoptic scale easterly waves were well developed and initially convection is suppressed for several hours in the ridge region of the wave apart from isolated clouds appearing in radar images. The development at Oceanographer is shown in fig. 2.2. At about 1700 to the south-east of the GATE ship Oceanographer more intense convection started and grew into several rain areas of 20 km in scale. By 1800 a clear east-west linear structure had developed with cells of strong precipitation embedded in it. Convection developing on this line's axis but not connected to it also grew rapidly in scale and became incorporated into the line. In this way the band grew to a length of 250 km by 2100. Subsequently it lost its linear form and split into two slightly elongated clusters and at 2400 there was no alignment apparent in the embedded cells. These clusters are labelled A and B



2.2 Radar development at Oceanographer, 1700-2400 GMT 3 Sept 1974. Range 250 km. R marks position of Researcher at 2100.

by Ogura et al.(1979) where the long term behaviour of several clusters is studied. During the whole period between initial development and final decay into clusters the band remained in almost the same position as is characteristic of such systems. Another interesting and typical feature was the almost total lack of convection to the south of the band which may be the result of the mesoscale circulation associated with the system producing an unfavourably high meridional wind at the surface and mid-level compensating subsidence.

The time resolution of 15 minutes in radar images makes it possible to determine some typical echo speeds in those cases where a feature remains distinct from one image to the next. This analysis shows a general cell velocity of 8 m/s from east to west along the band, some regions of intense rainfall being identifiable for over one hour.

Typical echo heights in the band are 8-10 km with a general tendency for these heights to increase with time. At 2000 they reach 7 km and by 2200 heights in excess of 12 km are observed. There was also a tendency for cells to move slower after 2100 indicating that the mid-level jet local to the band may have weakened or that the updraught cores, being more active, were less affected by the mid-level wind speed; the observation that the jet remained strong tends to support the latter conjecture.

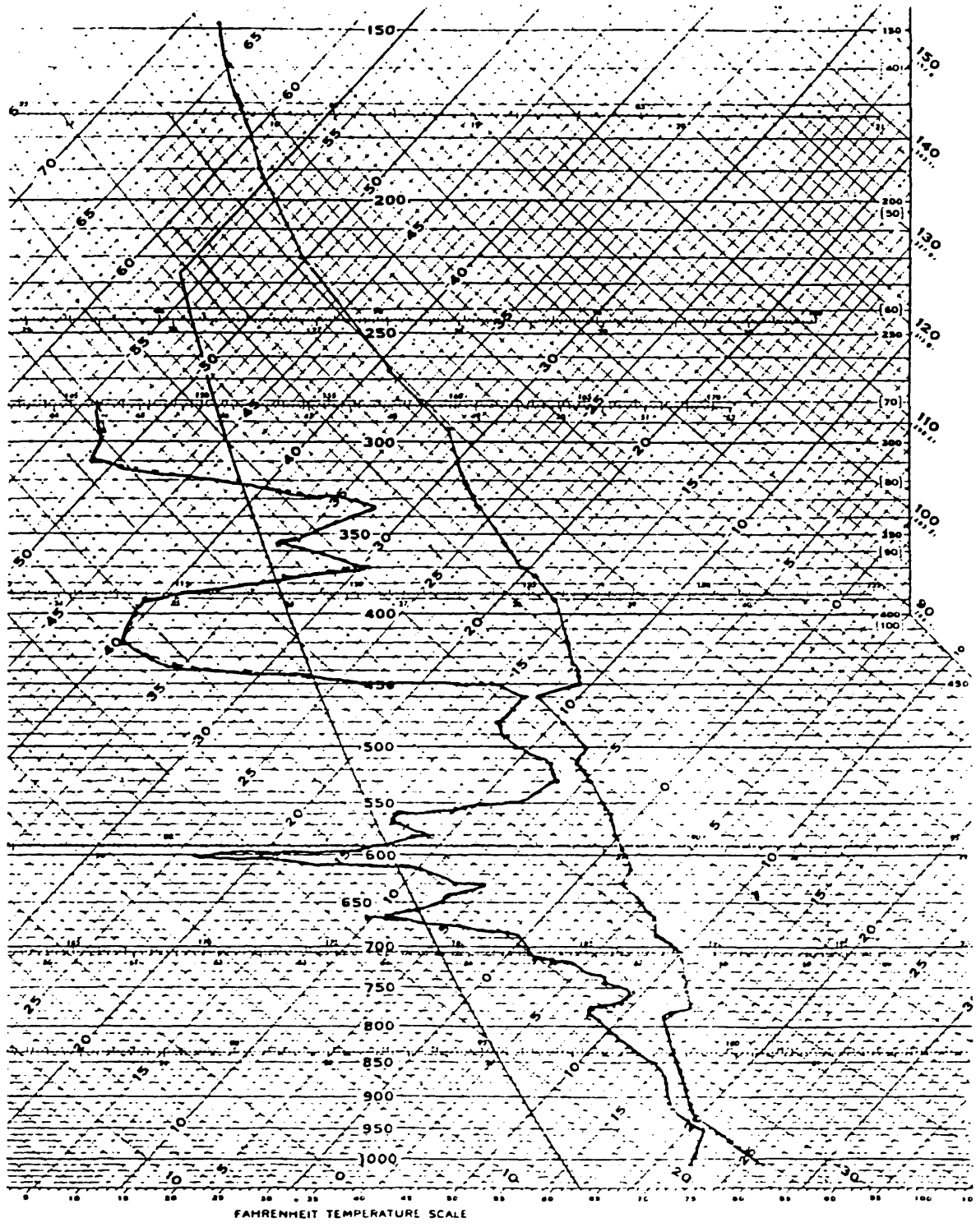
The area covered by echoes greater than 43 dbZ was over 400 km^2 indicating that rainfall rates were in excess of 25 mm/hr in this whole region by 2200. A rainfall rate of 7 mm/hr (35 dbZ) was estimated to cover an area of 1000 km^2.

2.5 Conditions Prior to 3rd Sept. Band

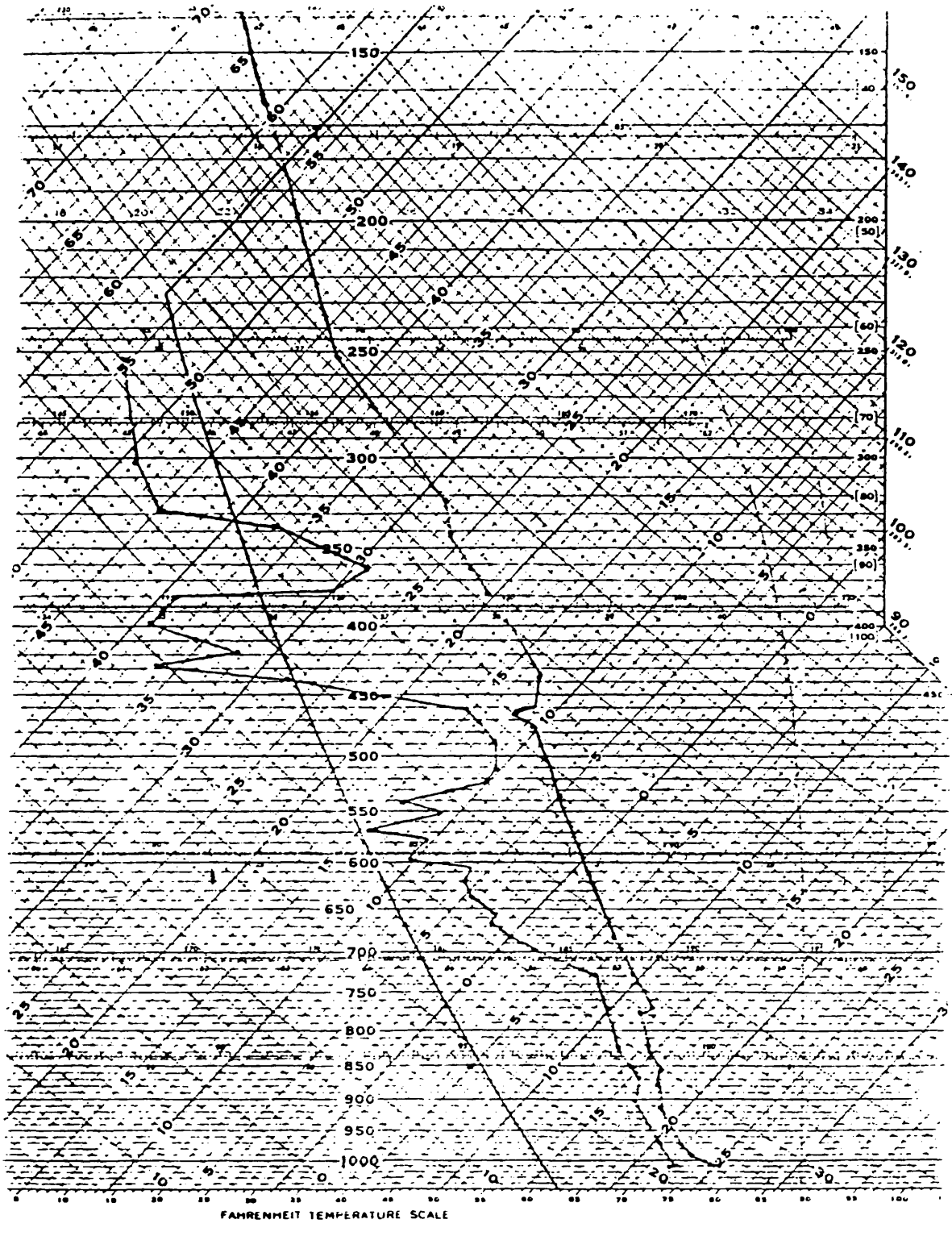
2.5.1 Temperature and Moisture Profile

The two ships nearest to the band provided soundings using balloon ascents at 3-hourly intervals. Oceanographer was situated about 50 km to the north and Researcher 100 km to the west of the area where the band first developed. Soundings from these ships at 1800 GMT (fig. 2.3) are therefore probably fairly representative of the thermodynamic structure at the time and position of the band. This is particularly supported by the strong similarity of the profiles produced by these ships which are separated by 100 km. The only major difference is at the surface where Oceanographer recorded a temperature of 24°C compared to Researcher's 26 C in the lowest 500 m. Such low-level variations would be expected as a result of the isolated showers which are seen on radar pictures in the vicinity of Oceanographer. It is possible that the cooling and slight drying is a remnant of a cold outflow. At Researcher the boundary layer is dry adiabatic and well-mixed up to the lifting condensation level at 950 mb showing no evidence of deep convection. This part of the sounding is thus typical of shallow boundary layer convection in equilibrium with heat and moisture fluxes from the sea surface. Below 800 mb the Researcher sounding is generally drier but both show a wet adiabatic lapse rate between 800 and 900 mb with a wet bulb potential temperature of 21-22°C which is evidence of shallow convection. Above 800 mb there is a 1 K temperature inversion at Researcher, 0.5 K at Oceanographer. At Researcher this marks the lower end of a very dry layer up to 525 mb with the humidity in the region of 30 per cent between 600 and 700 mb. Oceanographer also shows a distinct dry layer at the same heights but the humidity is greater possibly as a result of previous deep convection which may also account for the comparative weakness of the inversion at 775 mb. A layer of high humidity between 450 and 525 mb is capped by a second strong inversion with a humidity of 10 per cent immediately above it. Both ships' soundings also show a moist layer at 350 mb interrupting this upper dry layer.

The inversion at 2 km is a common occurrence in the tropics in



2.3a Thermodynamic sounding at Researcher, 1800.



2.3b As 2.3a for Oceanographer, 1800.

relatively suppressed conditions. It is the southern extension of the trade inversion which reached a strength of 5 K at 15 N. The air above has originally descended to the north of the convective belt where the strength of the inversion has totally suppressed convection so that the overlying air remains dry. Consideration of the large scale flow shows this air to have moved southwestwards into the region and it probably originated over the Sahara. Advection from the north is more likely to account for the presence of the 2 km inversion at this latitude (7 N) than descent because most studies indicate that large scale descent does not extend to such low levels. However, Reeves, Ropelewski and Hudlow (1979) have shown that there was mean descent at 700 mb in the GATE area of 0.5-1 cm/s for several hours on 3rd Sept. which is sufficient to produce a 1 K inversion according to a numerical study by Soong and Ogura (1980). The dryness above the inversion, however, implies that advection from higher latitudes is significant.

The upper inversion at 450 mb is consistent with composites by Chen and Ogura (1980) and Frank (1978) and the case study of Ogura, Chen, Russell and Soong (1979) which all show that a large scale subsidence is commonly found down to 450 mb during suppressed conditions.

Ogura, Chen, Russell and Soong (1979) have remarked that of all the GATE ships at this time, the inversion at 800 mb was least pronounced at Oceanographer and Researcher indicating this to be the most favourable area for convective growth at 1800 GMT. The inversion disappears gradually because of cumulus transports. As a cumulus cloud penetrates the inversion it evaporates, cooling and moistening the environment's warm and relatively dry air. The reason for cumulus activity being particularly effective in the region of these ships compared to the rest of the GATE area is not clear. As will be discussed later, a possible mechanism for forcing low-level mesoscale convergence is associated with a mid-level jet maximum as described by Beebe and Bates (1955). The convective activity in the vicinity of Oceanographer is also related to the surface meridional wind strength as described in the next subsection.

2.5.2 Wind Profile

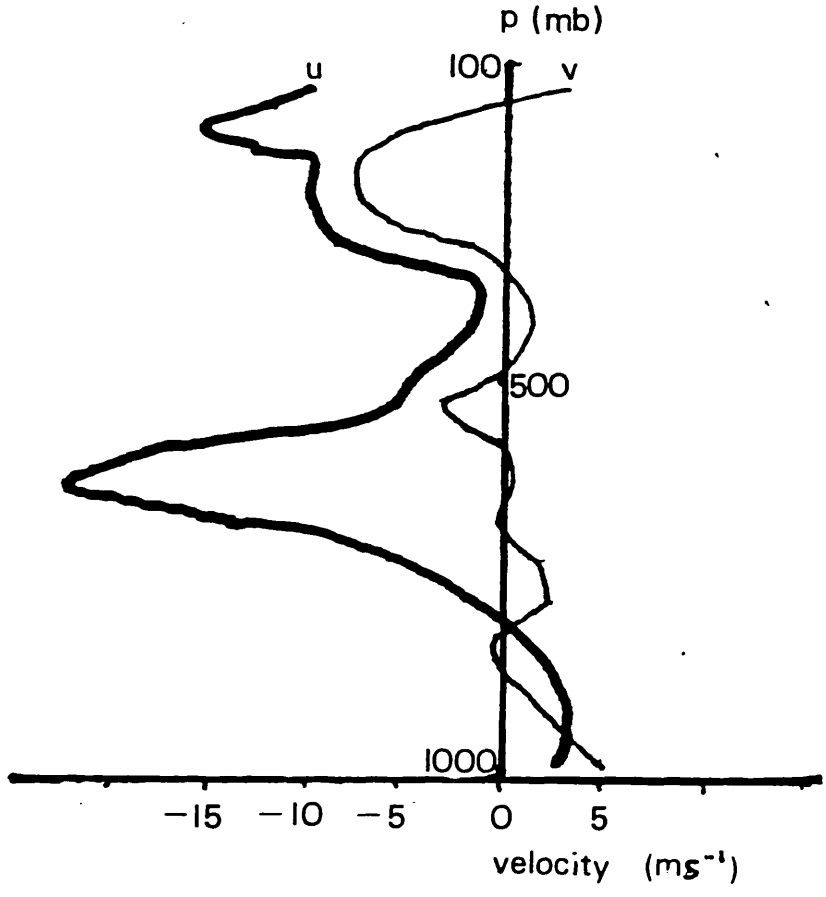
The most distinctive features of the 1800 Oceanographer wind profile (fig. 2.4) were the easterly jets at 600 and 200 mb. After 1200 on 3-9-74 the mid-level jet speed gradually increased reaching a maximum in excess of 25 m/s at about 1800. Researcher, to the south-west, recorded a peak strength of 33 m/s in the unsmoothed data at 2100 and other evidence indicated that the jet maximum moved gradually southwards through the GATE array during the latter half of the day.

At Oceanographer and Researcher, the jet persisted throughout the lifetime of the convective band studied implying that this convective feature developed in the presence of an extremely large easterly vertical shear between 800 and 600 mb. This jet can be identified as part of the African Easterly Jet which probably results from a persistent baroclinic zone between the Sahara and Equatorial Africa.

The 200 mb jet is also a commonly observed feature in this region and is part of the Tropical Easterly Jet associated with a persistent upper anticyclone over the Sahara which brings air equatorwards to its east leading to a westward acceleration due to angular momentum conservation.

The low-level zonal component was westerly and was part of the African monsoonal flow according to Chen and Ogura (1982) , who show that the Phase III mean depth of this westerly flow was 2 km, similar to that recorded in the 3rd Sept. case.

The meridional wind component was almost zero through most of the troposphere. There was a northerly maximum at the level of the upper tropospheric jet and a surface southerly up to 850 mb. Radar and satellite pictures at the time showed cloud top flow towards the south-west as a result of the Tropical Easterly Jet's direction. At 0900 there had been a southerly wind throughout the lower troposphere but this had disappeared by 1500 except for the strong surface southerlies which gradually reduced in speed to 5 m/s at 1800 GMT.



2.4 Wind profile at Oceanographer, 1800.

Thus there was a meridional shear of 5 m/s in the lowest 1500 m, this being a typical feature of the southern part of the GATE area just after the passage of an easterly wave ridge. This component of the shear was probably important in cloud development. Oceanographer was situated at a latitude of 7.5 N where the meridional wind component's surface convergence was large so that the strength of this vertical shear was very latitude dependent. The surface wind varied by 1 m/s per 100 km (or 1 m/s per deg). It may be for this reason that quasi-stationary convection had a tendency to be favoured in a narrow latitude band around 7 N. In agreement with this idea is that Chen and Ogura show the latitude of maximum precipitation to move with the surface confluence line remaining several degrees to its south during a composite easterly wave passage. Thus it seems typical for convection to develop and persist in the region of surface southerlies and not just at the surface confluence line several degrees further north.

CHAPTER 3
NUMERICAL SIMULATION OF BAND CONVECTION: PART I

3.1 The Numerical Model

To aid the understanding of the detailed structure of the convective band a numerical simulation was carried out. The numerical model employed was developed at the Atmospheric Physics Group, Imperial College, during the 1970s and is modified from the version used to simulate mid-latitude convection e.g. the Hampstead storm (Miller, 1978), multicell and splitting storms (Thorpe and Miller, 1978) and tropical convection (Moncrieff and Miller, 1976). The model uses a pressure coordinate system and thus the model levels represent layers of equal mass. The approximations involved in transforming the Navier Stokes equations into pressure coordinates are discussed in Miller(1974). The Boussinesq approximation is made whereby pressure and density deviations from their hydrostatic values are assumed small. This has become a standard procedure in all atmospheric numerical models and involves neglecting the contribution of non-hydrostatic density changes in the mass continuity equation but keeping their effect on the vertical momentum equation neglecting second order terms. The vertical momentum equation becomes:-

$$\frac{D}{Dt}\left(\frac{\omega}{\rho_0 g}\right) + g\left(\frac{\theta_v'}{\theta_{0v}} - q_l\right) + \rho_0 g^2 \frac{\partial h'}{\partial p} = 0 \qquad \text{(Eq. 3.1)}$$

$$\theta_v = \theta(1 + a q_v) \; ; \; a = \frac{R_v}{R_d} - 1$$

Continuity of mass becomes:-

$$\frac{1}{\rho_0} \nabla . \rho_0 \underline{V} \simeq \frac{\partial u}{\partial x} + \frac{\partial v}{\partial y} + \frac{\partial w}{\partial p} = 0 \qquad \text{(Eq. 3.2)}$$

Since the approximation that $\partial \rho / \partial t = 0$ has been made the equations are anelastic and sound waves cannot exist in the numerical model. This has the advantage that the time step required for stability which is determined by the fastest moving model wave is only limited by the speed of surface gravity waves (30 m/s) rather than

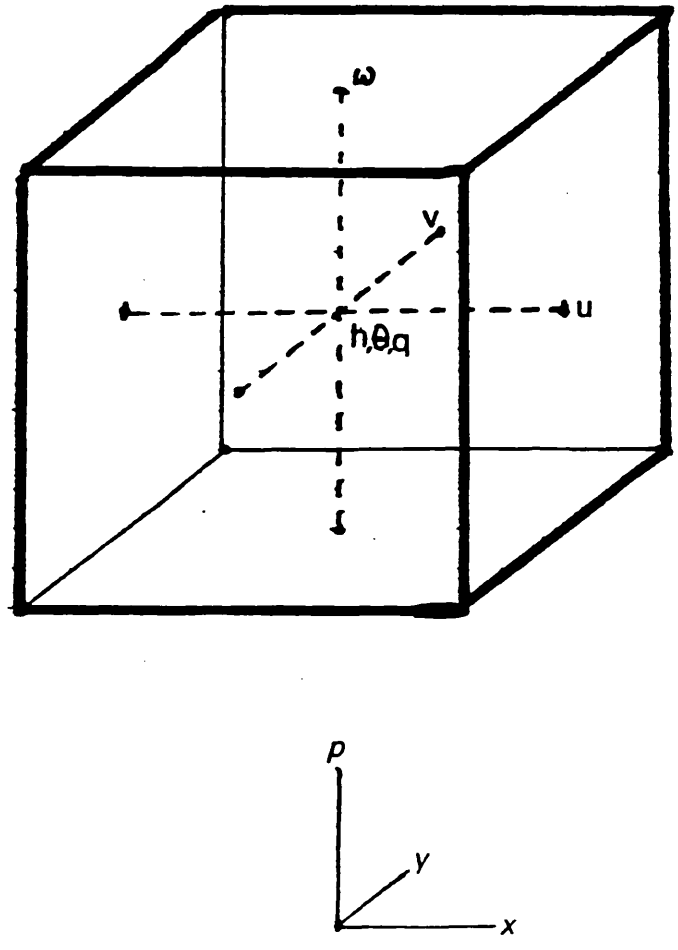
sound waves (300 m/s).

Using the momentum and continuity equations a diagnostic Poisson-type equation is obtained from the pressure (height) deviation from hydrostatic. Since the equations are expressed in flux form and are therefore conservative it is important to ensure that mass continuity is accurately preserved by the velocity fields. This is achieved by the Harlow and Welch (1965) method. The term $\frac{\partial}{\partial t}(\nabla . \rho . \underline{v})$ on the right hand side of the Poisson equation for h' is represented in finite difference form despite strictly being zero. This has the effect of causing the height field to damp any deviations from continuity each time it is calculated. As the lateral boundary values of h' are calculated in the model the Poisson equation is solved by transforming with sines in the horizontal directions and solving the resulting second order equation for each pair of horizontal wavenumbers in the vertical direction imposing the upper and lower gradient boundary condition. This second order equation is solved by the recurrence method. A reverse transform gives h'.

Apart from the three momentum components and height the variables carried by the model at each grid point are temperature, water vapour, cloud water and rain water. The variables are defined in the grid as shown in fig.3.1. making evaluation of the fluxes through the faces easier. The space derivatives are represented by second order centred differences with the flux term at a face defined as:-

$$(u\phi)_{i+\frac{1}{2}} = \frac{1}{2} u_{i+\frac{1}{2}} (\phi_i + \phi_{i+1}) \qquad \text{(Eq. 3.3)}$$

The exception to this is the rainfall flux where the upstream value of the rain is transported through the face at a fall speed which varies with rain water content. This is done to ensure that rainfall does not produce negative water because upstream schemes maintain positiveness at the expense of being only first order and producing unrealistic diffusion. The use of fluxes ensures that a variable is conserved during advection in that the domain total would remain constant in the absence of sources or boundary fluxes as long as mass



3.1 Model grid box showing points at which variables are defined.

continuity is preserved.

The equations for momentum, temperature and moisture are time integrated using alternately the Euler forward step and Euler backward step as in Miller (1974). The simple forward step predicts values at time n+1 using the fluxes at time n. However, the use of this time integration scheme with centred space differencing leads to a numerical instability in the advection of waves and thus these cannot be combined in a numerical scheme. To avoid this difficulty alternate time integrations are carried out using a 'backward' step . In this scheme the quantity at the future time step (n+1) is first estimated using a simple forward step and it is these estimated values which are used in evaluating the fluxes which finally determine the change from time step n to n+1. The 'backward' scheme is thus quasi-implicit in using the fluxes estimated for the future time step to determine the new values. The alternating scheme is marginally unstable in wave advection but the application of a selective 17-point filter every 16 timesteps keeps the instability from amplifying short waves. The filter is based on the application of a three-point second order diffusion-like term $\frac{D^2}{4}$ which completely removes 2 grid length waves followed by applying its inverse (Schapiro) to restore the long waves to their original amplitudes. The true inverse requires an infinite number of points and a 17-point truncated version is used in the model based on the first few terms in the expansion for $\left(1+\frac{D^2}{4}\right)^{-1}\left(1+\frac{D^2}{4}\right)$. In addition to this filter there is a smoothing applied to all fields (except height) which acts to represent subgrid scale mixing in a crude way aswell as keeping short wave amplitudes small. In deep convective modelling the effects of mixing on scales less than one grid length (1 km) are considered to be of secondary importance in comparison with the resolved scale atmospheric motions since most of the dynamics of storms depends on interactions between larger scale air masses viz. updraughts and downdraughts.

At the lateral boundaries normal velocity, temperature, water vapour and height are predicted using radiation conditions. The predicted value of a quantity at the boundary is determined by advecting it at a local 'effective advection' speed which is

calculated from nearby spatial and temporal gradients. This method allows gravity waves to propagate out through the boundaries with little reflection and has been used in simulations of storms with open boundaries by e.g. Klemp and Wilhelmson (1978) and Clark (1979). Because gravity wave speeds are high in comparison with typical model flow speeds the approximation of ordinary advection by the model wind at the boundary would be inaccurate and the inconsistency of the behaviour of boundary points with interior points would produce reflected gravity waves which could seriously disrupt the interior solution.

The upper and lower boundaries are pressure surfaces at 100 and 1000 mb and it is assumed that there is no flow across these. This is realistic because the upper boundary is in the stratosphere and the lower boundary is approximately at the surface. Subgrid scale transports across these boundaries are also set to zero. The vertical pressure velocity, Dp/Dt, is maintained at zero on the boundaries by keeping the nonhydrostatic pressure gradient in balance with the buoyancy there such that there is no net vertical acceleration. Thus the height field has gradient boundary conditions at the top and bottom and these are imposed on the Poisson equation solution.

After each time step, condensation and evaporation processes are calculated. If the water vapour content of a grid point exceeds the saturated value for that temperature the mixing ratio and temperature are changed, constrained by energy conservation, until the final mixing ratio is the saturated value for the final temperature. The excess water vapour is condensed into cloud water. Similarly if cloud water exists in subsaturated air it is evaporated with a corresponding temperature change until either saturation is obtained or no cloud is left. Thus, no model point has supersaturated water vapour nor cloud in subsaturated air and the time scale of cloud/water vapour conversions is taken to be small compared to the model time step (15 s).

Rain water in the model is distinguished from cloud by being allowed to fall relative to the air containing it. The Kessler (1969)

parameterisation scheme is adopted whereby cloud water can be converted to rain by coalescence of cloud droplets and by accretion onto pre-existing rain drops. Rain is also able to evaporate at a rate dependent on the subsaturation of the surrounding air. As has been desribed in chapter 1, the representation of rain and its evaporation is important to the dynamics of cumulonimbus convection and past use of the model has verified that the Kessler parameterisation scheme produces adequate results.

3.2 Simulation with a 100 mb Vertical Resolution

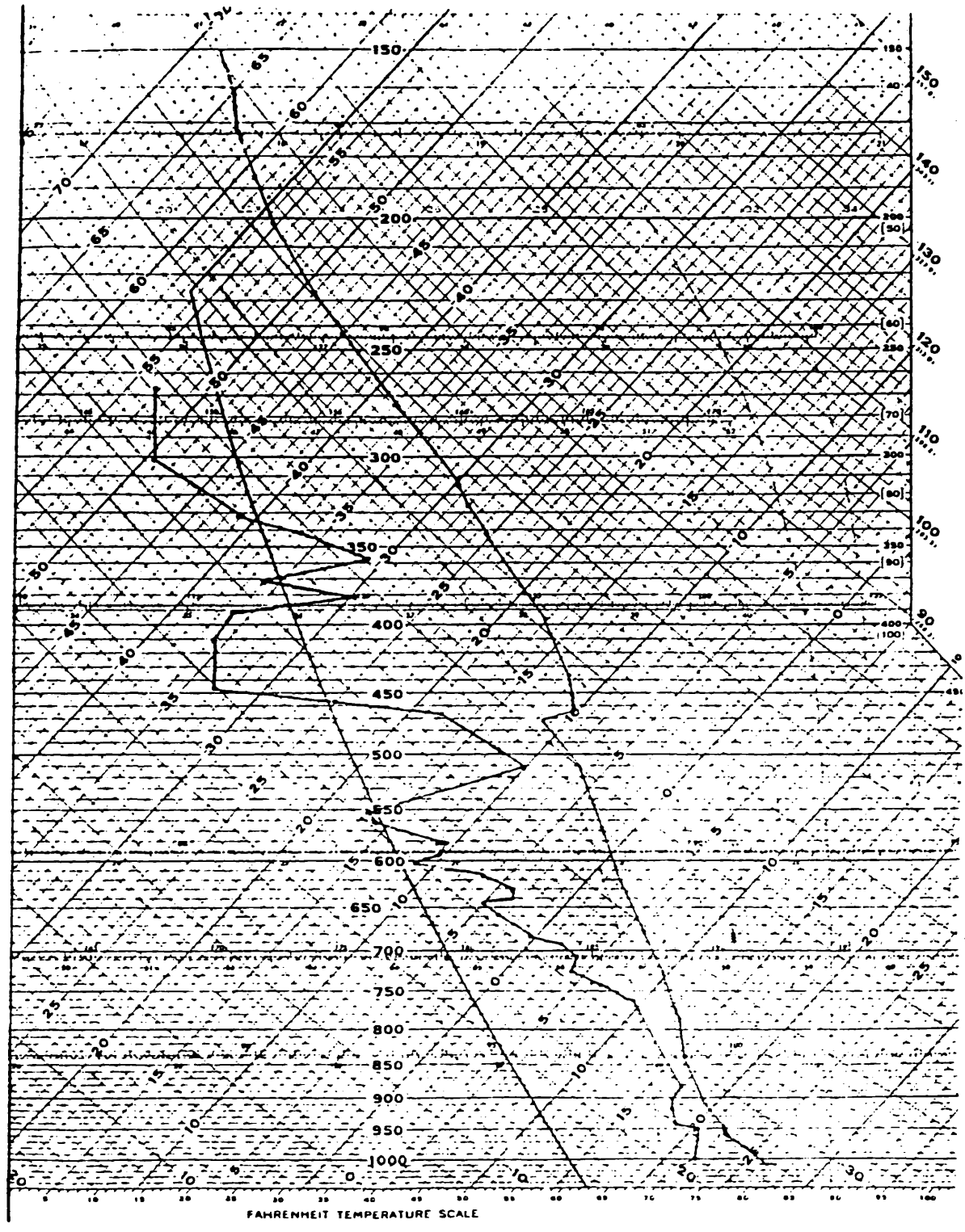
3.2.1 Introduction

In these initial simulations the vertical resolution was half of that used for the later research. This section describes the results obtained in the low resolution simulation and these are then compared with the 50 mb resolution results. By analysing the difference in the simulated storm behaviour, the importance of vertical resolution can be evaluated.

3.2.2 Domain and Sounding

The model domain consists of 30x30 grid points each representing 1 km^2 horizontally. There are 9 vertical levels between 100 and 1000 mb, each level being a 100 mb deep.

The thermodynamic profile was based on that observed at Researcher at 2100 GMT (fig. 3.2) because this was considered to represent most the sounding in which the band grew. The ship Oceanographer was closer to the site of initial development but the thermodynamic structure had already been modified at low levels by the effects of isolated showers before 1800. The Researcher temperature profile at 1800 showed a 1 K inversion at 2 km with an 800 m deep neutrally stable boundary layer and it was not until 3 hours later that convection developed strongly in this ship's region. Thus the sounding used was the only strongly unstable thermodynamic profile recorded during the band's development. The value of CAPE is



3.2 Thermodynamic sounding at Researcher, 2100.

1200-1300 J/kg but because of the high shear a small proportion of this is actually converted into updraught kinetic energy.

The wind profile considered most representative was that from Oceanographer at 1800 (fig. 2.4). The use of this is supported by the fact that qualitatively all the wind profiles recorded in this area at this time are similar. They all show low-level south westerlies, a mid-level easterly jet and upper level northeasterly jet.

To produce the model sounding these data are averaged over 100 mb layers to give a temperature and moisture typical of that air. This is necessary because the model advection is in flux form and thus the grid points represent boxes rather than point values.

The numerical simulation was initialised with a 4 km x 4 km x 300 mb block of saturated air 1.5-2.5 K above the environmental temperature and initially at rest. This method produces an extremely active convective cell in comparison with those later in the run because the wet bulb potential temperature of the air in this impulse is several degrees higher than that of the surface air. In a later 9-level simulation and most 18-level simulations described the initial impulse was made less active by only applying a gradual heating for the first 8 minutes. This produces an initial cell which is no more buoyant than surface air would be once saturated and thus has a more realistic strength.

3.2.3 Simulated Structure and Development

The model was run to 2 hours with a 15 sec. time step during which time a persistent east-west oriented line of convective clouds developed gradually eastwards from the position of the initial cell. These clouds (fig. 3.3) of 3-4 km in horizontal scale and with tops at 3-4 km are produced by ascent on a convergence line which is at the boundary between evaporatively cooled downdraught air from previous cells to the north and environmental inflow air approaching from the south-west. Thus the alignment of the system is governed by that of the gust front as is common with such multicell systems in nature.

The downdraught outflow (fig. 3.4) is 1.5-2 K cooler than the environment and occupies only the lowest model layer having an effective depth of 1 km. A balance is achieved whereby the environmental inflow is of sufficient strength to prevent this dense pool of air from spreading southwards and to thus keep the convergence zone almost stationary. During the simulation the cold air region expands northwards and eastwards but remains unable to spread upwind relative to the surface air throughout the 2 hours. In comparison with observations the clouds are small and convection is generally much weaker but the east-west alignment is common to both. This direction is probably determined by the low-level wind profile which governs the motion of developing cells. As cells grow they move slowly northeastwards before decaying and producing an intense downdraught which is sufficiently close to the convergence line to enhance the strength of the gust front. The northerly component of the surface shear is important because it enables developing cells to remain close to the surface front. The low-level westerly wind causes these clouds to move eastwards and this allows the surface gust front to develop eastwards.

The primary reason for the reduced activity of the simulated convection compared to that observed is the inability of the modelled updraughts to penetrate the mid-level shear layer. Taller, stronger updraughts such as those observed on radar images are able to produce much more rain and can aid low-level convergence by creating a region of low pressure in the lower troposphere and by increasing the strength of the downdraught. The updraughts in the model are active up to the 700-800 mb layer reaching a strength of 4 m/s and a temperature 4.5 K above the environmental value. These cores are about 3 km wide and tend to have no associated downdraught until their decay stage approximately 30 minutes after their initial formation. Above 700 mb these updraughts are capped by air up to 2 K below the environmental temperature, resulting from the updraught air mixing with jet level air in such quantities that the cloud almost totally evaporates. This is aided by the dryness of the jet air, its humidity being 60 per cent at 650 mb. It is noticeable in the simulations that cells growing downwind relative to the jet evaporate less as a result

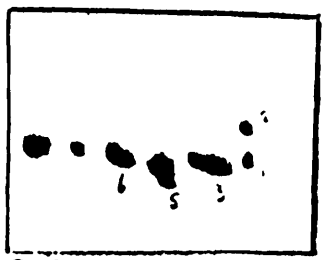
3.3



650 mb



750



850

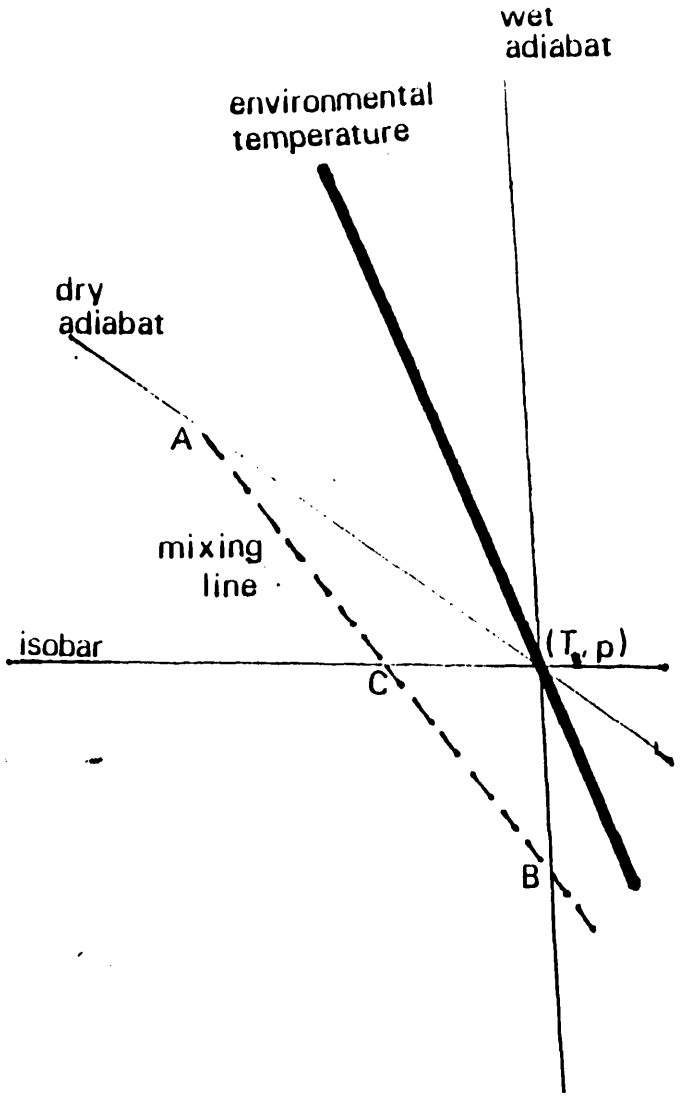
3.4



950

3.3 9-level model clouds at 120 min. Horizontal sections at 650, 750, 850 mb.

3.4 9-level model 950 mb air less than environmental temperature by more than 1 K.



3.5 Saturation Points of mixtures of distinct air types.

of the jet air's humidity being increased by the moisture transport of upwind cells. From consideration of the equivalent potential temperature of the mixed air compared to that of the updraught air and environment it can be estimated that only a quarter of the mixed air originated in the updraught. Thus it is the high degree of mixing which is destroying the convection. The possibility that this is a consequence of the low resolution of a strongly sheared flow will be discussed in the next section.

The downdraughts of decaying cells supply the surface layer keeping the gust front active. The wet bulb potential temperature of this air is typically around 19°C compared to 23-24°C for the surface environmental inflow. From the tephigram it can be seen that, assuming approximate conservation of θ_w , it must have originated from heights between 2.5 and 3 km. However, this can only be an estimate since numerical inaccuracies could affect θ_w .

Above the cold surface layer there is a 1 km layer of subsiding environmental air which is warm and dry compared to the ambient environment initially at that height. There is also a significant convergence (4×10^{-4} /s) up to 2 km above the surface indicating that the general subsidence extends to this height with descending air being replaced by horizontal convergence. There is no evidence of subsidence or convergence above 3 km.

In the sheared layer the correlation between westerly momentum and ascent is strong as surface air retains much of its eastward momentum during ascent in updraughts. Even in the lower jet there is eastward moving air which has originated from the surface. Similarly downdraughts tend to transport air of high easterly momentum downwards. An equivalent description of this momentum transport is that of vorticity tilting. The presence of updraughts or downdraughts produces a horizontal gradient of vertical velocity in a vertically sheared environment. Thus vertical vorticity is generated at the sides of the updraught and this appears mainly as a high transverse shear in the horizontal wind component parallel to the shear vector. Calculations confirm that the time scale of this generation of

vertical vorticity is consistent with the tilting term, $\frac{\partial w}{\partial y}\frac{\partial u}{\partial z}$, in the vorticity equation (cf. Zipser, Meitin and Lemone, 1981, observed band).

The southerly momentum component of the surface air is only maintained up to about 2 km as the air ascends in a northward sloping low-level draught. Above this height the north-south pressure gradient dominates this component of the motion and the effects of dynamic detrainment (from updraught deceleration) have a substantial effect at mid and upper-levels producing a strong divergent component in the meridional wind field.

The diverse behaviour of these two momentum components, one being quasi-conserved and one being unconserved, can be explained in terms of the relative strength of the two shear components. The strong easterly shear governs the alignment of the system and hence there is a symmetry in the pressure field. Low-level pressure gradients in the east-west direction are small compared to those perpendicular to the alignment and hence are less likely to affect momentum transports. This effect is enhanced by the strength of the zonal momentum's vertical transport which results from the high shear below the jet.

3.2.4 The Effects of Vertical Resolution

In cloud models a good vertical resolution is particularly important because of the need to represent the ascent of warm, moist air into an environment with substantially different thermodynamic properties. At the boundaries of such cells there are sharp gradients of quantities and it is vital that the numerical scheme and resolution can cope with with these. The simulation must allow air to move without significantly changing parcel-conserved properties such as θ_w along their path except through a reasonable degree of mixing with environmental air.

Preservation of a realistic value of θ_w by air ascending from the surface is crucial to the dynamics of the convection since it determines the buoyancy. Even an error of 1 C could significantly

alter the activity of the system because the instability of the surface air with respect to moist adiabatic ascent is critically dependent on its wet bulb potential temperature which should be conserved by unmixed air parcels in the absence of diabatic processes other than condensation/evaporation.

The effects of resolution can be divided into two classes. Those of mixing and dispersion.

3.3 Mixing

3.3.1 Introduction

MIxing on the scale of one grid cell is distinct from diffusion which is represented explicitly in this model and can be controlled in its effect. Grid scale mixing is implicit in any numerical model where points represent the average properties in a grid cell. Although the use of centred space differencing for gradients in advection is only a second order approximation in the model, the effects of numerical diffusion (∇^2 ,$\nabla^4\phi$ etc.) are eliminated totally leaving truncation error terms such as ∇^3 ,$\nabla^5\phi$ etc. which only affect the dispersive properties of waves. Thus there is no diffusion implicit in second order space differencing. First order schemes such as upstream differencing, where the leading Taylor series truncation term is in $\nabla^2\phi$ can have a significant implicit diffusion when applied to advection.

The horizontal resolution in the model is 1 km and this is considered sufficient to represent the more important mesoscale features in a mesoscale convective system. A lower resolution would lead to an implicit mixing on a scale of more than 1 km and would probably produce a high rate of entrainment of environmental air into updraughts which themselves are only several kilometres across and thus could be affected to an unrealistic extent by this process.

The vertical resolution in the 9-level simulation is 100 mb, which is about 1 km in the lower troposphere. In unsheared

environments this may be a sufficient resolution to represent the vertical scale of updraught cores. However, the presence of a mid-tropospheric jet and consequent low-level shear introduces a smaller scale to the vertical structure which tests the resolution requirements more severely. In particular, updraught cores reach 750 mb almost unmixed from the surface but there exists a shear of 15 m/s between the 750 and 650 mb levels and the updraught strength at 700 mb is only around 4 m/s. In the grid boxes above the updraught the jet air and the updraught air are mixed in a ratio approximated by:-

$$\frac{\Delta u \, \Delta z \, \Delta y}{w \, L \, \Delta y} \qquad \text{(Eq. 3.4)}$$

where Δu is the shear between 750 and 650 mb and w is the updraught speed and L is the east-west extent of the updraught. This ratio is sufficient for almost total evaporation of all the cloud in the ascending air and consequently the air cools below the environmental temperature. This cold air prevents any further updraught development above 750 mb. The unnatural part of this behaviour is the immediate mixing of all the updraught air passing through the 700 mb level with the jet air up to 1 km higher. The large quantity of environmental air included in this mixing process results from the shear and low vertical resolution and leads to a much higher evaporation rate than could realistically be expected. In the model a grid box is either totally saturated or clear whereas in reality there are possibly unmixed cloudy and clear air in 1 km^3 boxes at the jet level. The mixing of these two distinct air types, neither of which is negatively buoyant, produces an almost saturated cold mass of air which is thus far less buoyant than it should be and has a spurious adverse effect on convection. Although some mixing undoubtably occurs, the 1 km vertical scale does seem too large to represent the mixing length in this case. Alternatively to increasing the vertical resolution, the cloud evaporation rate could be limited in some way dependent on the likely entrainment rate so that cloudy and clear air are allowed to co-exist in a grid cell. In the present model the cloud evaporates at the same rate as its flux through 700 mb (4 000 000 m^3/s) implying a diffusion/entrainment speed of the same magnitude as the updraught's.

Doubling the vertical resolution would also reduce the initial evaporation rate for air ascending through 700 mb. This is because it is mixed with less environmental air for two reasons. Firstly, the reduced vertical grid length results in the scale of mixing being halved and secondly, the relative speed of the environmental air to the updraught's would be approximately half that with 100. mb resolution if the shear is linear. These together have the consequence that mixing of environment to updraught air below 650 mb is reduced fourfold when the resolution is doubled implying, possibly, a much lower evaporation rate.

3.3.2 Saturation Point Analysis

A method useful in the study of mixing of two distinct air types is Betts' Saturation Point analysis (Betts, 1982). By this method it is possible to find the effect of the degree of mixing on the buoyancy of the resulting mixture and hence to determine the effect of doubling the vertical resolution on the updraught at 700 mb.

When cloudy and clear air are mixed there is a method, using a tephigram, of determining the temperature of the final mixture and hence its buoyancy at a given height. The method involves finding the saturation point for each air type to be mixed. This is represented by two coordinates (e.g. θ_w and pressure) and is found as follows. For unsaturated air it is at the lifting condensation level. For saturated air it is the level to which air must descend wet adiabatically to evaporate out all its liquid water content.

The useful property of the SP is that when air parcels of two different SP's are mixed, the SP of the final mixture lies on an easily determined line connecting the two points. The values of θ and q for the SP of the mixture are just the average of the initial two SPs' weighted according to the mixing ratio.

In general, the SP of an air parcel is not conserved and can be changed along its path by variations in the total water (liquid plus vapour) content. This usually occurs as a result of rain fallout

which raises the SP along the wet adiabat and rain evaporation which lowers the SP along its wet adiabat.

Having determined the mixing line on a tephigram (fig. 3.5), several critical mixing ratios can be determined readily by the use of this line with the environmental temperature, T_e, at the required pressure level, p. Following the dry adiabat up from (T_e,p) intersects the mixing line at a point, A. Following the wet adiabat down from (T_e,p) intersects the mixing line at point, B. All the mixtures represented by SP's between A and B are cooler than the environment at pressure, p and all other mixtures are warmer. Following the isobar from (T_e,p) gives a point, C, between A and B where the mixture is just sufficient to evaporate all the liquid content of the cloudy air. This is the coolest possible mixture. Thus all points above C represent unsaturated mixtures and all those below are saturated. This idea can be generalised to all SP's to determine whether the air is thermally buoyant at a given pressure level at temperature, T_e. If the lines from (T_e,p) to A and B are continued all SP's to the left of the kinked line through (T_a,p) represent negatively buoyant air and all those to its right represent positively buoyant air. The presence of liquid drag and relatively buoyant water vapour means that the overall buoyancy is not solely determined by thermal buoyancy. Betts (1982) discusses the differences made by neglecting these two additional buoyancy terms.

This analysis is applicable to the 9-level numerical model because errors in the saturation point of the updraught air, which occur as a result of finite difference advection, are much smaller than the difference between the saturation points of the updraught and the jet air. Consequently, the change in saturation point as air is advected through the 700 mb level is almost entirely due to mixing. This is supported by the model results which show the mixed air properties to be consistent with those expected from SP analysis.

The minimum temperature of mixed air is 2 K less than the environment and corresponds to air which is just saturated (i.e. liquid content is nearly zero). If a typical saturation point for the

updraught core is taken, assuming a total evaporable water content of 15 g/kg, this temperature corresponds to a mixing ratio of 0.2 (one part updraught to four parts 650 mb environmental air). As has been stated previously this ratio can be expected from the shear and resolution of the 9-level model. Updraughts are capped by large plumes of this cold air particularly at the eastern end of the band. At the western end where the easterly jet has been modified by upwind cells there are regions of buoyant air at 650 mb consistent with a mixing ratio of 0.5 which, due to the horizontal scale of the updraughts, is only possible if the jet air has been mixed with two separate cores. This is discussed below.

The mixing ratio required to just achieve thermal buoyancy is 0.4. Comparing this to $wL/\Delta u\Delta z$ (updraught/environment) which is an estimated mixing ratio for an updraught of speed w, horizontal extent, L, and a shear of Δu with resolved height Δz gives $0.06wL/1000 = 0.4/0.6$ in the case being considered. Thus wL is about 10 km.m/s is the required updraught volume flux per unit width if surface air is to be mixed in sufficient quantities to result in a buoyant mixture. A single model updraught has typically only a sufficient volume flux to produce a mixing ratio of 0.25-0.3 thus it generally would require two updraughts before 0.4 is achieved and this is confirmed by the fact that buoyant air only exists above cells in jet air which has already been modified.

In a 9-level model the updraught air is mixed with all the jet air between 600 and 700 mb whereas an 18-level model's updraughts would initially only be mixed with that between 650 and 700 mb which has a lower relative speed. The SP of this 50 mb layer is close to that of the previously considered 100 mb layer but the mixing should be reduced approximately fourfold. If it is assumed that the 700 mb updraught flux remains the same in the higher resolution model, the typical mixing ratio produced by an updraught would rise from 0.25-0.3 to 0.6 which would be sufficient for positive buoyancy to persist up to 650 mb. Above this level the air would be further mixed as a result of the shear but it seems likely that the cloud activity would be increased by the increased resolution because of the reduced

effective entrainment rate.

3.3.3 Effects of Vertical Resolution on the Surface Layer

Another region in which vertical resolution is important is the lowest 1 km of the domain. In the 9-level model this is represented by one grid level and it is found that the cold downdraught outflow occupies only this layer with no trace of cold air above 900 mb. This leads to the question of whether the depth of this cold air, which is effectively 1 km in the model, is realistic. The depth is important to the dynamics of the system because it determines the height to which the environmental inflow air is forced to ascend. The lifting condensation level and level of free convection are both near 900 mb and it is, therefore, likely that the amount of forced ascent is a critical factor in the persistence of convection. The cold surface air is continuously supplied by downdraughts driven by rain evaporation from decaying cells. Thus there is a tendency to spread over the surface as a density current and this produces convergence with the surface environmental south westerlies. The relative speed of the density current depends on both its depth and temperature and an unrealistic depth could affect the motion of the convergence line. This fact may be important when simulating an almost stationary system.

Without the continuous downdraught supply the general descent of the density current air, which results from its horizontal divergence, would allow the overlying environmental air to descend through the 900 mb level. The consequent mixing would decrease the negative buoyancy of the density current. The temperature of the lowest model layer is thus determined by the net effect of the cold downdraught flux and the environmental air subsiding through 900 mb and mixing. In reality, the spread of the cold air causes the density current to get shallower than 1 km with warm subsiding air above it. However, the low model resolution prevents this process from being represented properly, causing the denser air to entrain more ambient air than in nature. Hence, the pool of cold air becomes deeper and warmer than it should be. Although the mean surface layer hydrostatic pressure would be

nearly correct, the vertical pressure gradient which should exist in the lowest kilometre would be unresolved.

In conclusion, the model resolution of 100 mb appears to be deficient in its treatment of cloud top detrainment in the high shear and the vertical structure of the surface layer's downdraught outflow area. In both cases a 50 mb resolution is likely to be sufficient to significantly increase the accuracy of the simulation.

3.4 Dispersion

3.4.1 Introduction

One of the most important effects of finite differencing is numerical dispersion whereby waves of different lengths are caused to propagate at different speeds relative to the grid. Dispersion exists in nature only when waves move relative to their medium (e.g. gravity waves, sound waves) and would not be expected to occur in simple advective motion. However, finite differencing introduces an artificial medium with respect to which the fluid moves, i.e. the grid. It is this fact which causes dispersion to occur even for advection in a numerical model.

Mathematically, dispersion arises from finite difference approximations of the time and space derivatives. A second order space derivative, such as is used in the model, has its largest truncation error term proportional to $\partial^3\phi/\partial x^3$. This is found from considering the Taylor expansion compared to the centred space difference. All even powers of $\frac{\partial}{\partial x}$ are eliminated and thus the space scheme produces no diffusion. The odd higher powers of $\frac{\partial}{\partial x}$ cause the relation between frequency and wavenumber to be nonlinear with shorter waves being deviated most from the true advection speed. Two grid length waves are severely affected by this scheme, being unable to propagate. The effect on other wavelengths is summarised below for 1-dimensional advection.

TABLE 3.1

WAVELENGTH/GRID LENGTH	WAVE SPEED/ADVECTION SPEED
2	0.0
3	0.41
4	0.64
6	0.83
10	0.94

It can be seen how much effect this dispersion has on ascent in the model with a vertical scale of 9 grid lengths. Much of the vertical structure has a scale of less than 4 grid lengths owing to the presence of a high shear in the lowest 400 mb and therefore vertical advection is highly dispersive.

The time integration scheme employed in the model, described in chapter 3, is alternate Euler forward and backward steps. This also produces a slight dispersion and small amplification but these effects are minor in comparison to those ascribed to space differencing.

Though the model is 3-dimensional and in flux form the above arguments for the 1-dimensional case apply equally and give a measure of the 3-d dispersion. This can be expected to have the severest effect in updraughts where, as a result of condensation and evaporation, there are sharp gradients of temperature and moisture in the direction of motion and the advection term dominates. In this sense the model is not behaving properly because latent processes are occurring continuously during parcel ascent in nature while in the model there are advections in the presence of large gradients followed by corrections for cloud processes. In view of the dispersion errors arising from advection, it may be more consistent with the natural process to apply advection to a parcel conserved property such as equivalent potential temperature which varies more smoothly along a trajectory as condensation and evaporation occur. In addition the advection of total water would be needed to define the parcel properties uniquely. The practical difficulty with this method is the

accurate conversion from θ_e and total water to potential temperature, θ, and water vapour, q_v, which are required for buoyancy calculations. The presence of rain which has a limited evaporation rate further complicates this procedure. Empirical functions would be needed to obtain the temperature and saturated mixing ratio from the equivalent potential temperature and pressure. If this exceeds the total of vapour and cloud water the temperature is corrected following

$$\Delta T = L\Delta q/c_p$$

and all the condensable (non-rain) water remains in vapour form. Otherwise, if there is more condensable water than the saturated mixing ratio the excess is condensed into cloud water and the temperature is unaltered.

3.4.2 Dispersion in the Low Resolution Simulation

The initial cell produces dispersion in its most distinct form owing to the presence of high thermal gradients between this cell air and environmental air. The method of initialisation was to allow a warm saturated bubble to rise from rest. By ten minutes the base of the cell rises from 1000 to 800 mb and the air immediately below cools by 4 K and also dries significantly. No natural processes can account for this change because dry adiabatic ascent and evaporative cooling can only cool and moisten the air. Subsidence over a distance of 1-2 km accompanied by rain evaporation would account for these properties but inspection of the velocity field shows no air to have descended far enough. Thus the effect is purely numerical.

It can readily be seen how the centred difference approximation to the gradient produces a negative perturbation to the rear of a positive moving block despite the absence of any upstream gradients (see eq. 3.5).

$$\frac{\partial \phi}{\partial t} = -u\frac{\partial \phi}{\partial x} < 0 \qquad \text{(Eq. 3.5)}$$

$$u > 0 \quad \phi_{i-1} = \phi_i < \phi_{i+1}$$

$$\frac{\partial \phi}{\partial x} \equiv \frac{(\phi_{i+1} - \phi_{i-1})}{2\Delta}$$

This effect is related to the inability of two grid length waves to propagate in this scheme since such discontinuities have a two grid length component. In the case of the initial cell the gradient discontinuity is an artificial result of the initialisation because the warm saturated inital perturbation has sharp boundaries. During the run itself, discontinuities in the temperature gradient along the direction of motion are small due to the common origin of the ascending or descending air in updraughts and downdraughts. However, the presence of condensation and evaporation does produce a discontinuity in the gradients of temperature and moisture where the parcel goes from unsaturated to saturated motion and vice versa. Thus, for the reasons described above, the air below the condensation level is numerically cooled by dispersion and that below the evaporation level (e.g. the mid-level jet) is warmed. Similarly, the effect of dispersion on the water vapour is to moisten the air below the condensation level more than would be expected from simple advection in a continuous fluid. Below the jet the updraught air is also dispersion-moistened because of the relative dryness of the mixed air above. This saturated updraught core being both warmed and moistened, has a wet bulb potential temperature significantly higher than would be expected from thermodynamic considerations, i.e. 25°C compared to 24°C estimated for surface air from the tephigram. Such warming is found as a common feature in the low resolution model updraughts between 700 and 800 mb. The surface cold outflow is also strengthened by dispersion cooling below the LCL and thus may be more effective than is realistic in forcing convergence.

It should be noted that the lack of preservation of parcel properties following trajectories does not conflict with the overall conservation of the flux form differencing scheme. The volume integrated total would be conserved in the absence of sources and boundary fluxes but dispersion acts to redistribute the heat and moisture within the volume.

In the case of the model updraughts, this redistribution is, crudely, a removal of heat from below the condensation level and a supply to the updraught below the evaporation level. Moisture is

gained, as has been stated previously, in both these stages and this is compensated for by the loss of moisture in the jet air approaching the evaporated updraughts. Thus the redistribution is not all necessarily in air of the same origin when a three-dimensional system is considered. It can be seen that dispersion in this way can affect the wet bulb potential temperature and total water conservation of moving air parcels.

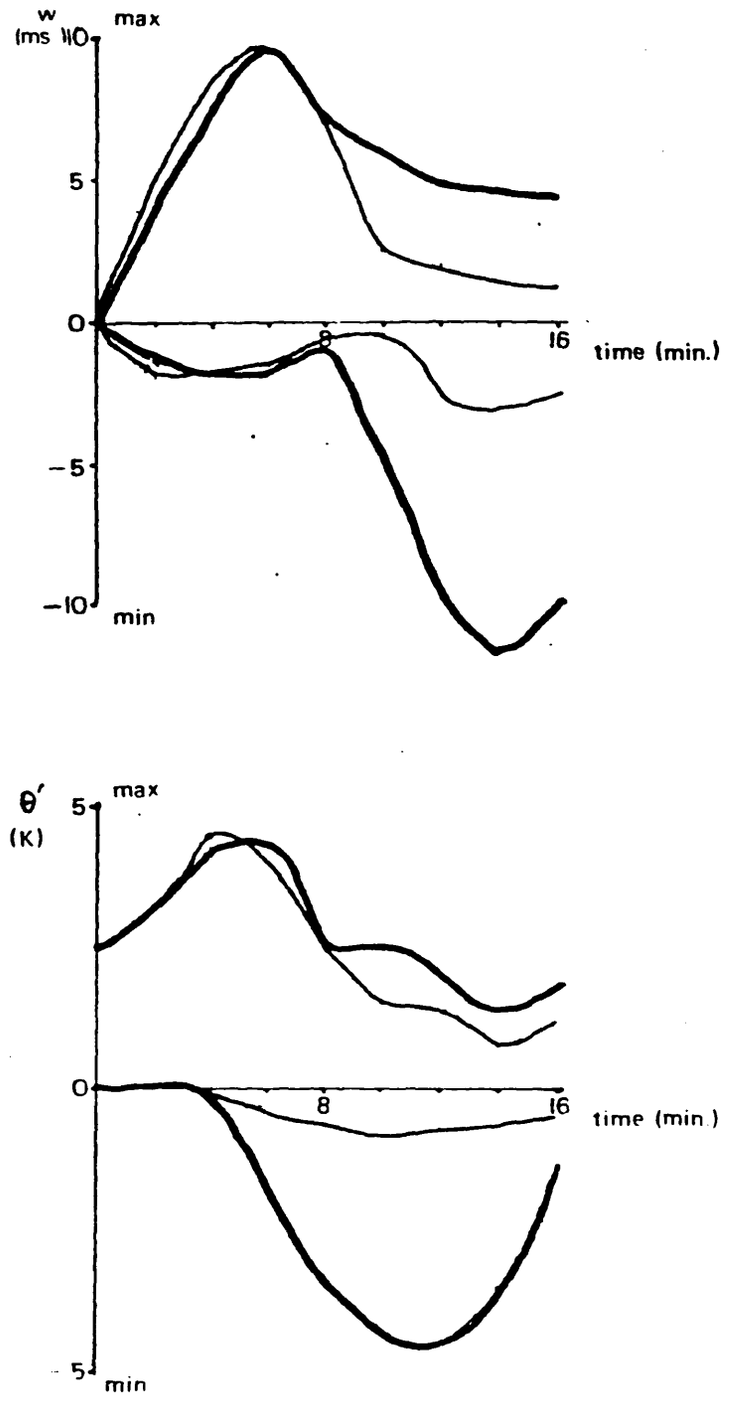
3.4.3 Resolution and Dispersion

A run of the numerical model identical to the 9-level run except with twice the resolution provides a useful comparison for assessing the effect of the vertical grid length on dispersion in the model.

As would be expected the difference in behaviour shows best in that of the initial cell where gradients of heat and moisture are sharpest. Fig. 3.6 shows the temperature and vertical velocity extremes between 800 and 900 mb. This layer is represented by two levels in the 18-layer run and these are averaged to give a direct comparison with the 9-level results.

The simulation behaviours diverge almost immediately as the cold perturbation in the low resolution run grows at approximately five times the rate of that in the 18-level simulation. At ten minutes into the run the minimum temperature is over 4 K less than the environment and a downdraught is generated which grows to 12 m/s by 14 minutes. With twice the resolution the cold perturbation remained around 0.5 K below the environmental value and consequently the downdraught strength was only about 3 m/s.

As has been discussed, this cooling is purely dispersional and therefore the strong downdraught is a product of too low a resolution and the large temperature gradient behind the initial ascending bubble. The higher resolution model's behaviour is more realistic in not producing such an effective downdraught but the presence of even a small volume of cold air shows that the effects of dispersion could



3.6 Vertical velocity and temperature deviation. Max. and min. point values in the 800-900 mb layer.
18-level (thin), 9-level (thick).

still be important. In terms of gradients along the direction of motion the initial cell is an extreme case and it is likely that doubling the resolution is sufficient to almost completely remove the effects of dipersion described in the last section.

As an example of the improvement expected from a higher resolution we consider the following system. Air ascends steadily through its LCL. Below cloud base the lapse rate is dry adiabatic and above it is wet adiabatic. Thus a discontinuity exists in the potential temperature gradient to which numerical advection is applied. Centred space differencing causes the air below cloud base to cool at a rate (assuming w is constant along the trajectory, i.e. 1-dimensional ascent):-

$$\frac{\partial \theta}{\partial t} = -\frac{1}{2}\omega \Delta p \frac{\partial^2 \theta}{\partial p^2} \qquad \text{(Eq. 3.6)}$$

This cooling occurs at the grid point immediately below cloud base, which in the natural system would remain at the same potential temperature, and is thus a measure of the departure from reality produced by the numerical scheme. In the case being considered $\Delta p\, \partial^2\theta/\partial p^2$ is governed by the dry and wet adiabatic lapse rates and may be taken as a physical constant so that the cooling rate due to dispersion is approximately proportional to the vertical velocity. In addition, the volume over which the cooling occurs is proportional to the grid length and thus there would be a decrease in volume integrated cooling expected as a result of doubling the resolution. In the case of an ascending hot perturbation with a small vertical scale such as the initial cell, the resolution increase has the further advantage of allowing it to ascend at a more realistic speed because of the reduced relative importance of the two and three grid length components in a better resolved perturbation.

Aswell as reducing cooling below the condensation level the 18-level simulation would be expected to decrease the warming below the evaporation (jet) level and also aid moisture preservation by

advected air parcels. This is confirmed by the results which show that the maximum θ_w of updraught air is 24°C which is consistent with that of the surface air in the 18-level sounding. There is also a much smaller bulk of cold outflow air at the surface.

The 18-level simulation will be described in more detail later.

3.4.4 Diffusion and Dispersion

It can be seen from the mathematical form of the numerical cooling rate that the addition of a diffusion term with a coefficient, $K=\frac{1}{2}\omega\Delta p$ would cancel its effect. This, however, is nearly an order of magnitude larger than the diffusion explicitly in the model which represents sub-grid scale mixing. An unphysically large diffusion coefficient would be required if this method is to be used to reduce numerical cooling . As the Euler forward/backward scheme in the model is effectively time- centred the inclusion of diffusion to counteract dispersive effects would have to be done carefully to avoid numerical instability. Simple analysis (e.g. Potter, Comp. Phys.) shows that diffusion terms have to be evaluated at the earlier rather than time-centred timestep to prevent numerical amplification. It is for similar reasons that the upstream and Lax space differencing schemes, which are highly diffusive, cannot be employed in conjunction with the time-centred scheme despite their advantage of not producing numerical cooling at discontinuities in the temperature gradient.

A similar problem to this is discussed by Pearson and O'Connor (1977), who conclude that damping is required to prevent dispersive effects from being amplified by a dynamical feedback mechanism. In their model a hot perturbation is amplified by dispersion which causes it to ascend more rapidly because of its increased buoyancy and this acceleration in turn further increases the effects of dispersion.

Though artificial damping has the desirable effect of causing the more dispersive shorter waves to decay faster it leads to rather more mixing transverse to the direction of motion than would be realistically expected. Entrainment into updraughts would be

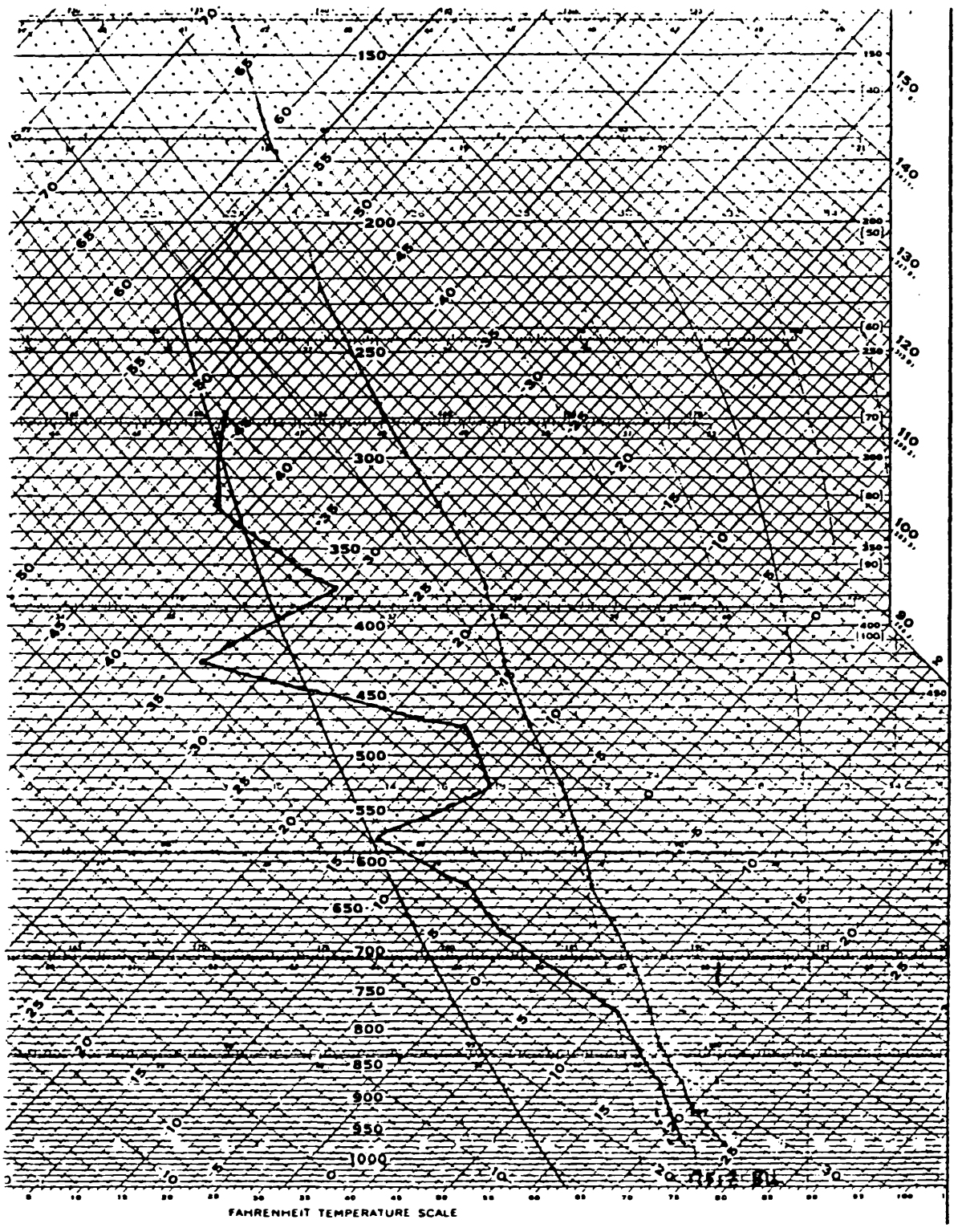
over-estimated in the simulation weakening them significantly. When employing a low order space differencing scheme, the choice between excessive diffusion and dispersion has to be made since it is impossible to eliminate both without greatly increasing the computational cost of the scheme. As it was found that doubling the resolution automatically reduced dispersive effects to an acceptable level, there was considered to be no need of damping to further control them.

3.5 Simulations with 50 mb Resolution

3.5.1 Introduction

The high resolution simulation has already been mentioned in connection with dispersion. In this section the emphasis will be on the simulated cloud behaviour.

As with the low resolution run already described, the wind profile was based on the Oceanographer observations at 1800 GMT and the thermodynamic structure is that recorded by Researcher at 2100. The increased resolution of the wind profile sharpens the easterly jet maximum to 22.1 m/s in the 600-650 mb layer compared to 18.6 m/s in the 600-700 mb layer of the 9-level profile. Small scale variations in the vertical moisture distribution are also better resolved. One feature of this sounding which was considered unrepresentative of pre-band conditions was the dryness of the air between 900 and 950 mb compared to that below it. A possible explanation is that it results from subsidence in the neighbourhood of the band which is well-developed by 2100. This also accounts for the slight increase in potential temperature gradient at the base of the dry layer. In the absence of subsidence, the whole subcloud layer would be uniformly mixed as observed 3 hours earlier. It was for this reason that the lowest kilometre of the model sounding was based on the boundary layer properties at 1800 in which the air is nearly 1 g/kg more moist (fig. 3.7). As has been discussed earlier, the reason for not using the whole 1800 Researcher sounding is the existence of a marked 1 K inversion at 800 mb which is unlikely to be representative of the



3.7 Thermodynamic sounding used in the 18-level simulations.

atmosphere at the time of development of deep convection, especially as there is evidence that this inversion eroded in the vicinity of the band prior to its growth. At Oceanographer, which is nearer to the site of the initial deep cells, the inversion was 0.5 K at 1800 but the surface air has a value of θ_w 1 K less than that at Researcher being cooler and drier possibly due to modification by convective downdraughts leaving it significantly less conditionally unstable. Thus the modified 2100 Researcher sounding selected for the simulations was the only one sufficiently unstable to produce the highly convective conditions observed on radar.

3.5.2 Comparison with 9-Level Results

The earlier 18-level simulations were directly comparable with the 9-level simulations because they used an identical initialisation procedure and were based on almost the same soundings. The resulting convection, however, was rather weaker and not self-sustaining. The cause of this difference was ascribed to the dispersion-aided downdraught produced by the hot initial perturbation. In the 9-level case, a deep cold pool was created capable of providing an almost stationary front to incoming south-westerly environmental air. The relative weakness of the higher resolution simulation's cold pool was due to the reduced effect of dispersion rather than any physical mechanisms (e.g.rain evaporation) because there was a similar amount of rain in the early stages to that before.

With a shallower and less cool downdraught outflow far less convergence is forced since the front moves northwards. This leads to a reduction in ascent and cloud development. Effectively the cold layer has insufficient inertia to remain slow moving and force environmental surface air to ascend.

3.5.3 Dependence of Development on Initialisation

From the thermodynamic sounding the initial perturbation used thus far is stronger than any subsequent cells would be in terms of relative buoyancy. There may be two reasons for such a rapidly ascending impulse hindering the formation of a downdraught of sufficient volume to sustain ascent. Firstly, a strong updraught has little slope with height in a sheared environment so that most of the rain produced falls through saturated air and evaporative cooling is limited to that below cloud base. A weaker updraught would slope downshear allowing rain to fall into unsaturated environmental air producing a cool downdraught. Secondly, the strength of the ascent in the core is of a similar magnitude (5 m/s) to the rain fall speed and a weaker core could enable more rain to fall out immediately despite producing it at a lower rate.

To test whether these were the reasons for the 'hot saturated bubble' initialisation failing to produce an adequate downdraught, a more gradual 'heat source' initialisation was tried. A heating rate of .005 K/s was applied for 8 min to the 2 km layer between 900 and 700 mb over a 4x4 km square near the centre of the domain. This method gives an initial unsaturated warm block of air which has a more realistic wet bulb potential temperature. I.e. θ_w is not higher than that of the surface air and the initial cell is thus more physically justifiable. The resulting downdraught outflow was weaker and covered a much smaller area than the previous run. This reduction in area results from the initial cell not penetrating the high shear layer as the previously employed strong cell had done. This had allowed rain to be carried westwards falling in a long zonally oriented line whereas with the weaker initialisation evaporation dominates over rain production in the jet. By 50 min into the simulation the lack of new cell generation meant that the surface rainfall rate had decayed to zero. Even increasing the size of the initial perturbation to 6 km x 6 km was not sufficient to extend the lifetime of the system. It can be concluded that the strength of the initial perturbation has little bearing on the subsequent ability of the system to persist.

Since it appeared to be impossible to grow the convective band from a cloud scale impulse the use of a mesoscale initialisation was investigated. It was considered that a pre-existing gust front of sufficient length transverse to the incoming surface flow may be capable of forcing enough ascent to sustain itself because a linear convergence region is more efficient.

To generate this front an 8 km x 8 km heat sink of .01 K/s was applied to an initially undisturbed domain for 5 min. By 40 min the cold surface air had extended northwards out of the domain but only moved about 2 km southwards (1 m/s) aligning against the prevailing wind. Its height was confined to the lowest grid level with the air immediately above showing evidence of subsidence warming except at the front where ascent cooling predominated. Throughout the 80 min simulation cells were generated at the 10-20 km front which continued to move slowly southwards. These clouds moved north developing to less than 4 km in height and producing about 5 mm/hr of surface rainfall compared to 10 mm/hr in the low resolution simulation.

Thus, having reduced the effects of dispersion by employing a higher resolution, the convection is weaker and remains so even with a mesoscale gust front to organise it. There is no evidence that the modelled system's scale can amplify into that observed and it is for this reason that the representativeness of the sounding used in the model must be examined more closely.

3.5.4 Dependence of Development on Jet Strength

The inhibitng effect of shear on convection is well known and it may be important to represent the wind profile accurately in the simulation when a strong shear is present as in this case.

The lack of convective growth in the simulations so far may be indicative of the shear being over-estimated. The two ships nearest the band provided wind profiles at 1800 and 2100 GMT all of which show evidence that a shear of approximately the magnitude of that employed in the model was present. The lowest jet strength observed was that

at Researcher at 1800 with a maximum of 16 m/s. This is three quarters of that in the model sounding adopted hitherto. To test whether this reduction in shear had a significant effect on convection a simulation was carried out with the 1800 Researcher jet profile. The previously described downdraught initialisation was again used so that a direct comparison could be made.

The initial cells produced twice the rain in the first hour of the simulation and cloud tops reached 8 km compared to 4 km with the stronger jet. This activity did not persist although cloud tops remained near 8 km up to the end of the simulation at 80 min. The later cells were weaker producing only 5 mm/hr of rainfall and the surface convergence showed no sign of intensification.

Thus, the only difference made by this 25 per cent reduction in jet speed was to allow the weak cells to develop through the shear layer. This result showed that the lack of activity was not primarily caused by the high shear in the model wind.

Since the wind profile and thermodynamic sounding both seem to be representative of the observed band's environment and assuming, reasonably, that the weakness of modelled convection is not solely the result of a numerical inaccuracy there must be another factor, as yet unaccounted for which aids cloud growth in nature. Such a factor may be the continuous interaction of the model domain scale with the larger scale flow. In the following chapters the implementation of the effects of this interaction on the model will be described.

CHAPTER 4
LARGE SCALE INFLUENCES ON CONVECTION

4.1 Introduction

In the simulations described so far no account has been taken of synoptic scale motions which may have an effect on the numerical domain scale. The methods by which this influence can be imposed on a numerical model will be discussed in the next chapter.

This chapter deals with the observational support for the presence of large scale tendencies in the flow. In particular, the forcing of mean ascent in the GATE region by several mechanisms is discussed. Firstly, it is known that deep convection can provide mean ascent and this can be modelled reasonably in the simulation. However, other mechanisms of forcing mean ascent exist on scales too large to be represented explicitly in the model. These forcings may have to be included for thir effect on the thermodynamic sounding and hence on convective activity. It will be seen that it is possible for ascent to be forced almost independently by mesoscale, synoptic scale and global scale dynamics, the causes being respectively jet maxima, easterly waves and the Hadley circulation.

4.2 Evidence for Large Scale Ascent on 3 Sept.

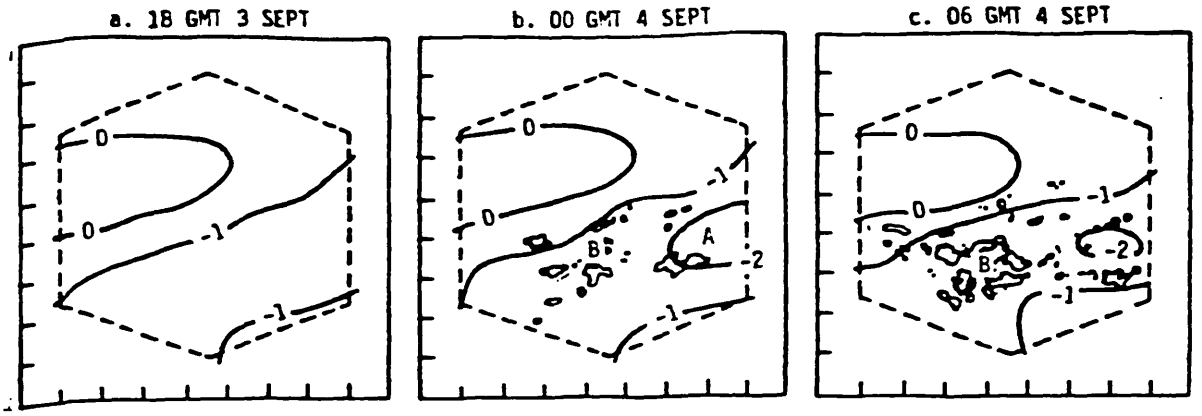
It is necessary, before describing how low-level ascent is forced, to find proof that it could have influenced the development of the band under study. Ogura et al. (1979) have analysed the GATE data at the time of this convective band. They derive the vertical velocity from the wind data supplied by the 6 outer hexagon ships and one inner hexagon ship in the GATE array giving a resolution of about 400 km. The data at 3-hourly intervals is interpolated and smoothed onto a 6x6 grid and then further interpolated onto a 25x25 grid. This fine mesh data was then used for divergence calculations from which the vertical pressure velocity, ω, was calculated assuming that $\omega=0$ at the surface. To ensure that the vertical velocity at 100 mb was negligible the divergences had to be corrected. The assumption of

O'Brien (1970) that the divergence error increases vertically as a linear function of pressure was used. Comparison of the mean vertical mass flux generated by this procedure with the observed area mass divergence gave agreement to within 10 per cent. Their results (fig. 4.1) show that even before any significant deep convection developed at 1800 GMT, there was a general ascent at 900 mb of 1 μb/s in the south-eastern half of the array where the band eventually developed. An area averaged ascent rate of 0.5 μb/s (approximately 0.5 cm/s) was present between 800 and 950 mb and this result is supported by Reeves et al. (1979) who show the surface convergence to be 10^{-5} /s . This latter study gives more evidence of large scale forcing in terms of the correlation between the mean 700 mb vertical velocity on the B and A/B scales measured independently. All the ascent episodes on the B scale are matched by increases in the mean A/B scale ascent including that observed late on 3rd Sept. Thus, even on the A/B scale of 700 km, there was evidence for non-convective forced ascent prior to the development of the band.

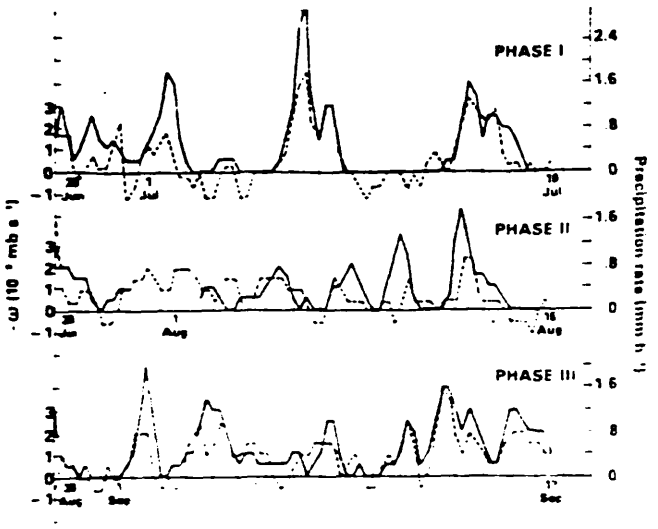
The time series of 700 mb vertical velocity of Reeves et al. (1979) (fig. 4.2) shows that until very late on 3rd Sept there was mean subsidence. However, there is a longitudinal dependence introduced by the traveling nature of large scale disturbances and 100 km to the east of the array's centre it is likely that the mean ascent set in several hours earlier than the time series indicates.

Frank (1978) in a composite study (fig. 4.3) shows that before convective growth there is a distinct low-level ascent of 0.5 cm/s averaged over the B scale area. Reeves et al. also show that there is an almost constant background meridional ITCZ convergence present in GATE independently of easterly wave convergence. As clouds develop, the vertical velocity maximum remains in the lower troposphere typically for 6-9 hours. Then mid-level divergence gives way to upper level divergence at 250 mb and the mean vertical velocity maximum moves into the upper troposphere. At this stage the B scale ascent profile is dominated by that resulting from deep convective towers.

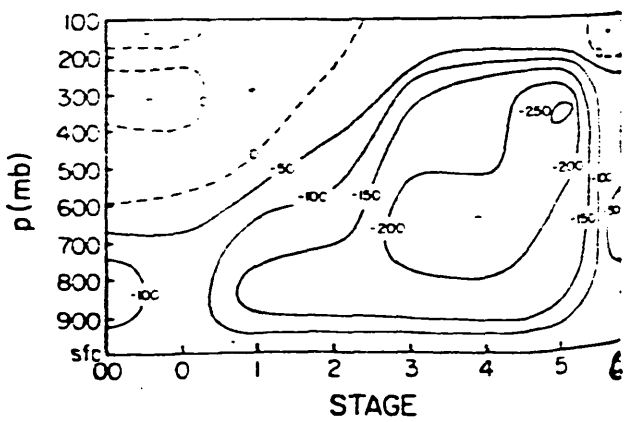
It is almost certain that the convective band being simulated



4.1 Vertical velocity in GATE area (μb/sec) at 900 mb and radar echoes. (Ogura et al., 1979)



4.2 Time series of 700 mb vertical velocity (dashed) and precipitation rate. (Reeves et al., 1977)



4.3 Composite vertical velocity (mb/day) in relation to convective events. Stages 00 and 0 before convective growth. (Frank, 1978)

occurred in the presence of at least 0.5 cm/s forced ascent which is the B scale mean ascent rate at the time. Several factors are likely to enhance this value locally such as easterly wave flow patterns and possibly vorticity conserving motion near a jet maximum. The erosion of the inversion in the neighbourhood of Researcher and Oceanographer seems to support this fact.

4.3 Easterly Waves

4.3.1 Easterly Waves in GATE

In the summer months the wind direction varies fairly periodically with a time scale of 3-4 days in the tropical Atlantic region. The basic flow remains easterly but the strength and meridional wind component change in a well-defined way. The meridional component becomes northerly as the easterlies increase and southerly as they decrease. The depth of the atmosphere over which this change occurs is about 8 km, being most marked at 4 km, the height of the strongest easterly wind. These waves have a typical length of 2000-3000 km and a phase speed of around 10 m/s as they move westwards from the African continent.

Several studies, including those by Thompson et al. (1979) and McBride and Gray (1974) have shown convective activity to be modulated by easterly wave passages. The GATE program has shown that there are periods during which the whole region is convectively suppressed and others where the radar echoes dominate demonstrating the importance of large scale influences on tropical convection. During Phase III of GATE (Aug 30 - Sep 18) the relation between easterly wave phase and precipitation is more strongly correlated than in Phases I and II and the easterly waves themselves are also more active.

Although a connection between easterly waves and precipitation exists it is far less explicit than that between mid-latitude cyclones and their associated rain patterns. In mid-latitude systems there are regions of large scale vertical motion of warm, moist air especially at the fronts where two air masses of different temperature meet.

This vertical motion is important to the dynamics of mid-latitude systems where the conversion of mean available potential energy to eddy kinetic energy is the primary process. However, in the eastern tropical Atlantic horizontal temperature gradients are too small for potential energy to be a source of wave energy and the basic motions in these waves are barotropic. Whereas in mid-latitudes much of the precipitation is a direct consequence of the motion of a large scale system, tropical precipitation is all the result of deep convection with the large scale motion playing a comparatively minor role once the convection has developed. As easterly waves are mainly barotropic, their associated vertical motions are only a consequence of the secondary circulation resulting from vorticity conservation. Alone this ascent is too small to saturate environmental air but a major theme of this thesis is the importance of this background ascent during cloud development. This vertical motion is probably a primary link between the convective and easterly wave scales. Later it will be seen that another link could be the way that horizontal advection by the waves affects the mid-level humidity which in turn has an influence on clouds. The clouds' behaviour is also dependent on the large scale wind shears associated with these waves.

4.3.2 The Origin of Easterly Waves

It is generally considered that easterly waves are closely associated with the African Easterly Jet (AEJ) found at a height of 4 km and originating over the African continent between the Sahara Desert and equatorial Africa. In support of this connection is that easterly waves have a maximum amplitude at the 4 km level and at the same time of year as that when the jet reaches its maximum strength.

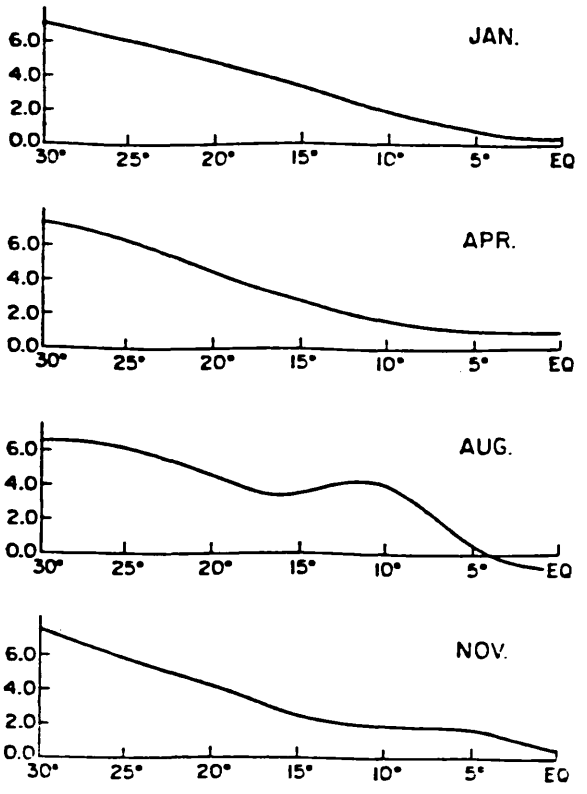
The jet maximum is approximately 25 m/s and is usually at 10-15 N. It has been studied by Burpee (1972), who concludes that its origin is a thermal wind response to a sharp temperature gradient. During the summer, the Sahara region lower troposhere reaches a temperature which is 10 K warmer than that over the equatorial forested part of Africa. This difference exists across a latitude band only 5 degrees wide. To the south the air is cooler and much

moister as it comes directly from the Atlantic in the westerly low-level summer monsoon flow. Over the Sahara the air is constantly heated by the high surface temperature and remains very dry. Thus a reverse temperature gradient builds up and persists for several months in the lower troposphere. The response of the tropical atmosphere to such a persistent forcing is similar to that in mid-latitudes in producing a wind shear perpendicular to the thermal gradient. Although the tropical atmosphere is normally considered to be very ageostrophic, it can still produce a geostrophic-like response if the time scale of the pressure gradient is sufficiently long compared to the inertial period at that latitude. At 15 N this period is about 4 days which is much less than the thermal gradient's lifetime and is similar to the time a westward moving parcel of air experiences the temperature gradient. However, in considering moving pressure patterns such as those caused by easterly waves the geostrophic approximation cannot be made because the inertial period is too long as a result of the small value of the Coriolis parameter, f. The pressure gradients also tend to be much less than in mid-latitudes due to the small ambient temperature gradients over the oceans.

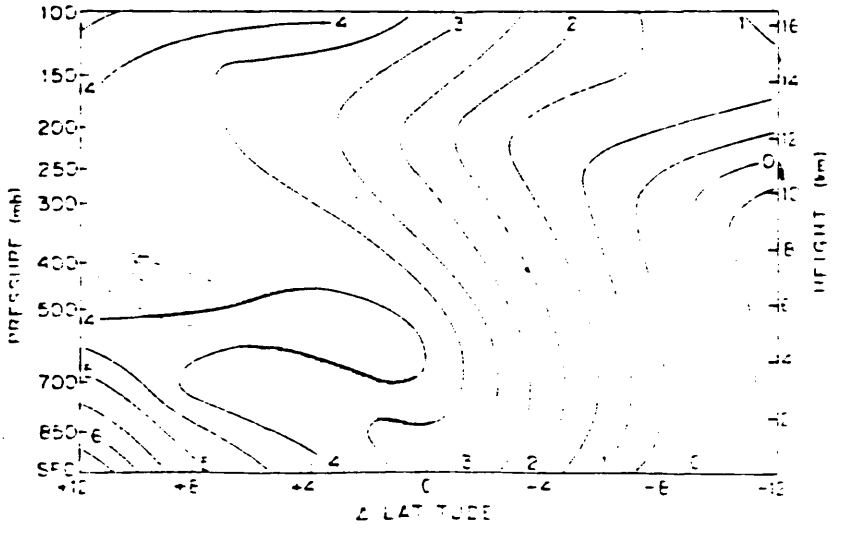
Thus the formation of the jet seems to be accounted for by the above arguments. However, the cause of the waves requires an explanation in terms of the stability of the flow with this jet embedded in it. Burpee (1972) has put forward a now generally accepted view that easterly waves owe their existence to a joint baroclinic-barotropic instability of the easterly flow pattern when a jet is present. As has been noted, the baroclinic process, whereby ambient potential energy is released, is known to be relatively unimportant in the tropical oceanic region. Although a large temperature gradient exists over the continent and is responsible for the initial formation of the jet, the jet itself persists over the ocean in the absence of this temperature gradient possibly because of the long inertial response period of the air to changing pressure gradients as the air moves from continent to ocean. Barotropic instability is probably, therefore, the more important mechanism in the generation of these waves. Its importance in fluid dynamics has been known for several decades and Kuo (1949) first applied it to

atmospheric dynamics. In its purest fluid dynamical form barotropic instability occurs only when an inflection point exists in the horizontal velocity's profile. I.e. $\partial^2 u/\partial y^2 = 0$, where y is the horizontal direction perpendicular to that of the flow which has velocity u(y). Lin (1945) gives a physical interpretation of this instability as follows.

An inflection point in the velocity profile is an extremum in the vorticity profile. If the vorticity in a region changes monotonically it can be shown that a perturbed vortex experiences an acceleration towards its initial position and the vorticity has a tendency to remain stratified. However, if a vortex is perturbed past an extremum it will not be accelerated back and it is possible for a disturbance to persist and amplify under these conditions. Kuo (1949) applies this idea to the atmosphere where instead of vorticity extrema it is absolute vorticity extrema that are necessary for instability. Absolute vorticity is conserved by air parcels in a barotropic atmosphere and is defined by $\zeta+f$. This can be further extended to an atmosphere with temperature gradients where it is potential vorticity gradients that are important (Charney and Stern, 1962). However, a plot of mean potential vorticity against latitude in the tropics is very similar to one of absolute vorticity demonstrating the relative unimportance of temperature gradients. Rennick (1976) and Reed et al.(1977) show the way absolute vorticity varies with latitude and height (fig. 4.4a,b). These plots show that in the summer the strong easterly jet has a significant effect on the latitudinal profile of absolute vorticity. To the south of the jet maximum there is a vorticity maximum at about 10 N. This only exists in the summer and is most marked at a height of 3 km where the easterly jet is strongest. Thus it seems probable that the strengthening of the easterly jet which results from a strong reverse temperature gradient over the African continent is sufficient to destabilise the atmosphere to barotropic instability. Rennick (1976) shows in a numerical model that waves generated by this instability have a similar scale to that observed. Their effect is to broaden and weaken the easterly jet by transferring easterly momentum down-gradient and hence they tend to stabilise the velocity profile.



4.4a Absolute vorticity ($x10^{-5}$/sec) versus latitude at 5°E, 700 mb. (Rennick, 1976)



4.4b GATE Phase III mean absolute vorticity ($x10^{-5}$) for 10°E-31°W. (Reed et al., 1977)

4.3.3 Flow Associated with Easterly Waves

Easterly waves are basically barotropic in that vertical structure and motions are unimportant to their transport properties. This is particularly true in the Eastern Atlantic where it will be seen that ascent possibly removes eddy kinetic energy (in contrast to baroclinic waves). The most important feature of these waves is their transport of easterly momentum horizontally away from the 700 mb jet maximum such as to tend to stabilise the mean easterly flow with respect to barotropic instability. Thompson et al. (1979) show northerly and easterly perturbations ahead of the trough and southerly and westerly perturbations to its east in a composite GATE easterly wave. This shows that the streamline trough tilts from south-west to north-east as is characteristic of a region where easterly momentum is transported southwards. This is consistent with the GATE area's location to the south of the mean jet maximum (about 12 N).

Easterly waves propagate westwards at approximately 8 m/s and are therefore often slower than the air at jet level (600-700 mb) which can move at 20 m/s. Thus in the region ahead of a trough (i.e. to its west), there is a significant mass of air overtaking the wave. At lower and upper levels the wave overtakes the environmental air. In this situation potential vorticity considerations necessitate the existence of a secondary circulation involving vertical motion forced by the wave. Mid-level jet air gaining on a wave ridge has to decrease its absolute vorticity for two reasons. Firstly, because it is approaching a region of relative anticyclonic vorticity ($D\zeta/Dt<0$) and the easterly wave is considered comparatively steady on this time scale and secondly because it is moving southwards to where the Coriolis parameter is less ($Df/Dt<0$). Thus the absolute vorticity of mid-level air decreases but since potential vorticity is conserved this air undergoes horizontal divergence. This will have the effect of forcing lower and upper level compensating convergence to the west of the trough. In addition convergence at the surface may be forced by a similar mechanism to mid-level divergence. If the wave had been purely barotropic, i.e. had no variation in wind with height, the two effects described above would oppose each other for surface air being

overtaken by the wave trough because $D\zeta/Dt$ is positive and Df/Dt is negative. However, it is observed that the surface strength of the fluctuation in the meridional component of the wind is only about a quarter of that at mid-levels and the position of the confluence line remains north of 9 N throughout the composite easterly wave as presented by Chen and Ogura (1982). Thus, in the southern part of the GATE region Df/Dt is always positive because of the southerly wind at the surface and reinforces $D\zeta/Dt$ ahead of a trough leading to convergence. It is observed that convection is favoured to the south of the surface confluence line rather than on it or to its north (Chen and Ogura, 1982) and this seems to be consistent with the easterly wave forced convergence pattern.

Reeves et al. (1979) show that during suppressed conditions there is upper level subsidence and low-level ascent which indicates a significant mid-level divergence and could be evidence of the dynamical processes above taking place. Their results also show a high variability of mid-level divergence in Phase III though this may be partially accounted for by variable medium cloud activity and its associated cloud top divergence. Another possible mechanism for upper tropospheric subsidence which should be mentioned is the secondary motion associated with the 200 mb Tropical Easterly Jet maximum. Reeves et al. (1979) provide mean profiles of velocity gradients showing that the TEJ is decelerating and the GATE mean 200 mb vorticity is anticyclonic (Reeves et al., 1979). This is indicative of upper level convergence being forced in the right front quadrant of the jet maximum (Riehl, 1954). The TEJ is a quasi-stationary feature associated with the African continent. Air to its north becomes gradually less anticyclonic as it moves westwards ahead of the jet maximum and hence has to converge to conserve potential vorticity. However, the results of Reeves et al. show that the mean divergence at this level over GATE is positive but very variable. This is probably associated with cloud top divergence which dominates the mean but during suppressed periods it is possible that convergence associated with the TEJ could produce upper level subsidence in this region.

Thus there are three possible mechanisms which may account for

the upper level subsidence frequently observed in GATE convectively suppressed conditions. It may be a response to mid-level divergence associated with motion of the easterly jet at 600 mb relative to the easterly waves, it may be a continuous background feature resulting from the positioning of the GATE array below the right front quadrant of the 200 mb jet maximum where there is a tendency for convergence or thirdly it could be a compensating response to convective ascent at other longitudes. Note that mid-level divergence of a significant magnitude could be forced by motion relative to the mid-level jet maximum but the data resolution makes it difficult to determine its position as a function of time. The possibility of jet maxima providing a mesoscale destabilisation mechanism has been discussed by Beebe and Bates (1955) in connection with tornado-producing storms.

4.3.4 Energetics of Easterly Waves in the Eastern Atlantic

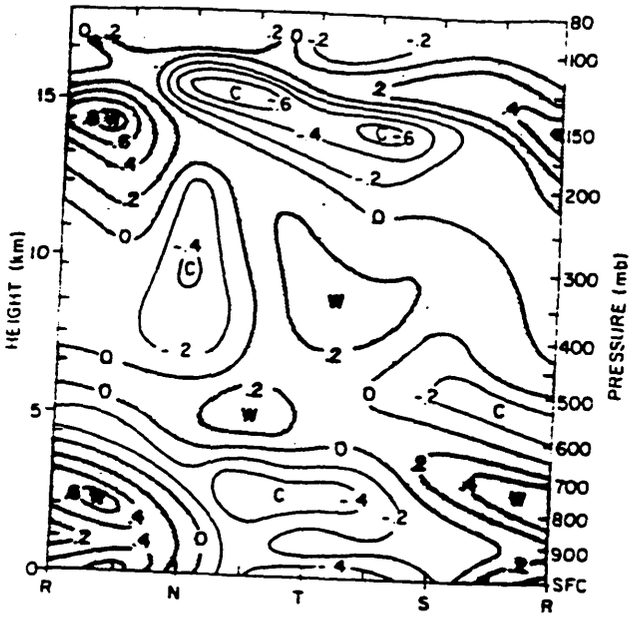
A study of wave energetics by Norquist et al. (1977) indicates that eddy kinetic energy is generated primarily by barotropic processes in this region, i.e. it is converted from mean zonal kinetic energy rather than from potential energy. This contrasts with waves in the W.Pacific and Africa as noted by Thompson et al. (1979) and Norquist et al. respectively. In these regions waves seem to derive their kinetic energy mainly from the conversion of eddy available potential energy in clouds and diabatic (latent) heating. Thus these large scale systems in the Atlantic seem to be energetically different from those elsewhere in being sustained by the available kinetic energy generated over Africa rather than by condensational heating and buoyant acceleration. Studies by Chen and Ogura (1982) and Thompson et al. show that the mean ascent is correlated with unbuoyant air in their GATE easterly wave composite trough on the cluster (B) scale. This implies that the ascent is forced. It therefore appears that the cloudy region in GATE is a sink of eddy kinetic energy in contrast to Africa and the Pacific where eddy kinetic energy is generated by the positive correlation between mean temperature and vertical motion.

However, it may be misleading to interpret the correlation

between θ' and w in the GATE area because it is likely that ascent is concentrated in small updraught cores of warm air and hence there is a large unresolved eddy contribution to these correlations which could possibly even reverse the sign. Hence, although it can be said that kinetic energy is not generated on the cluster scale in the GATE region it is possible that it is generated on the scale of updraught cores. The major source of the large scale difference in behaviour between the E.Atlantic and other regions seems to be the presence of relatively cool air in the trough (fig. 4.5) and ahead of it below 700 mb where there is also a maximum in the mean ascent (fig. 4.6). Evaporative cooling by rain has been proposed by Riehl (1954), Thompson et al. (1979) and Chen and Ogura (1982) as a mechanism by which air can cool in the presence of strong precipitation. This idea, however, seems to conflict with the observation that condensation dominates over evaporation at these levels. Horizontal advection would be unimportant because of the negligibility of horizontal temperature gradients over the GATE oceanic region. The size of this observed cooling is very small in comparison with the mean latent heating which is almost cancelled by mean ascent cooling (Thompson et al., 1979). From this cancellation it can be concuded that most ascent in the GATE region is saturated. However, the presence of a 10 per cent residual may indicate a small amount of dry low-level ascent existing in the initial stages of convection. This implies an external forcing of GATE ascent which may result from either the Hadley circulation or easterly wave dynamics.

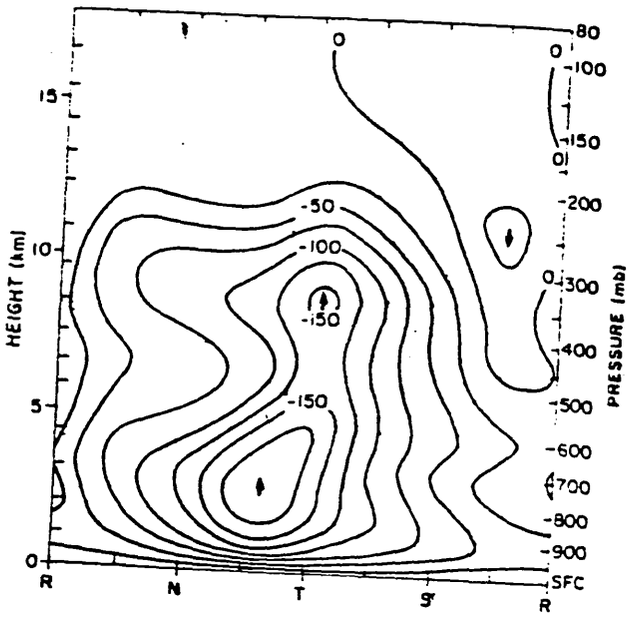
The low-level cold core is relatively less important in Africa and the W.Pacific because these have a maximum of vertical velocity in the upper troposphere which is correlated with warmer air. This overcomes the effect of the low level negative correlation providing a net generation of eddy kinetic energy.

Note that a low-level negative correlation between ascent and warming which is observed in all ITCZ regions may be evidence for large scale convergence aiding initial convection. As the environmental temperature falls because of large scale ascent, updraughts become more buoyant and active and increase the net

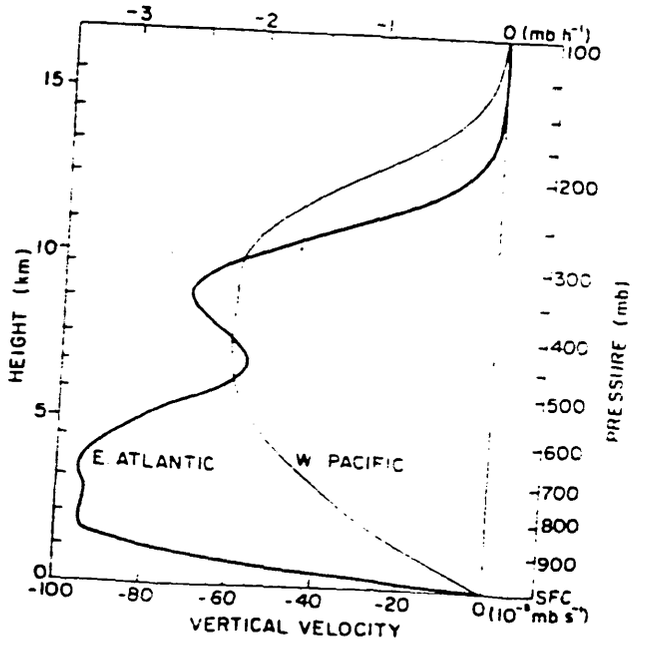


Vertical cross section of temperature deviation (°C).

4.5 Easterly wave composite temperature deviation. (Thompson et al., 1979)



4.6 As 4.5 for vertical velocity (mb/day).



4.7 Mean Phase III vertical velocity profile in B-scale area compared to W. Pacific. (Thompson et al., 1979)

vertical mass flux.

Kung and Burgdorf (1978) show that on the GATE A/B scale (5 deg) there is a positive correlation overall between ascent and warming. This may be support for the idea that large scale ascent cooling occurs mainly in the B scale (2 deg) cluster region itself where the convergence is concentrated. If compensating subsidence associated with these clusters occurs on the A/B scale the sign of the overall correlation could be reversed provided that the subsiding air is cooler than the time mean, i.e. it has previously been subjected to large scale ascent or radiative cooling. Unfortunately, there is insufficient data to test this hypothesis.

The weakness of the upper tropospheric maximum in mean ascent (fig. 4.6) and presence of a strong mid-level divergence in the E.Atlantic is the primary reason for the overall negative eddy kinetic energy generation. This may be because the E.Atlantic is a less favourable region for convection partially as a result of the strong low-level shear below the African Easterly Jet. This shear is especially pronounced ahead of easterly wave troughs where convection tends to develop. Also, because of coastal upwelling, the sea surface temperature is generally less than in the W.Pacific where convective towers therefore tend to be higher because of the lower stability of the surface air with respect to moist ascent (fig. 4.7). During convective periods the E.Atlantic vertical velocity profile shows mean maxima at 750 and 350 mb with a relative minimum above the jet level, 600 mb. This is a distinctive feature of this part of the ITCZ and shows two cloud populations with outflows at mid and upper levels. The mid-level divergence may be associated with clouds which are unable to penetrate the high shear layer. There is enough CAPE for the surface air to ascend buoyantly well above this level in the absence of shear. The only mechanisms by which this available energy can be reduced significantly in its conversion to ascending kinetic energy are (i) the dynamical pressure gradients resulting from ascent in a horizontal shear opposing the buoyancy and (ii) liquid loading becoming sufficiently high to decelerate the warm air. Though the latter may contribute to the weakening of updraughts because of the

high moisture content of low-level tropical air, it cannot alone account for the difference between Pacific and E.Atlantic convection since the Pacific boundary layer is equally moist. A run of the numerical model without any shear shows that a far stronger updraught can exist than in the case where the observed shear is imposed and thus it is probably the shear which distinguishes these two regions' ascent profiles.

4.4 The Inter Tropical Convergence Zone

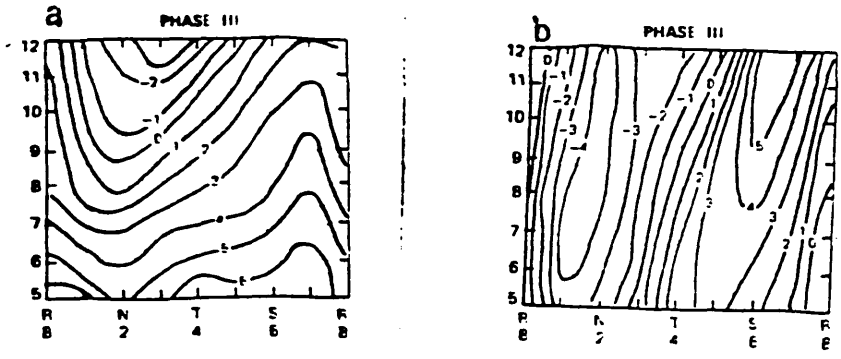
Tropical Atlantic convection is concentrated in a region which has a latitudinal extent of 5 degrees and forms part of the ascending branch of the Hadley circulation. The width of this convective area is typical of the whole equatorial region and on time mean satellite images over a few days it is usually easily discernible as a cloudy band parallel to the equator. This is known as the ITCZ and is at the latitude where trade winds at the surface from both hemispheres converge. The height of the converging layer is quite sharply defined in observations as about 1500 m in the GATE area. As the trade wind air moves equatorwards it is continuously moistened and heated by the surface so that when the two air masses meet both have very similar thermodynamic properties. It is observed that the position of the ITCZ shifts several degrees with season such that the trade winds from the winter hemisphere have a longer contact with the surface enabling them to come into equilibrium before reaching the ITCZ. Riehl and Malkus (1958) note that the updraught mass flux in the ITCZ is similar to the mass convergence in the lowest 2 km of the trade winds. However, only the lowest kilometre is capable of buoyant ascent in updraughts so an important part must be played by shallow downdraughts bringing air from 1-2 km to the surface where it can be modified by surface fluxes until it is sufficiently unstable to ascend to the upper troposphere.

In the E.Atlantic the ITCZ is situated around 10 N in the summer but, as shown by Chen and Ogura (1982) in fig. 4.8a, its position is modulated by easterly waves between 9 N and 12 N (as defined by the surface confluence line). The meridional wind in easterly waves has

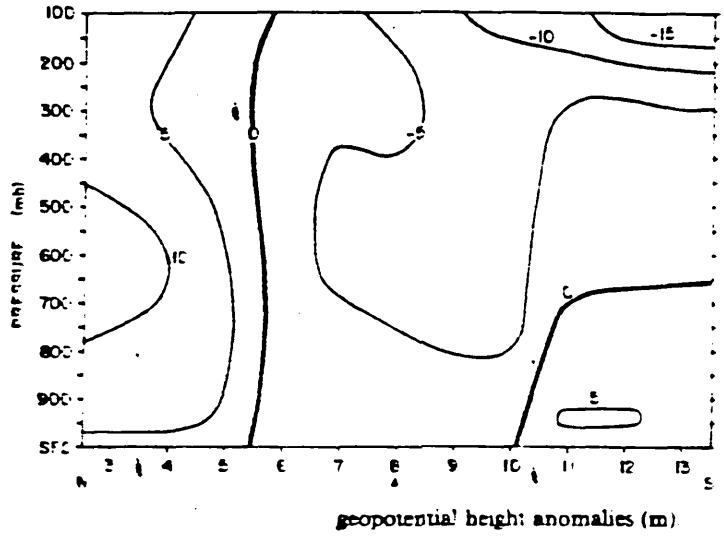
the strongest variation at 600-700 mb, the jet level (fig. 4.8b). At this height this component reverses during wave passages. The effect of waves at the surface is smaller and is combined with the continuous large scale confluence. This has the net result that the confluence line itself shifts but stays within the GATE region (5 N to 12 N) and in the southern part of the area the wind remains southerly but varying in strength with wave passages. Estoque and Douglas (1978) and Chen and Ogura (1982) give evidence that there is a precipitation and vertical velocity maximum situated 100 km to the south of the GATE confluence line and this seems to move northwards ahead of easterly wave troughs with the confluence region. In this ascending air the mean southerly component of the surface wind is about 3 m/s with a northerly shear component at low levels. The existence of this shear perpendicular to the easterly jet is probably important in the organisation of convection into quasi-stationary bands as will be seen later.

Estoque and Douglas (1978) have shown that the region of ascent and precipitation is not associated with a warm perturbation from the north-south mean in the E.Atlantic upper troposphere whereas in other tropical regions there is evidence of a warm core overall. This lack of correlation between ascent and warm air is important because it demonstrates that GATE ITCZ convergence may not be aided by large scale convection and must be produced by some other mechanism. In other tropical regions warm air is correlated with ascent and a feedback mechanism operates whereby eddy kinetic energy is generated from eddy available potential energy and the convergence resulting brings more unstable surface air into the convective region.

The above observations indicate that convective feedback does not operate to provide convergence in the E.Atlantic ITCZ. Estoque and Douglas suggest that this convergence must therefore depend on another process such as barotropic instability or 'pressure energy flux'. The former is easterly wave convergence which has already been discussed. The latter is the effect of descending cooler air in the subtropical part of the Hadley cell. If the latter is the case, the Hadley cell can be seen as being driven by convection in parts of the ITCZ where



4.8 Meridional wind component at (a) surface and (b) 700 mb for easterly wave composite. (Chen and Ogura, 1982)



4.9 ITCZ composite height anomalies. (Frank, 1983)

convection generates convergence, but acting to drive convection in other ITCZ areas where the stability of the atmosphere to deep convection inhibits the growth of cells. In these latter regions which include the E.Atlantic, convection is restricted in its ability to provide large scale convergence by such effects as those of high shear and relatively low surface temperatures. The prominence in the mean E.Atlantic divergence profile of a mid tropospheric maximum supports this idea. Medium height clouds with outflow at about 4 km are not active enough to produce large scale convergence. Therefore, the existence of these clouds could be an indication that large scale forcing is present and it is hence likely that any other regions of the ITCZ with a strong divergence maximum in the mid-troposphere are similarly forced by the Hadley circulation and/or barotropic waves.

A more recent study by Frank (1983) indicates that the ITCZ in the E.Atlantic may, in fact, be warm core. The composite in this work was centred on the latitude of strongest convection and showed that the time mean convergence into this part of the ITCZ is distinctly down the mean meridional pressure gradient (fig. 4.9), hence generating kinetic energy. The mean ITCZ pressure determined by Frank has a relative surface low and upper high which aids a direct circulation and is consistent with higher temperatures in the convective region.

This finding does not detract from the idea that large scale forcing is required to account for the observed mean convergence when high clouds are absent from the GATE area; it shows that the average easterly wave provides net convergence through the correlation between latent heating and ascent in the trough.

In conclusion it can be said that the initial development of convection occurs in the presence of easterly wave and Hadley cell forced convergence. Following the growth of clouds into the upper troposphere, Frank's results demonstrate that convection is capable of maintaining convergence through convective feedback in the E.Atlantic ITCZ.

CHAPTER 5
NUMERICAL SIMULATION OF BAND CONVECTION: PART II - INCLUDING LARGE SCALE INFLUENCES

5.1 Introduction

Having established from observation, the theory of tropical easterly waves and the dynamics of the Hadley circulation that surface convergence probably exists independently of that produced by convection, it is necessary to include this effect in the mesoscale simulation.

In this chapter the methods of imposing larger scale motion on the numerical domain will be discussed. Several authors have already done work in this field and nearly all have taken different approaches to the problem. These will be compared and the primary method used in this study will be introduced. The physical factors governing convection in large scale convergence and the sensitivity to the degree of imposed ascent will be evaluated from modelling results. A detailed description of the band's structure and its effect on large scale transports will be left to the next chapter.

5.2 Large Scale Ascent in Numerical Models

5.2.1 Review of Methods of Imposing Large Scale Motion

The inclusion of the interaction of the domain scale with larger scales in numerical modelling is always problematical because of the important part played by the boundary conditions. These have to be capable of maintaining large scale forced motion whilst simultaneously allowing domain scale disturbances to propagate through without reflection. Another situation in which a problem arises is the case of mean convergence produced by convection in the domain in addition to that forced by larger scale dynamics. Here, there is no way of distinguishing the two scales of motion at the boundaries so the boundary conditions are insensitive to the difference between domain produced convergence and background forced convergence and hence may

allow the latter to decay or grow.

An illustration of this is given by Chen and Orville (1980), who descibe an earlier simulation, Chang and Orville (1973), where the effects of large scale convergence are imposed in a streamfunction/ vorticity 2-dimensional model in the following manner. Having specified the initial horizontal velocity profile's streamfunction, a symmetric convergence field producing a uniform ascent rate across the domain is added with a maximum vertical velocity of 6 cm/s at mid-levels. The model is then allowed to run normally but the mesoscale convergence is not maintained at its initial value. Chen and Orville ascribe this to a deficiency in the boundary conditions and adapt the model to keep the mesoscale convergence field constant with time. This is done by the addition of a constant ascent streamfunction to the model predicted values and using the resultant velocity field for advection.

As well as Chang and Orville (1973), several other authors impose mesoscale convergence only through the initial velocity profile and do not attempt to continuously maintain its effect. Tripoli and Cotton (1980) employ a dynamic initialisation in a 3-dimensional simulation of deep convection initiated by a sea breeze in S.Florida. The scale of convergence within the domain is varied such that the initial ascent is concentrated in a specified area. Schlesinger (1982) also included initial convergence in a simulation of a severe Oklahoma storm in three dimensions.

A distinctly different method of forcing is employed by Kreitzberg and Perkey (1977) who, in a two dimensional study of mesoscale rain bands, apply convergence continuously through the horizontal velocity component transverse to the domain (cf Chang and Orville, 1973, where convergence is applied within the plane of the domain). To avoid boundary problems all the fields are damped at the lateral boundaries where there is no vertical velocity. However, the influence of this boundary condition on the results limits the length of the time integration.

Another way of including the effects of large scale ascent was that of Soong and Ogura (1980). In a 2-dimensional simulation of trade wind cumuli and another of deep tropical cumuli (Soong and Tao, 1980), they add a large scale vertical advection term based on the observed mean vertical velocity and the model predicted mean vertical temperature or moisture gradient at each level. Thus the additional term is horizontally uniform but approximately represents the effects of large scale ascent on the model domain scale. Initially the imposed vertical velocity was time dependent, being based on the variation of the observed ascent profile with time but in a later simulation (Ogura, 1982) this was kept fixed at its initial value. The reason for making this change was that it was considered that the time variation in the profile was primarily due to the effects of deep convection itself on the mean vertical velocity. It is thus unrealistic to include this in the large scale forcing term and this raises an important question in choosing how much forcing to apply to a model. When deciding from observations whether and how much mean ascent is forced by non-convective motion care must be taken not to include the component of mean ascent accounted for by clouds because this is already represented in the model explicitly. Therefore one can only be confident that non-convective convergence is present if there already exists a large scale ascent prior to deep cloud development.

Another method conceivable for representing ascent is to modify the initial thermodynamic sounding by an amount consistent with, for instance, an hour's ascent so that convection can take place in conditions more representative of the destabilised atmosphere resulting from a continuous imposed low-level convergence. This modified sounding would generally have more CAPE because this is supplied by the forced ascent and thus represents, properly, the available potential energy increase provided by large scale motion.

There may also be more complicated procedures for putting in large scale motion with a boundary condition on the pressure field. An increase from the hydrostatic value of the low-level pressure at the boundary and a corresponding decrease at upper levels would tend

to force low-level convergence and divergence aloft. However, in employing this method care must be taken that the imposed ascent field is reasonably uniform in the absence of perturbations in the domain as this scheme is sensitive to the behaviour of the model near the boundaries. In practice it could be difficult to have a simple boundary condition on the pressure which forces a uniform steady convergence. A boundary condition on the velocity in which the initial convergence is kept constant with time is also impractical because it does not allow cloud scale convergence to build up. In all finite area domains the effects of compensating subsidence around clouds tends to extend beyond the boundary and thus the surface convergence at the boundary should be allowed to increase to account for the net vertical mass flux change. If all the subsidence occurred within the domain there would be no change in total vertical mass flux when convection develops and it may be realistic, in this case, to impose the large scale velocity convergence at the boundaries but this would require a rather large domain.

In conclusion, the methods used by modellers so far of imposing large scale ascent fall into two categories. There are those such as Chang and Orville (1973), Schlesinger (1982) and Tripoli and Cotton (1980) who apply convergence only as an initial condition and let the model run as normal and there are those such as Chen and Orville (1980), Kreitzberg and Perkey (1977) and Soong and Ogura (1980) who continuously apply the effects of convergence throughout the simulation. Another point in which modelling is divided is whether to apply the convergence uniformly as is done by most or to have it varying horizontally within the domain (e.g. Tripoli and Cotton, 1980). This latter choice depends upon which large scale effect one is trying to represent. Tripoli and Cotton simulate convergence provided by a mesoscale sea breeze front which is likely to be fairly concentrated in comparison with that produced by synoptic scale motions justifying their line of approach.

5.2.2 Review of Results of Past Models

Chang and Orville (1973) apply a mesoscale ascent rate with a maximum of 6 cm/s between 1 and 5 km above the surface. Above this there is a divergence layer extending to 17.5 km. They find that this large scale forcing can produce much larger and more vigorous clouds accounting for the strength of some observed severe storms in the Great Lakes region. The forcing is attributed to upper air disturbances and mesoscale surface inhomogeneities providing upper divergence and lower convergence respectively.

Chen and Orville (1980) found that synoptic convergence sufficient to produce a mesoscale ascent rate of 30 cm/s between 2.4 and 5.4 km was present prior to the 1972 Black Hills flood and include this forcing in their model. In another case with an initial inversion which is also sometimes present before the occurrence of severe storms (e.g. Rapid City, 1972 and Big Thompson Canyon, 1976) the imposed ascent was sufficient to destabilise the atmosphere so that strong, deep convection could occur. In general random impulses developed into larger deeper clouds with ascent than without.

Kreitzberg and Perkey (1977) simulate extra-tropical cyclone rainband development in the presence of a 7 cm/s ascent rate imposed between 5 and 8 km altitude. The model represents mesoscale development with a resolution of 20 km. They find that there is a tendency for forced ascent to produce a broader precipitation band than in the unforced case.

Schlesinger (1982) in a three dimensional study of severe storms finds that convergence is required to enable the convective activity to persist in a steady state without decaying.

Tripoli and Cotton (1980) simulate deep convection in sea breeze convergence which is concentrated within the domain and reaches a maximum horizontal mean magnitude of 14 cm/s at 750 mb with divergence up to 4 km. The kinetic energy is found to increase with convergence in sensitivity tests where the ascent rate is varied up to 3.5 times

that observed.

Soong and Tao (1980) and Ogura (1982) apply low-level convergence to a GATE sounding, successfully simulating deep convective development which is forced by an ascent rate of 1-2 cm/s below 3 km. Without such ascent clouds were found not to develop above 600 mb which is much lower than the observed cloud top height at the time of the sounding. Another study by Soong and Ogura (1980) shows that large scale subsidence of about 1 cm/s in the lower troposphere is sufficient to produce and sustain a strong inversion in the presence of cumulus activity.

5.3 Numerical Simulation with Imposed Ascent

5.3.1 Method of Imposing Ascent in Band Simulations

The method adopted is most closely related to those of Soong and Ogura (1980) and Chen and Orville (1980) described in the previous section. It was considered that imposing the effects of ascent continuously during the simulation was more realistic because if this is not done the equilibrium state of the modelled atmosphere would be one of no ascent. In the absence of convection the simulation would tend towards this background rest state rather than that of large scale convergence. This is because the model equations do not retain any information on the initial state whereas in reality the domain scale atmosphere is continuously affected by large scale convergence. Later in this chapter simulations in which convergence is only applied initially will be compared to these continuous convergence cases.

The main assumptions are that the time and space scales of the imposed convergence are both much larger than the model's. Hence, a steady horizontally uniform ascent is applied by adding a mesoscale term to the model predicted fluxes of heat and moisture. The mesoscale velocity field is analogous to the time-independent streamfunction added by Chen and Orville (1980) and satisfies the continuity equation. Convergence and divergence are assumed to occur in the meridional plane as is consistent with the observations of

surface convergence by Reeves, Ropelewski and Hudlow (1979). Thus the meridional component of the total surface wind varies linearly from north to south but this variation of up to 0.5 m/s is small compared to the magnitude of the surface wind so its direction changes minimally across the domain. The initial zonal component is constant throughout the domain.

Thus the equations for heat and moisture take the form:-

$$\frac{\partial \phi}{\partial t} = -\nabla_p \cdot \underline{v}\phi + Q + D + F_m \qquad \text{(Eq. 5.1)}$$

$$\nabla_p \cdot \underline{v}\phi \equiv \frac{\partial}{\partial x} u\phi + \frac{\partial}{\partial y} v\phi + \frac{\partial}{\partial p} \omega\phi \qquad \text{(Eq. 5.2)}$$

where $F_m \equiv -\nabla_p \cdot \underline{v}_m \phi$ is the mesoscale induced flux

and $$\frac{\partial u_m}{\partial x} + \frac{\partial v_m}{\partial y} + \frac{\partial \omega_m}{\partial p} = 0 \qquad \text{(Eq. 5.3)}$$

$\underline{v}$ is the model predicted velocity field, Q is the source term, D is subgrid scale diffusion, ϕ is θ or q, q_c, q_r. The mesoscale velocity $\underline{v}_m$ is constant with respect to time, u_m is zero, ω_m is horizontally uniform with a specified vertical profile and v_m varies in such a way as to satisfy continuity, being zero in the centre of the north-south section.

The essential difference between this scheme and that of Soong and Ogura (1980) is the use of the flux form, $\nabla_r \cdot \underline{v}\phi$, in the mesoscale advection which ensures that the total heat and moisture are conserved by advection. The advective term employed by Soong and Ogura is effectively a source of moisture and a sink of heat and overall conservation is not achieved in their domain. Another major difference is that the scheme used in this work represents the effects of large scale ascent locally rather than applying a horizontally uniform large scale term as is done by Soong and Ogura. Hence the

mesoscale ascent cools the air at a rate proportional to the local vertical potential temperature gradient rather than the domain mean gradient.

The dominant term in the expansion of F_m if the domain is considered as a whole, is the vertical advection term, $\omega_m \partial\phi/\partial p$. The other advection terms are small in the horizontal mean and terms such as $\phi \frac{\partial \omega_m}{\partial p}$ are cancelled by continuity. Hence, the general effect of the applied mesoscale flux term is that of a horizontally uniform vertical advective velocity with a specified vertical profile.

5.3.2 Imposed Ascent and Momentum

It should be noted that the scheme of adding mesoscale fluxes to the model predicted values does not include their effect on the momentum equation. There are several reasons for this omission.

Firstly, large scale motion accounts for the strength of the easterly jet and its level in the atmosphere so its properties cannot be considered local to the domain as can temperature and moisture. It is sustained in its position and strength by the effects of easterly waves, the Coriolis force and large scale advection and pressure gradients none of which can be included in the model. The fact that surface convergence and low-level ascent occur may be expected to weaken the easterly flow below the jet through simple vertical advection but observations show that the easterly jet is strengthening at the time the convection occurs. This demonstrates the importance of other omitted large scale forcings in determining the momentum profile in the domain. It would thus be wrong to include the vertical advection by the mesoscale surface convergence without also including the effects of these other forces. In practice, therefore, all large scale forces are excluded and the momentum profile would not change in the absence of domain resolved influences, i.e. clouds.

Secondly, even if large scale ascent was allowed to influence the momentum profile its effect on convection would be rather less than those of ascent on the thermodynamic sounding which is destabilised

providing more CAPE. A reduction in the shear caused by vertical advection of momentum below the jet would aid convection but if the magnitude of this reduction is calculated it is found to be about 0.4 m/s/hr for a 1 cm/s ascent rate and it is difficult to see that such a small change in a 10 m/s wind could have a significant effect.

A third reason for not including the mesoscale flux on momentum was the behaviour of a test run in which it was included. Instead of a reduction in the easterly momentum of the sub-jet layer as might be expected from straight vertical advection, the surface westerly flow reduced in strength. This was traced to a build up of a linear zonal pressure gradient across the domain in response to the forcing. The resulting underestimated surface inflow is detrimental to the simulated system because the moisture supply is reduced below its true value. At the height of maximum shear, forced mesoscale vertical advection almost cancels the model produced pressure gradient and little acceleration occurs at this level. However, as the pressure gradient extends almost unchanged to the surface and mesoscale vertical advection reduces towards the surface, the net effect is a deceleration of the surface westerlies by an uncancelled pressure gradient. Qualitatively, it seems that in the presence of forcing which changes the momentum profile, the model may produce a spurious mean pressure gradient such as to oppose this change at an arbitrary level. In the case described, the level appears to be that at which the momentum would change most rapidly in the absence of such a pressure gradient i.e. that at which $w_m \partial u / \partial z$ is greatest. A simulation with no initial heat perturbation showed no such pressure gradient to develop implying that the effect arises from the amplification of a mode present in the perturbation.

5.3.3 Imposed Ascent and Boundary Conditions

It is always vital in a numerical simulation that the influence of boundary conditions on the time integration is kept to a minimum. The most important such effect is the reflection of gravity waves propagating out from the domain and the radiation conditions described earlier are helpful in preventing this.

In the present simulations with a uniform ascent across the domain a problem arises from using ordinary radiation conditions. To understand this problem, first we consider an undisturbed domain subject to uniform ascent. The gradients of all variables near the boundary are negligible initially but there is a uniform rate of change at all internal points due to vertical advection. Thus, there is a local time derivative but a negligible local space derivative. Hence the estimated phase speed is greater than the CFL speed, i.e:-

$$c = \frac{\partial\phi/\partial t}{\partial\phi/\partial x} \gg \frac{\Delta x}{\Delta t} \qquad \text{(Eq. 5.4)}$$

Under these circumstances the normal procedure employed when applying radiation conditions is to set the new boundary value equal to that one grid point in at the old time step. This is a reasonable approximation unless there is a large scale vertical motion in which case the boundary points would be caused to lag the interior points. The assumption in using radiation conditions is that all changes at the boundary occur as a result of waves moving at speeds less than the CFL speed (60 m/s). However, large scale ascent should also be allowed to change the boundary values even in the absence of a local gradient and radiation conditions have to be modified to account for this.

It can be seen that if nothing is done to prevent this boundary lag there can be a significant impact on the dynamics of the interior domain. The most important effect of this lag is the creation of an unrealistic temperature gradient which, in the presence of ascent, would make the boundary points relatively warm and hence buoyant. This would eventually lead to spurious ascent especially near inflow boundaries and the initially uniform vertical motion would be disrupted purely by boundary effects. Test runs show this to become significant compared to the magnitude of imposed acsent within a few minutes of the start. Another model field in which a time lag would introduce important perturbations is the pressure (height) field. Horizontal gradients are formed at the boundary through the pressure

lagging its hydrostatic value which changes steadily with the temperature. The nature of the pressure field would immediately cause this disturbance to spread into the domain and force non-uniform boundary dependent motion. The momentum component normal to the boundary is also predicted with radiation conditions but large scale ascent is not applied to this field.

In two dimensional modelling the use of periodic boundary conditions as is done by Soong and Ogura (1980) removes this problem. Chang and Orville (1973) have zero gradient conditions but these reflect gravity waves. Kreitzberg and Perkey (1977) damp all waves at the boundaries and apply a reduced ascent rate at points near the boundary. This method leads to horizontal gradients of variables even in the absence of any disturbances and the effects gradually spread into the domain limiting the useful length of the time integration. Tripoli and Cotton (1980) and Chen and Orville (1980) employ Klemp-Wilhelmson radiation boundary conditions in which the gravity wave speed is assumed constant and not calculated locally as in this study. However, the method has the same problems with regard to uniform ascent.

The priority in selecting boundary conditions for this modelling study was that they should not interact with the large scale ascent. To be useful they must allow pressure, temperature, moisture and vertical velocity to remain horizontally uniform in the absence of any perturbations within the domain and hence to test them the forced model was run for several minutes without an initial perturbation. Most boundary conditions currently employed in models would fail this test unless they were periodic, which are unsuitable for 3-dimensional modelling, or zero gradient, which reflect gravity waves. They would produce vertical velocity perturbations comparable with the mean ascent imposed in the first two minutes of the simulation unless precautions are taken to account for steady large scale trends.

5.3.4 Modified Boundary Conditions

It has been shown that radiation conditions cannot cope properly with changes in the domain which occur in the absence of horizontal gradients and will produce a lag which can have important dynamical effects on the results.

The modified boundary condition is to time extrapolate for the new boundary value when the horizontal gradient is small, i.e. when:-

$$|c^*| = \frac{\Delta t}{\Delta x}\left|\frac{\partial\phi/\partial t}{\partial\phi/\partial x}\right| > 1 \qquad \text{(Eq. 5.5)}$$

If the effective wave phase speed, c^*, is less than unity and outwards at the boundary, normal radiation conditions are applied whereby normal advection at the speed $c^*\Delta x/\Delta t$ is assumed.

For a negative c^* less than unity, zero gradient conditions are applied.

The time extrapolation assumes a linear variation from the past to present to future time step and the future boundary value is assumed the same as that of the first interior point because the horizontal gradient is small.

Thus if

$$\left|\frac{\partial\phi/\partial t}{\partial\phi/\partial x}\right| > \frac{\Delta x}{\Delta t} \qquad \text{(Eq. 5.6)}$$

$$\phi_b^{n+1} = 2\phi_{b-1}^{n} - \phi_{b-1}^{n-1} \qquad \text{(Eq. 5.7)}$$

b: boundary, b-1: first interior point

In the absence of gravity waves such as at the beginning of the simulation the effect of this change is important in preventing the

boundary lag from developing.

If gravity waves are present ordinary radiation conditions can cope reasonably with their effect superimposed on a large scale steady change provided that their length is sufficiently great in comparison with the grid length. The following considerations illustraete this point.

For a long sinusoidal wave propagating through a boundary, the value of c^* calculated will remain approximately constant being independent of phase. However, if the effect of a steady uniform change in time is superimposed on this wave the value of c^* calculated from Eq. 5.5 would vary, typically 10 per cent in the simulations, with phase. It is less ahead of wave troughs and greater ahead of ridges. As c^* is estimated a grid length from the boundary point any such variation with phase would be important unless this length is small compared to the total wavelength. In addition c^* is estimated a time step earlier and it is required that the local phase does not vary too much in one time step. As gravity wave speeds are about 30 m/s and the CFL speed is 67 m/s, these constraints are met because waves move typically half a grid length per time step and their lengths generally are about 15 km (15 grid lengths). Thus the phase change is about 12 deg at a given point per time step and about -24 deg at a given time per grid length. It can be seen that these two errors in the estimation of c^* tend to oppose and, in fact, would cancel exactly for a wave moving outwards at the CFL speed.

Another boundary condition change is required in the initial forward part of the Euler backward time differencing scheme to remove a systematic error that is produced in the presence of a uniform time variation. Normally, the boundary values are left unchanged in the initial forward step but this would result in a lag and a consequent accumulative error in the estimation of fluxes near the boundaries. To prevent this, zero gradient conditions are applied after the initial forward step.

The extrapolative nature of the changed radiation conditions

makes it necessary to use zero gradient conditions in the first time step of the simulation because here the time extrapolation procedure cannot be carried out. As the only perturbation in the domain is initially well away from any boundaries, this is a consistent boundary condition. However, this cannot be done for the pressure (height) field since the boundary values are needed in advance of calculating the interior values. Therefore, the height field is assumed hydrostatic and the boundary values are determined from the density profile. At all later time steps modified radiation conditions are applied to height, temperature, moisture and normal velocity.

The test runs without an initial heat source show temperature deviations, θ', resulting from ascent to vary only 5 per cent across a 10x10 point domain after 8 minutes and this is considered acceptable. The boundary conditions in this modified form are thus capable of sustaining large scale tendencies aswell as allowing gravity waves to propagate through without too much reflection. If the pressure at the boundaries is forced to remain hydrostatic throughout a test run, the variation of vertical velocity across the domain becomes negligible but this boundary condition is unsuitable for a simulation in which gravity waves are produced because of their associated non-hydrostatic pressure fluctuations. This test shows that the 5 per cent temperature deviation variation is mainly caused by the time extrapolation procedure applied to the pressure field but this is a reasonable compromise between properly treating gravity waves and allowing steady ascent.

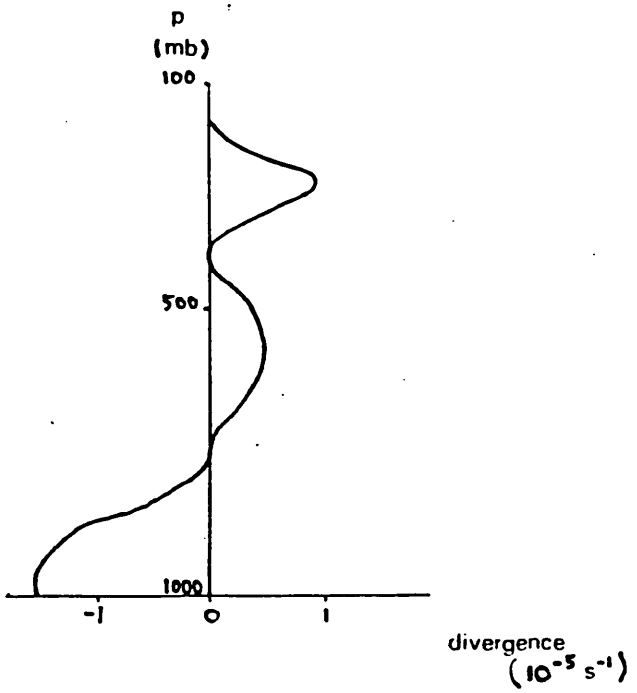
5.4 Magnitude of Imposed Ascent

The wind profiles in GATE are only accurate enough to provide a 400 km resolution in the derived vertical velocity. The results of Ogura et al. (1979) in fig. 4.1 show that the 900 mb ascent rate at 1800 in the south-eastern half of the array was approximately 1 cm/s but it is difficult to determine from this a magnitude appropriate to the domain scale which is a tenth of the resolved scale. However, these results give an indication of the minimum forcing to impose on the simulation.

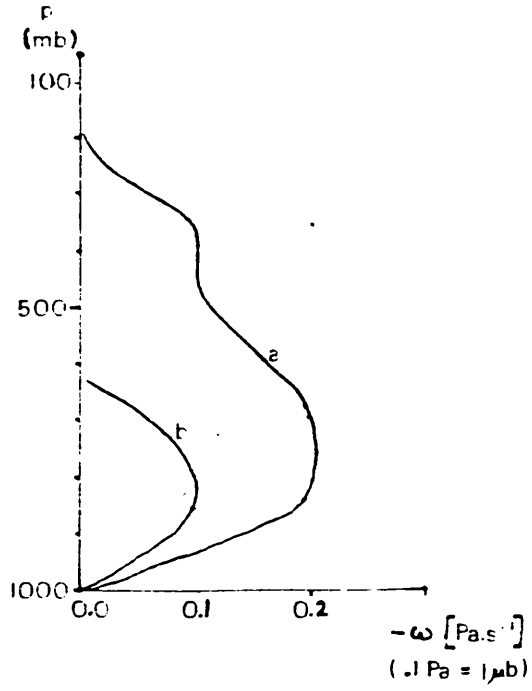
The mean divergence profile presented by McBride and Gray (1978) for the GATE A/B scale area in the convectively active periods (fig. 5.1) could be taken as another estimate for the large scale forcing because it represents motion on the scale of 1000 km. The low-level vertical velocity maximum obtained from this profile is 2 cm/s. The overall GATE mean vertical velocity has a maximum of 1 cm/s at 800-850 mb and hence global scale motions associated with the surface trade wind convergence must provide at least this amount of upward motion in the model domain continuously and possibly independently of resolved convective motions.

The separation of the observed mean behaviour into convective ascent and large scale forced ascent is a central problem in deciding the magnitude of imposed convergence. During periods of active convection the mean ascent in the whole GATE array increases significantly and upper level divergence becomes much larger than that at mid-levels as a consequence of deep cloud top outflow. This shows that convection is not passively influenced by larger scale convergence but provides some large scale convergence itself. Reeves et al. (1979) show that the results from GATE cluster scale ships (B-scale) and large scale (A/B) ships independently produce vertical velocity time sequences with a strong correlation and it can be concluded that the influence of clusters on the large scale convergence is at least as important as that of large scale convergence on cluster development. This implies that in the presence of active convection it is impossible to distinguish imposed ascent from convectively produced ascent since all the large scale upward motion is occurring in cloud updraughts.

The way of isolating the influence of non-convective large scale motion in the observations is to consider only those periods when convection is not contributing to the convergence. Clouds are only capable of providing mean convergence if there is a net latent heating in them which would have the effect of lowering the surface pressure. Steady non-precipitating cumulus convection is thus unlikely to generate convergence because the overall condensational warming and evaporative cooling tend to cancel. The presence of surface



5.1 Divergence profile during convectively active periods in GATE. (McBride and Gray, 1978)



5.2 (a) Vertical velocity from fig. 5.1 profile. (b) 1 cm/sec imposed ascent employed in simulation BD45.

precipitation, however, shows that there must be a net condensation and heating and hence cumulonimbus convection may generate convergence.

Observations showing low-level ascent to exist in the absence of precipitation confirm that non-convective convergence occurs in GATE and is usually present prior to deep convection as shown by the composite study of Frank (1978) and the analyses of Ogura et al. (1979) and Reeves et al. (1979). Ascent seems to be restricted to below 600 mb and this is consistent with the large scale trade wind convergence which is confined to the lowest 1500 m. In the absence of deep convection, compensating divergence occurs at mid-levels.

As there is no detailed data for the vertical velocity on 3rd Sept 1974 the majority of simulations with imposed ascent employed a convergence profile based on that of McBride and Gray (1978) as in fig. 5.1. This shows low-level convergence with a maximum of 1.5×10^{-5} /s balanced by divergence at 600 and 250 mb. The upper divergence is probably a consequence of cloud top outflow because the profile was composited from cloud dominated periods. However, most of the ascent is in the lower troposphere and its maximum magnitude of 2 cm/s at 750 mb is the average observed on the whole A/B scale GATE array and therefore represents convergence over a 700 km diameter area. This can reasonably be taken as a typical large scale forced convergence because events on the domain scale are unlikely on their own to influence the behaviour of such a comparatively large mass of air on the simulation's time scale.

The upper tropospheric ascent in this profile is likely to be primarily convective and, as has been said, strictly should not be included as part of the forcing. Later simulations employ a profile, as shown in fig. 5.2, in which no ascent is imposed above 600 mb, consistent with pre-convective conditions found in most GATE analyses. Soong and Tao (1980) encounter a similar difficulty in deciding the convergence profile to force on their deep tropical cumulonimbus simulations. They impose the observed mean vertical velocity but as noted by Ogura (1982), this evolves in time in a way dependent on

updraught mass fluxes until much of the mean mass flux is in strong localised updraughts. Hence, Ogura (1982) only forces the simulation with the initial convergence observed in undisturbed conditions and does not allow the forcing to evolve in time.

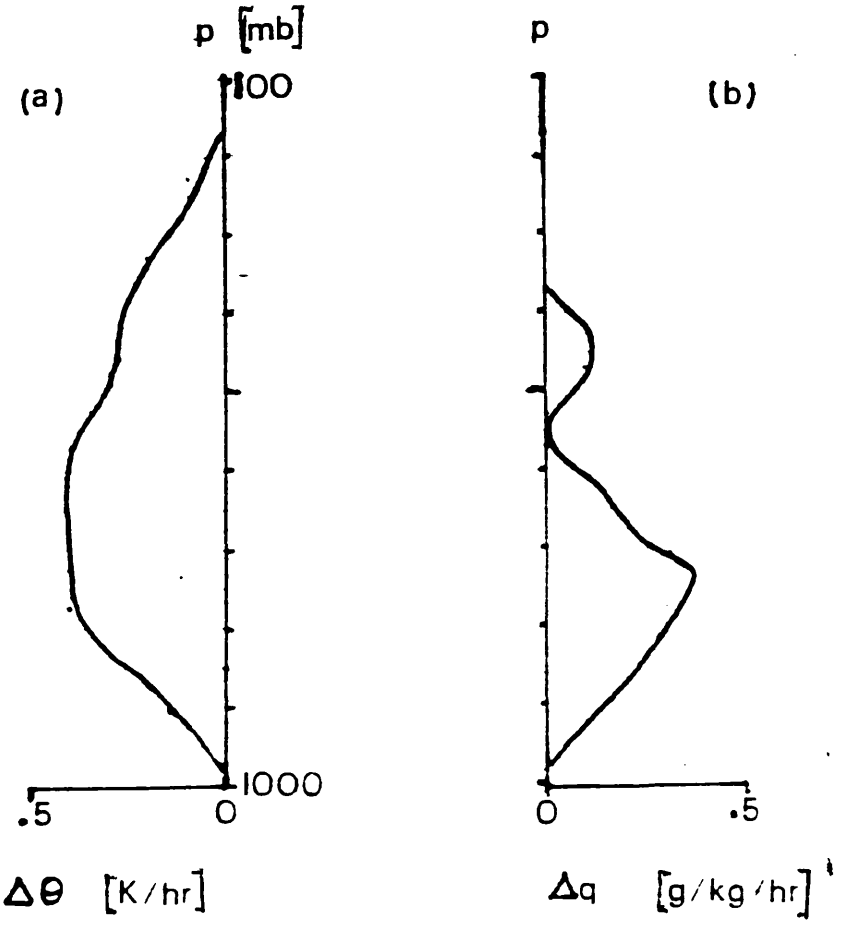
In summary, the applied convergence, being a mean for a scale ten times that of the domain is the minimum that one would need to impose and in the absence of more accurate data the model was run with this minimum forcing. The McBride and Gray (1978) profile has twice the ascent rate of that generally observed before GATE convection but the small scale of the domain compared to GATE resolution justifies this enhancement. Hence, the first simulations described below are forced with this profile.

5.5 Effect of Ascent on the Thermodynamic Sounding

If the atmosphere, as specified by the 2100 Researcher sounding is lifted in the absence of any other processes such as convection and advection there are small but significant changes to the thermodynamic structure.

Fig. 5.3 shows that a 2 cm/s low-level ascent rate would cause a cooling of 0.4 K/hr between 600 and 800 mb, a moistening of 0.4 g/kg/hr at around 700 mb and a lifting of 7 mb/hr at 750 mb.

CAPE for this sounding is 1350 J/kg and mid-level cooling increases this by 90 J/kg/hr. This 7 per cent change per hour may seem quite negligible but is actually important when it is considered where most of the CAPE is released. Due to the high shear it is mainly CAPE in the lowest 4 km which determines the ability of the updraught to grow into the upper troposphere and of the 1350 J/kg in the sounding only about 300 J/kg is available in the 4 km below the jet maximum. It is this value which should be compared with the 45 J/kg/hr supplied by imposed ascent in the same layer. This gives a 15 per cent increase in the sub-jet CAPE per hour, this being an indication of how much more active updraughts would be at the jet level in a lifted sounding.



5.3 Rate of change of (a) temperature and (b) moisture content with ascent as in fig. 5.2a.

The upper diverging air is potentially warmer and drier than the surface converging air but there is a net moist static energy supply to the domain because the difference in latent energy between these two layers is greater than that in dry static energy so that, energetically, moisture convergence dominates.

However, not all this additional energy, averaging 200 J/kg/hr over the domain, is available to convection since it is the properties of the boundary layer which determine the convective activity. In the lowest kilometre the ascent rate is small and the value of θ_w changes by only 0.05 K/hr adding 1-2 per cent to the value of CAPE determined for this layer. The moistening of air above the boundary layer may aid updraughts indirectly by reducing the cooling caused by low-level entrainment.

5.6 Comparative Simulations with and without Imposed Ascent

5.6.1 Simulations

The initial comparisons made with the adopted method of imposed ascent were between simulations which were identical apart from the presence or absence of this forcing. In addition, there were two other simulations like these but with an initial sounding modified by the equivalent of one hour of ascent at the imposed rate. Again, one of these latter simulations had the forcing terms applied and one did not.

Hence, the results of these simulations would make it possible to determine the relative importance of continuous forced ascent and the effect of just modifying the initial sounding.

The question to be answered by these results is whether convergence acts just to trigger convection by destabilising the initial sounding or whether its influence continues to be important once convection has started developing.

In order to isolate the relevant features of the comparison

between these four simulations, the development and structure of the band will not be described in this section in detail. Only a few parameters related to overall growth will be considered.

One parameter is the total surface rainfall accumulated over 20 minute intervals (most of the simulations were run to 2 hours) and another is the area of surface air more than 1 K below the environmental temperature. The latter is a useful measure because the area only increases if it is sustained by fresh downdraught air driven by rain from active updraughts. In the absence of this supply, the cold layer spreads, subsides and warms gradually aswell as being forced north-eastwards by the ambient wind in the lowest 500 m.

The four runs chosen for the comparison are:-

BD47	unforced	unmodified sounding	60 min
BD44	unforced	modified sounding	120 min
BD39	forced	unmodified sounding	120 min
BD40	forced	modified sounding	120 min

Note :- the 'unmodified' sounding was made neutral in the lowest kilometre whereas the 'modified' sounding was marginally stable being based on the observed sounding with added mid-level cooling and moistening. Runs earlier with the unmodified sounding and stable observed boundary layer were less active than those being described in this comparison.

The initialisation procedure and choice of soundings were described in chapter 3.

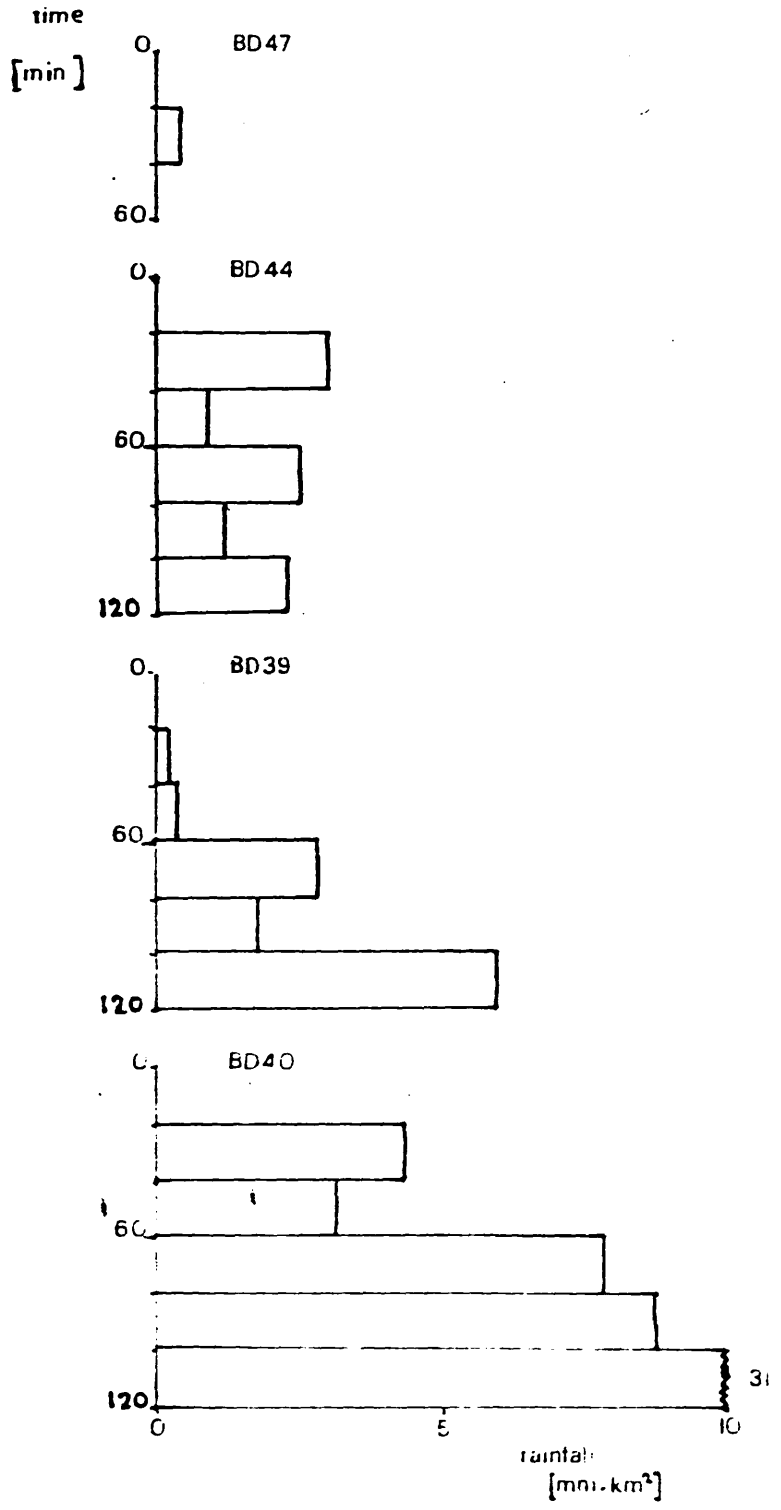
5.6.2 Results and Discussion

It can be seen from the rainfall rates (fig. 5.4) that neither of the unforced simulations showed signs of convection amplifying into a mesoscale system in the 2 hours of the run. The run, BD47, actually decayed after one hour with the surface cold pool showing no expansion in the last 20 minutes. BD44, which was also unforced but had a less stable initial sounding, continuously grew but at a rate far less than in the other two simulations, BD39 and BD40. Cloud tops remained below 5 km throughout and rainfall rates reached 10 mm/hr under the most active cells (cf observed 25+ mm/hr).

BD39 and BD40 both showed an almost explosive development starting at about 100 and 60 minutes respectively. The former developed more slowly because of the reduced CAPE of its initial sounding. Cloud tops reached 8 km and surface rainfall rates of 50 mm/hr in BD40 and 20 mm/hr in BD39 were attained by 120 minutes. In both cases the cold pool expanded rapidly to 300 km^2 (fig. 5.5) and spread out of the domain's northern boundary. Thus, the area was four times that in BD44 and ten times the size of the cold area produced by the initial cell at 40 minutes illustrating the rapid rate at which this system expands. This tenfold increase is eastwards, westwards and northwards from the initial convection with almost no expansion southwards as is consistent with the shear below 1.5 km. The gust front thus aligns east-west.

Although the modification of the sounding aids the initial cells in producing more rain in the first hour, it is not sufficient alone for strong convection to develop with the cloud heights and rainfall rates observed as is demonstrated by the lack of activity of BD44. The two forced simulations produce more realistic convective development rates.

These results demonstrate that the importance of forced low-level convergence is not merely restricted to destabilising the initial sounding in order for convection to develop. Its effects are critical during the growth stage of the simulated mesoscale band possibly



5.4 Rainfall in 20 min. intervals for simulations BD47, BD44, BD39, BD40.

because it provides a continuous supply of CAPE and low-level moisture counteracting the effects of convectively induced environmental subsidence, which itself tends to stabilise the atmosphere.

5.7 Sensitivity of Development to Forced Convergence Profile

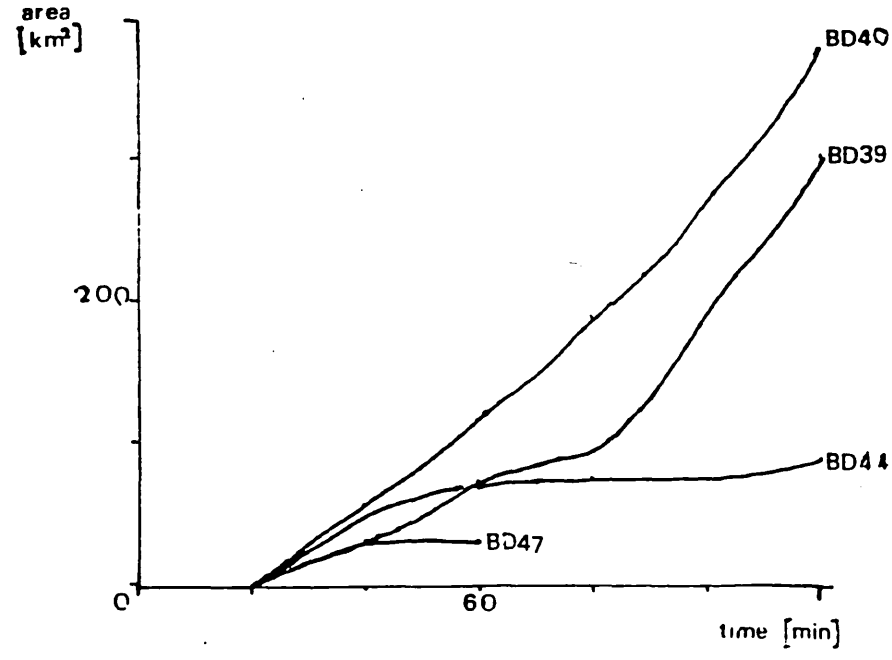
5.7.1 Simulations

It was stated earlier that the mean vertical motion profile in the GATE A/B hexagon during convectively active episodes (McBride and Gray, 1978) may not be representative of large scale forcing because of the presence of upper divergence which is cloud top outflow. As can be seen from the composite of Frank (1978) and the data analysis of Ogura et al. (1979), all divergence is restricted to that at mid-levels prior to deep convection.

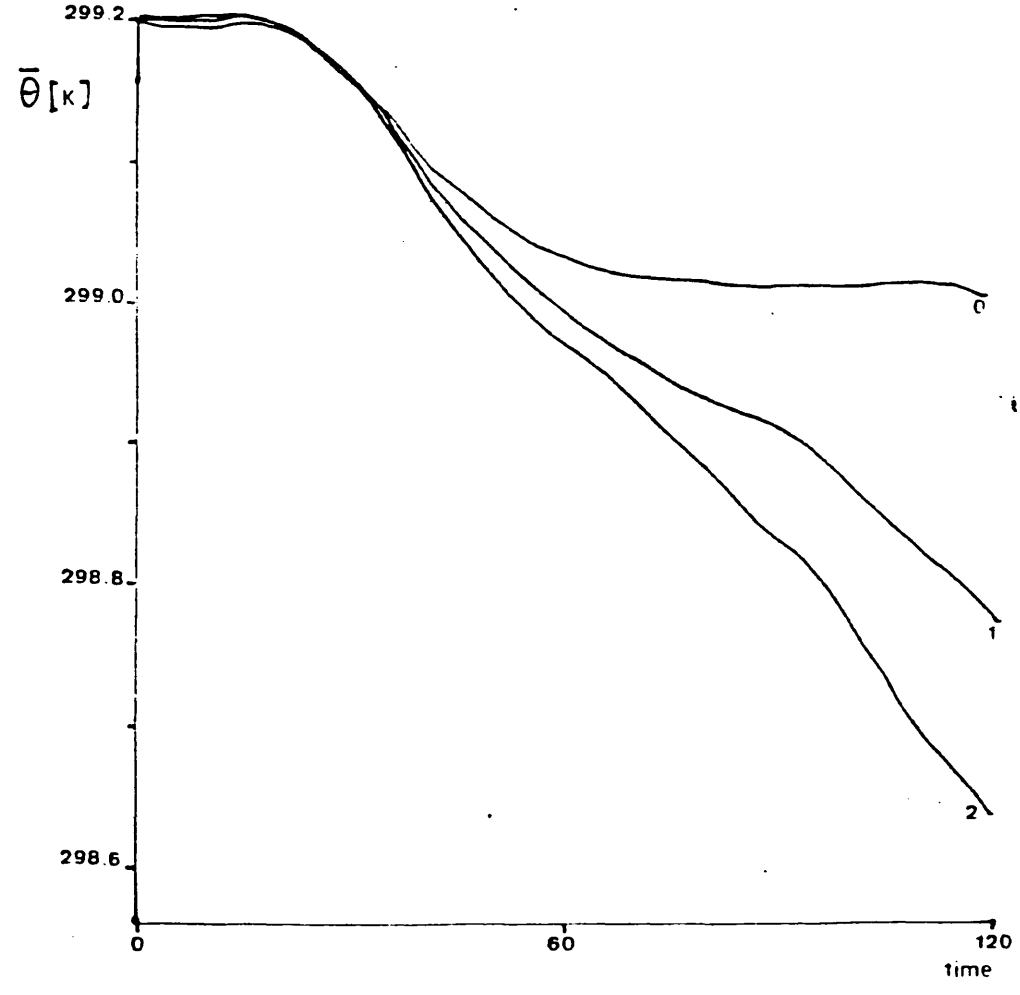
Hence, simulations were carried out with a low-level maximum ascent rate of 1 cm/s and no imposed motion above 600 mb (as in fig. 5.2). The initial simulation was modified as before because this produces band convection more quickly and saves computing time. This simulation with less imposed ascent, BD45, is thus directly comparable with two of the runs previously described, BD40 (which was re-run as BD43 with a larger domain) and BD44. All these have domain dimensions of 51x25 km and are identical apart from the forced ascent profile.

BD44	no imposed ascent	120 min
BD45	1 cm/s max imposed ascent	180 min
BD43	2 cm/s max imposed ascent	180 min

The 1 cm/s ascent rate is the minimum one would expect on the domain scale since observations suggest it to represent a mean over an area two orders of magnitude greater and it is of interest to find whether this alone is sufficient to aid the growth of a mesoscale system.



5.5 Area with temperature 1 K cooler than environment at 975 mb in BD47, BD39, BD44, BD40.



5.6 Mean temperature at 975 mb for simulations BD44 (0), BD45 (1), BD43 (2).

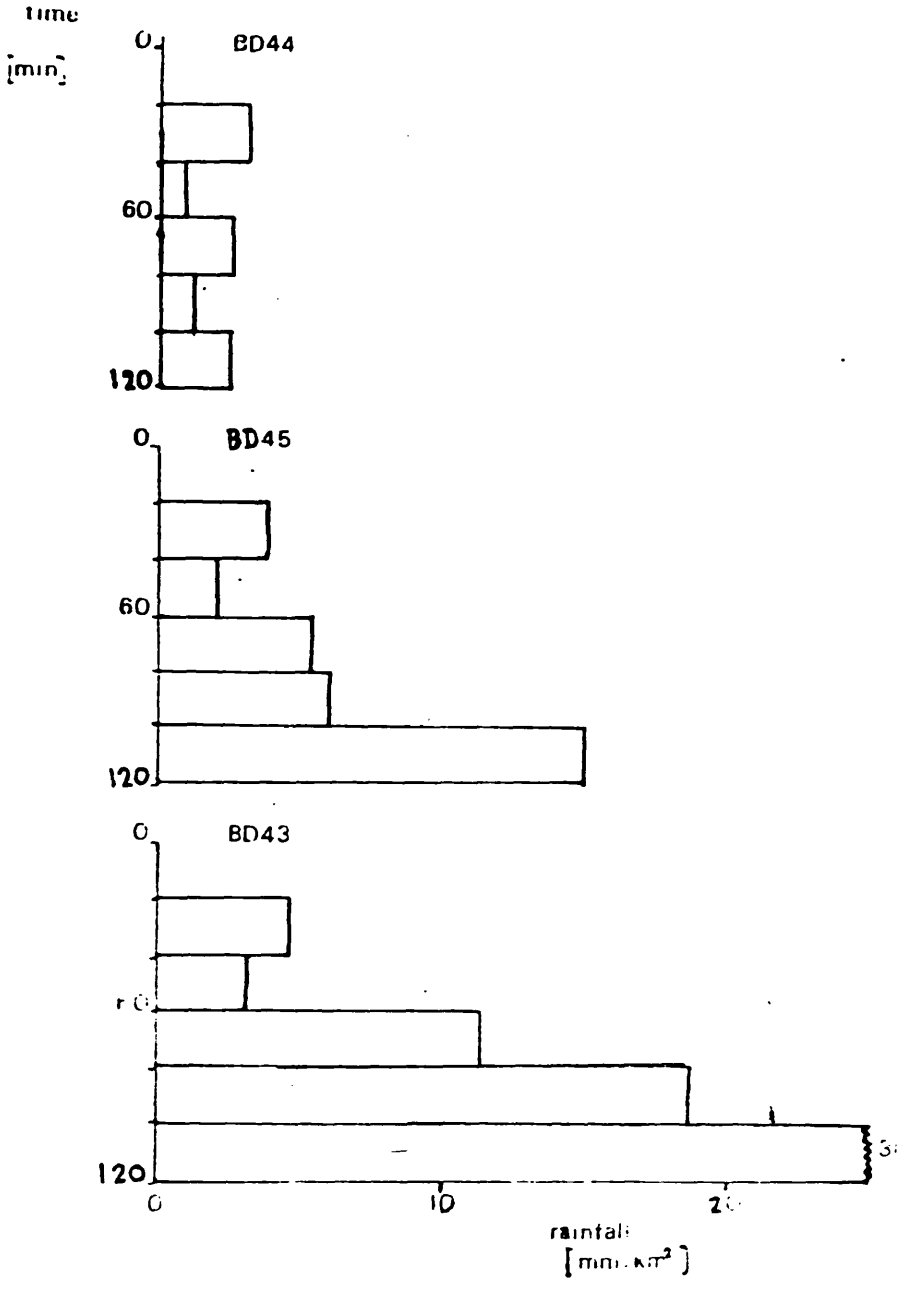
Another simulation, BD43.5, was run where the maximum ascent rate was reduced from 2 cm/s to 1 cm/s after one hour in order to test the senstivity of development to forcing at a later stage of growth. After one hour of BD43 clouds had started to generate their own convergence of a similar magnitude to that forced so BD43.5, in which forced convergence is halved at this stage, provides a useful comparison with BD43's continued development.

5.7.2 Results and Discussion

For these simulations it was decided that the mean surface temperature would be used as an indicator of convective activity since it only decreases through downdraught transports and rain evaporation. The comparative time developments of mean surface temperature (fig. 5.6) show both the forced runs, BD43 and BD45, to be convectively active throughout the first two hours and, in fact, they continue strengthening in the third hour. The unforced simulation, BD44, stops cooling at the surface after one hour and this is indicative of convective transports ceasing as the system decays.

In terms of both the surface temperature and rainfall (fig. 5.7) the 1 cm/s forced run is intermediate between the two earlier runs as might be expected. This shows that the degree of forced ascent is a primary factor in determining the development rate of these simulated mesoscale bands and that fluctuations in behaviour resulting from the random divergence of different numerical integrations are comparatively unimportant.

The rainfall rate at two hours for BD45 is about half that in BD43 and six times more than BD44's. By three hours the overall development of BD45 seems to be similar to the stage reached by the more strongly forced run, BD43, at two hours showing that the growth rate judged in terms of outflow area and surface rainfall rate is approximately two thirds when the low-level forced convergence is halved. The removal of the unrealistic upper tropospheric forced ascent seems not to change the structure of the resulting band implying that low-level ascent alone is sufficient to aid growth in



5.7 Rainfall in 20 min. intervals for simulations BD44, BD45, BD43

these cases.

Reduction of forced ascent one hour after the initialisation of the run, BD43.5, has the effect that after a further two hours the rainfall rate is approximately half of the value it would have reached had the forcing continued unreduced. The amplification rate of the system therefore shows a marked sensitivity to the imposed forcing throughout its simulated lifetime even when the mean vertical mass flux in the domain is an order of magnitude greater than that imposed.

5.8 Mechanisms of Forced Convection

5.8.1 Simulations

The above results have established a strong correlation between cloud activity and imposed low-level convergence. The GATE observed profile of wind and thermodynamic properties seems to be particularly sensitive to this type of forcing because of the amount of available energy which cannot be released by small unorganised convective clouds due to the high ambient shear. Large scale convergence provides a means of releasing more of this energy by allowing an organised mesoscale system to develop because convection is able to persist and amplify in the presence of a continuous destabilisation and moisture supply. Discussion of the organisation will be left to the next chapter. In this section the relative importance of the two primary mechanisms in forced convection will be evaluated. These mechanisms are ascent cooling and moisture convergence which provide respectively convective destabilisation and an energy supply.

By applying ascent to mid-levels the atmosphere is cooled and moistened. Since a convective updraught core comprises mainly air which has originated from the boundary layer its temperature is comparatively unaffected by such ascent and therefore its relative buoyancy is increased. Mid-level forced moistening tends to oppose this by increasing the environment's buoyancy but the magnitude of this change is only 20 per cent of that due to ascent cooling which thus has the dominant effect.

Moisture convergence by the imposed velocity field provides latent energy, Ldq, to the low-level atmosphere but this effect is significantly reduced by the cooling, $c_p dT$, and the overall increase in low-level moist static energy is only 60 per cent of the latent energy increase. However, this aids updraughts by raising the low-level wet bulb potential temperature by up to 0.1 K/hr thus slightly reducing the cooling effect of entrainment and increasing the updraught core's temperature.

It would be of interest to know if either of these mechanisms predominates in its effect on cloud development as it would simplify the parameterisation of these processes. Hence, simulations were carried out in which the mesoscale flux term was applied to either the heat or moisture equation, i.e. not both. The former provides a simulation in which the effects of mid-level destabilisation by ascent cooling are isolated. The latter simulation has no such destabilisation but includes the latent energy convergence provided by the mesoscale moisture flux.

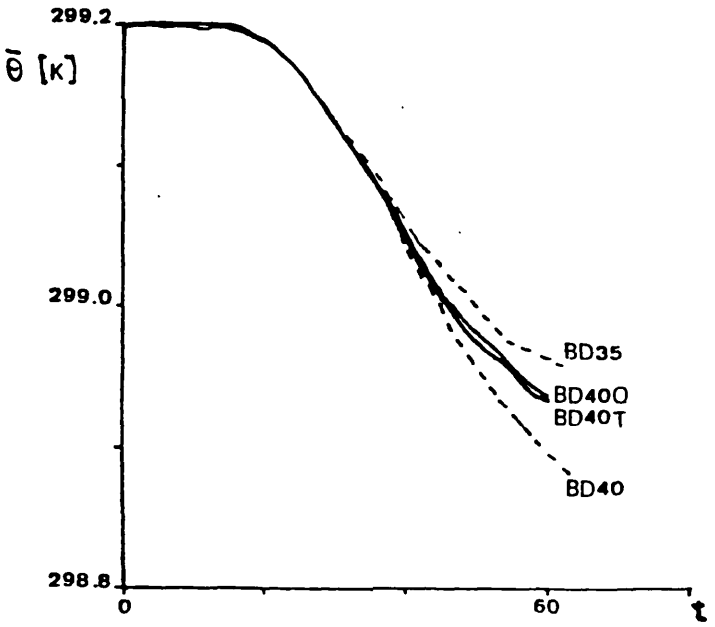
The above described changes to the equations are physically unrealistic but this procedure serves to isolate the importance of each additional term and is more like a mathematical exercise.

The sounding and forcing profile were those of BD40. The domain size was 31x31 km.

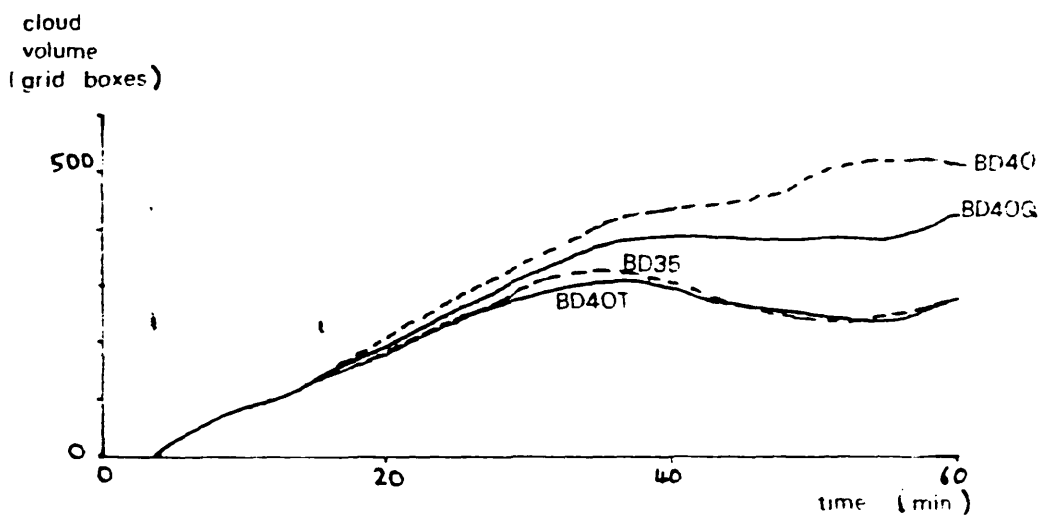
BD40T	mesoscale flux applied to heat	60 min
BD40Q	mesoscale flux applied to moisture	60 min

5.8.2 Results and Discussion

Despite being different from each other in many respects the runs, BD40T and BD40Q, had the same overall strength of downdraught transport and rainfall as can be seen from the mean surface temperature (fig. 5.8). Both were more active than the unforced run, BD44, and significantly less active than BD40.



5.8 Mean temperature at 975 mb in simulations BD40T, BD40Q, BD35, BD40.



5.9 As fig. 5.8 but for total domain cloud volume.

Fig. 5.9 shows that BD40T had no more cloud by volume than the unforced run, BD35, but produced more rain. BD40Q had a cloud volume intermediate between those of BD35 and BD40.

The most marked differences between BD40T and BD40Q were that the former had much more environmental subsidence, smaller and cooler clouds and a lower net vertical mass flux.

This is consistent with the idea that ascent cooling has a destabilising effect which increases the convective circulation strength, i.e. ascent in clouds, descent outside. Moisture convergence allows larger, warmer clouds to grow enhancing the net vertical mass flux. Thus the distinction between these two forcing mechanisms is that ascent aids the updraught strength by cooling the environment whereas moisture convergence warms the updraught itself. The effects of both forcings in isolation are equal in their contribution to convective growth and neither can be neglected in parameterisation.

5.9 Simulation with Ascent as an Initial Condition

5.9.1 Simulation

In all the simulations described so far ascent has been continuously imposed by the addition of a mesoscale velocity field to the model predicted velocity.

In this section a different approach is taken. The large scale motion is only specified as an initial condition and no attempt is made to force the model continuously.

Again care is taken that in the absence of any horizontal gradients within the domain, the boundary conditions do not introduce them. In addition to the modifications already described, the fact that ascent is now explicitly represented in the velocity field makes a further change necessary. It is no longer satisfactory to apply radiation conditions to the normal horizontal component of velocity

and integrate the continuity equation to determine the boundary vertical velocity because this does not ensure horizontal uniformity in the ascent field. Instead radiation conditions are applied to the vertical velocity with the normal component being derived from continuity.

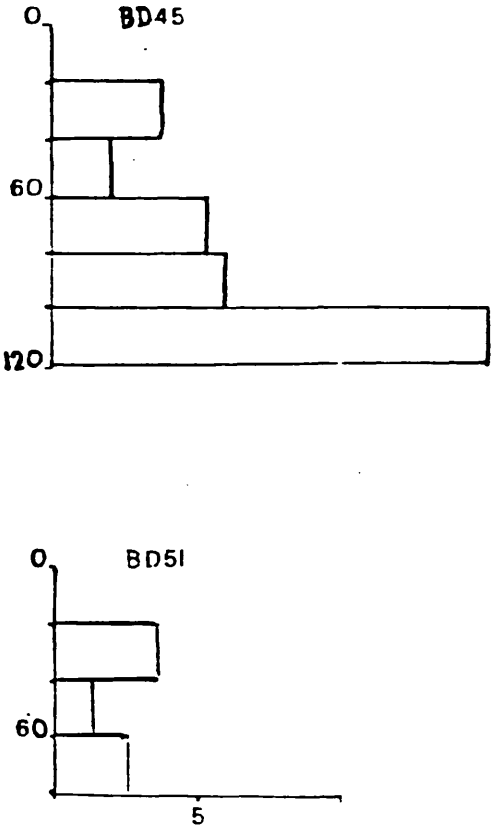
A test run in a 10x10 km domain to 20 minutes shows that in the absence of an initial perturbation these boundary conditions can maintain a uniform ascent field.

The run, BD51, in a 51x25 km domain is directly comparable with BD45 and was time integrated to 80 minutes.

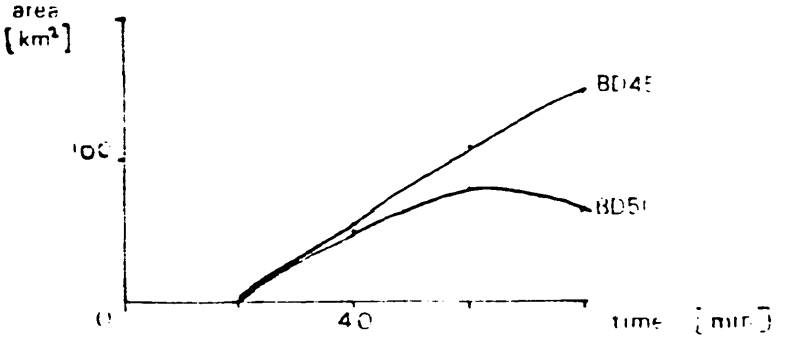
5.9.2 Results and Discussion

In the first 40 minutes the rainfall rate and surface outflow area (figs. 5.10 and 5.11) were intermediate between BD45, the continuously forced run, and BD44, the unforced case. Later into the simulation the rainfall rate increased more slowly than in BD45 and between 60 and 80 minutes the total surface rainfall was only equal to that of BD44.

It is apparent from these results that the forced ascent applied initially has not persisted after the development of convection and this is further supported by the reduced low-mid-level cooling around the clouds in BD51 compared to BD45, i.e. more subsidence must have occurred. The test run showed that the boundary conditions do not affect the initial mean ascent yet it seems that the convecting model cannot maintain such motion. As was stated previously, this is unrealistic because the background equilibrium state of the domain in this simulation is one of no vertical motion whereas in reality for the ITCZ there should be a tendency towards mean low-level convergence. It may be possible to use this initial condition method to force convection for longer if the domain size is increased. With the current domain it seems that a continuous forcing is required to retain information on the background state in the model since perturbations resulting from convection appear to remove it.



5.10 Rainfall in 20 min. intervals for simulations BD45, BD51.



5.11 As 5.10 but for area with temperature 1 K cooler than environment.

CHAPTER 6
SIMULATED BAND DEVELOPMENT, STRUCTURE AND TRANSPORT PROPERTIES

6.1 Introduction

In this chapter the band simulated will be described in more detail. The various interactions between convective motion and the environmental wind profile will be discussed and a conceptual model of tropical band convection wiil be proposed on the basis of these modelling results.

Chapter 5 dealt with the influence of the large scale on convection and the latter part of this chapter completes the picture by analysing the overall effects of convection on the large scale. This is done by considering domain mean transport properties and evaluating the clouds' vertical flux profiles of heat and moisture, these being useful guides to the way in which such clouds should be parameterised in global models.

Most of the description will be based on the run BD43, which is the most strongly forced case, because this produced a well-developed band in the three hours of simulation time. The less forced run, BD45, showed the same overall structure but its development had not reached the stage of BD43's by three hours.

6.2 Convective Band Development

6.2.1 Initial Growth Stage

In the first hour of the simulation, the initial cell's downdraught provides surface convergence which enables a secondary cell to grow to its east. This side is favoured for new cell generation because of the low-level westerly flow which displaces downdraught air downwind from the initial updraught. Consequently, the coolest part of the surface outflow and hence the most active part of the initial gust front are to the east of the original cell.

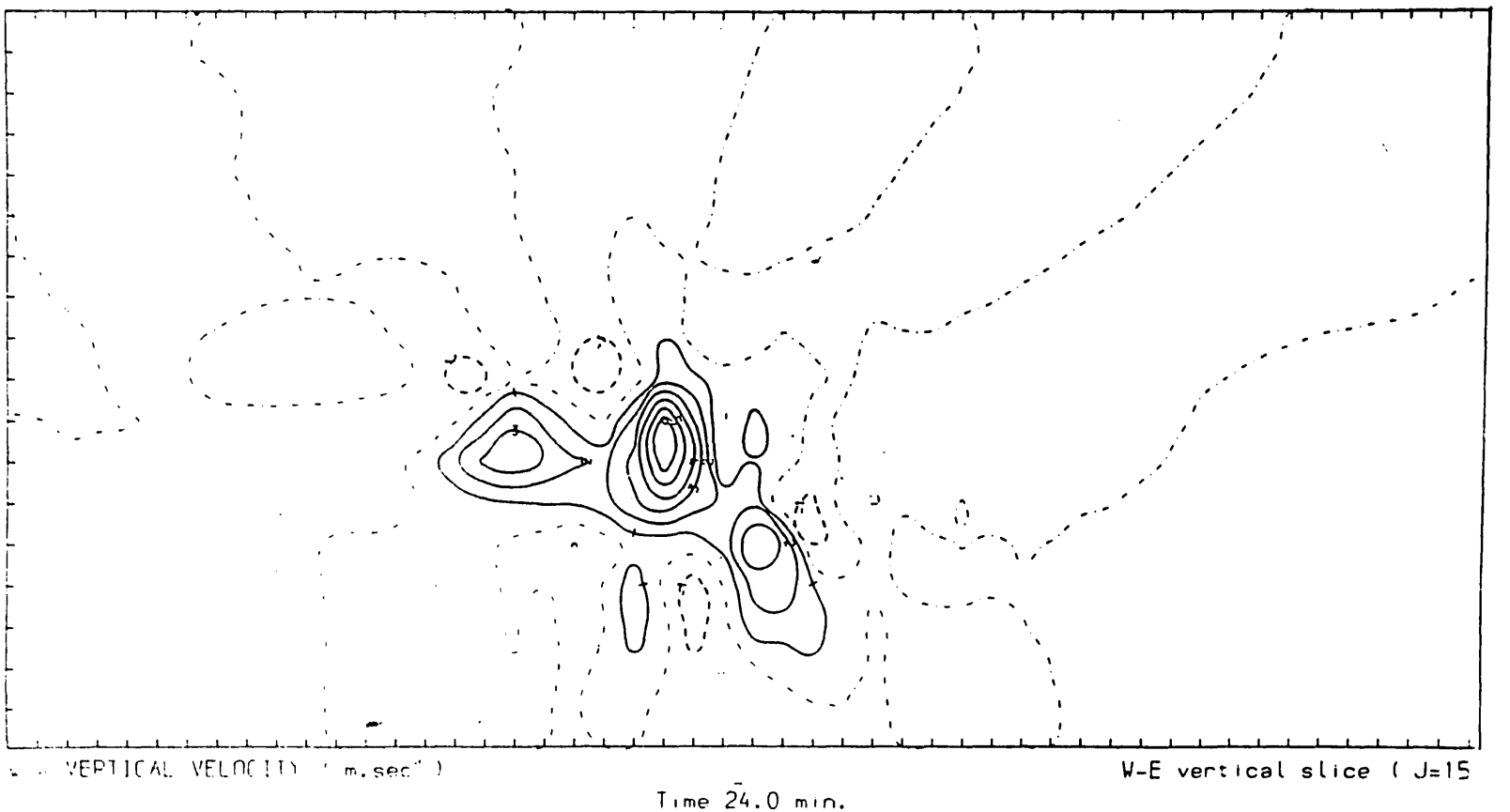
The gust front also extends westwards and is distinctly linear by 40 minutes into the simulation being 12 km east to west. The westward development is the result of rain falling from the initial cell at the jet level where the easterlies have carried the cloud downwind. This generates a downdraught to the west.

The behaviour of the initial cell as it develops in the high ambient shear is of an impulsive type whereby the low-level updraught below 3 km remains stationary and gradually weakens as a succession of cells are detached at 4 km (fig. 6.1) and carried downwind at approximately 10 minute intervals (cf Brunt-Vaisala frequency: 8 min.). None of these upper remnants develop much higher having been cut off from their energy supplying parent cell. By 60 minutes the initial lower updraught has decayed and the secondary cell grows to its east.

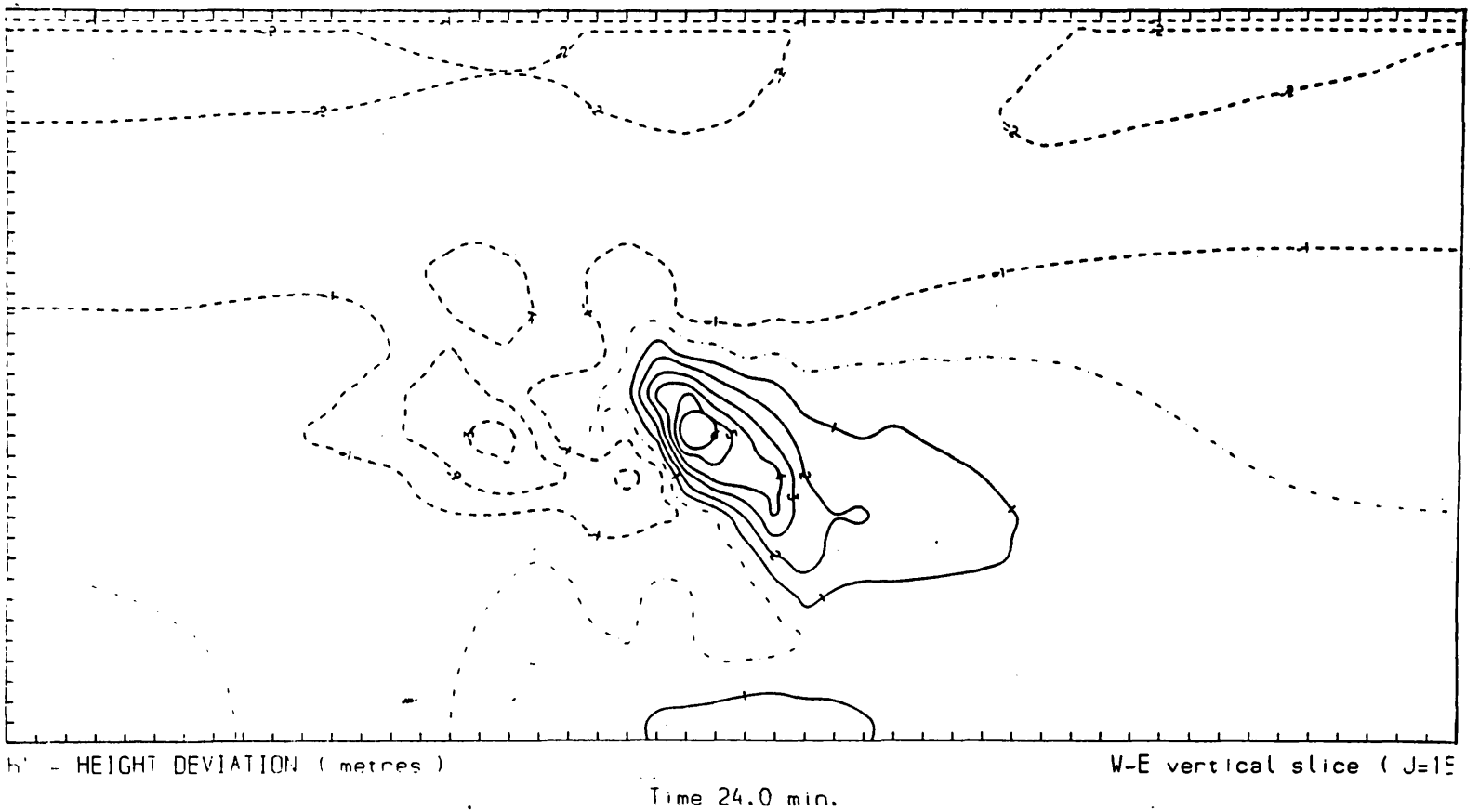
The dynamical pressure gradient set up as the updraught develops into the jet is of sufficient strength to bring the environmental easterly flow to stagnation on the upwind side of the updraught. Thus all the jet air is diverted around the ascending core which acts similarly to a solid obstacle. However, in order to produce this mid-level high pressure, work has to be done by the updraught which therefore has a tendency to be decelerated. This causes the updraught to diverge horizontally as it conserves mass flux and there is a distinct downshear elongation of the cloud at 4 km consistent with this divergence. The pressure downshear (west) of the updraught at the jet level is low (fig. 6.2) and this corresponds to the 'wake low' behind obstacles in fluid flows (Tripoli and Cotton, 1980, Newton and Newton, 1959). It is this low pressure region which organises the mid-level detrainment of the updraught as converging dry environmental air mixes with cloudy detrained air.

In the initial hour of the simulation dynamic deceleration and detrainment mixing are sufficient to prevent buoyant ascent from reaching above 5 km and the convection is shear dominated.

The behaviour of the jet environmental air as it deviates around



6.1 Vertical velocity at 24 min. E-W section. NB all figs. have linear pressure scale from 100-1000 mb.



6.2 As fig. 6.1 for height (pressure) deviation.

the updraught is also interesting in terms of vorticity. As this easterly flow passes to the north and south of the ascending air which has a negligible easterly motion, regions of high vorticity are generated at the core's boundaries. This mesovortex couplet, with a positive vorticity centre to the north and a negative centre to the south, influences the downstream behaviour of the jet air and aids its convergence into the wake region. Simpson, Van Helvoirt and McCumber (1982) also find that such mesovortices may organise entrainment into updraughts in a sheared environment in their three dimensional GATE simulation. In this study it is cloud top detrainment which is helped by these mesovortices and this process is especially well-defined in the early stages of growth when few other cells are present to complicate the flow pattern.

The mid-level wake low influences the pressure field even at the surface (fig. 6.2) where the south-westerly inflow is accelerated towards the convective region by gradients of 0.01 mb/km. Thus surface convergence of 10^{-4}/s occurs to the west of the initial cell almost perpendicularly below the wake of the initial updraught and is probably partially responsible for the westward elongation of the band. Tripoli and Cotton (1980) in their numerical simulations show that the surface influence of a wake low may strongly affect the motion of cold downdraught outflow air and hence determine the surface convergence field.

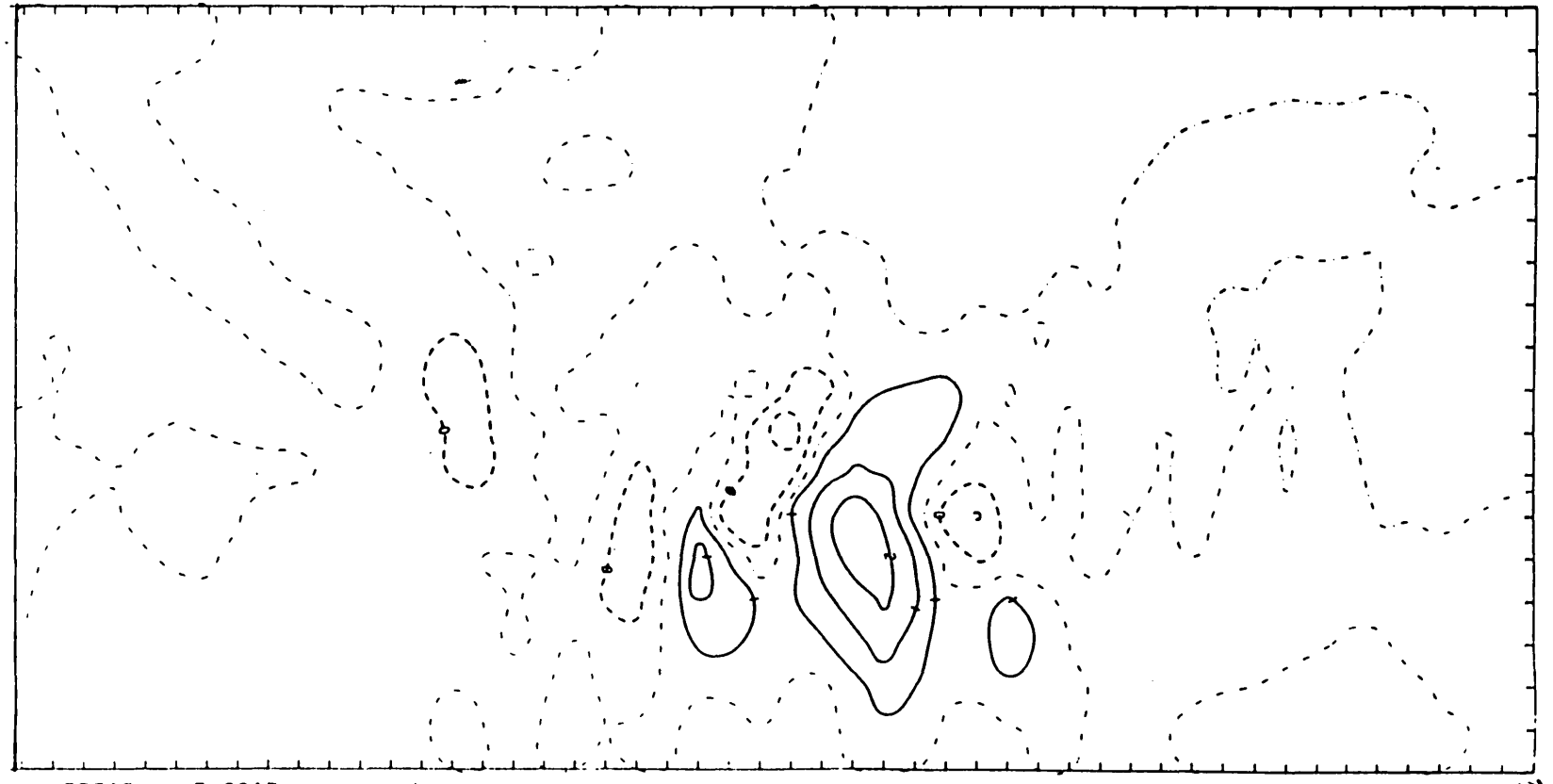
The primary determining factor in the alignment of the growing band is probably the interaction of the downdraught outflow, which is 1-2 K below the surface environmental temperature, and the ambient wind. This cool layer is 500 m deep in the model and is mainly supplied by shallow downdraughts in the lowest 1-2 km. For such a surface front to remain stationary relative to its supply there has to be a strong low-level shear and when the lowest 1000-1500 m of the model wind profile is considered (fig. 3.7) it can be seen that there is a much stronger meridional than zonal shear. This has a magnitude of 5 m/s/km and is sufficient to halt the gust front relative to the convection which produces it. Cells growing at this almost stationary convergence line have little northward motion because the ambient

meridional wind is almost negligible above 1000 m. Note that any other alignment of the gust front would have a lower shear component perpendicular to it and hence would be unable to remain comparatively stationary relative to the low-level convective cells. I.e. this east-west alignment maximises the shear perpendicular to the front in the lowest 1000-1500 m.

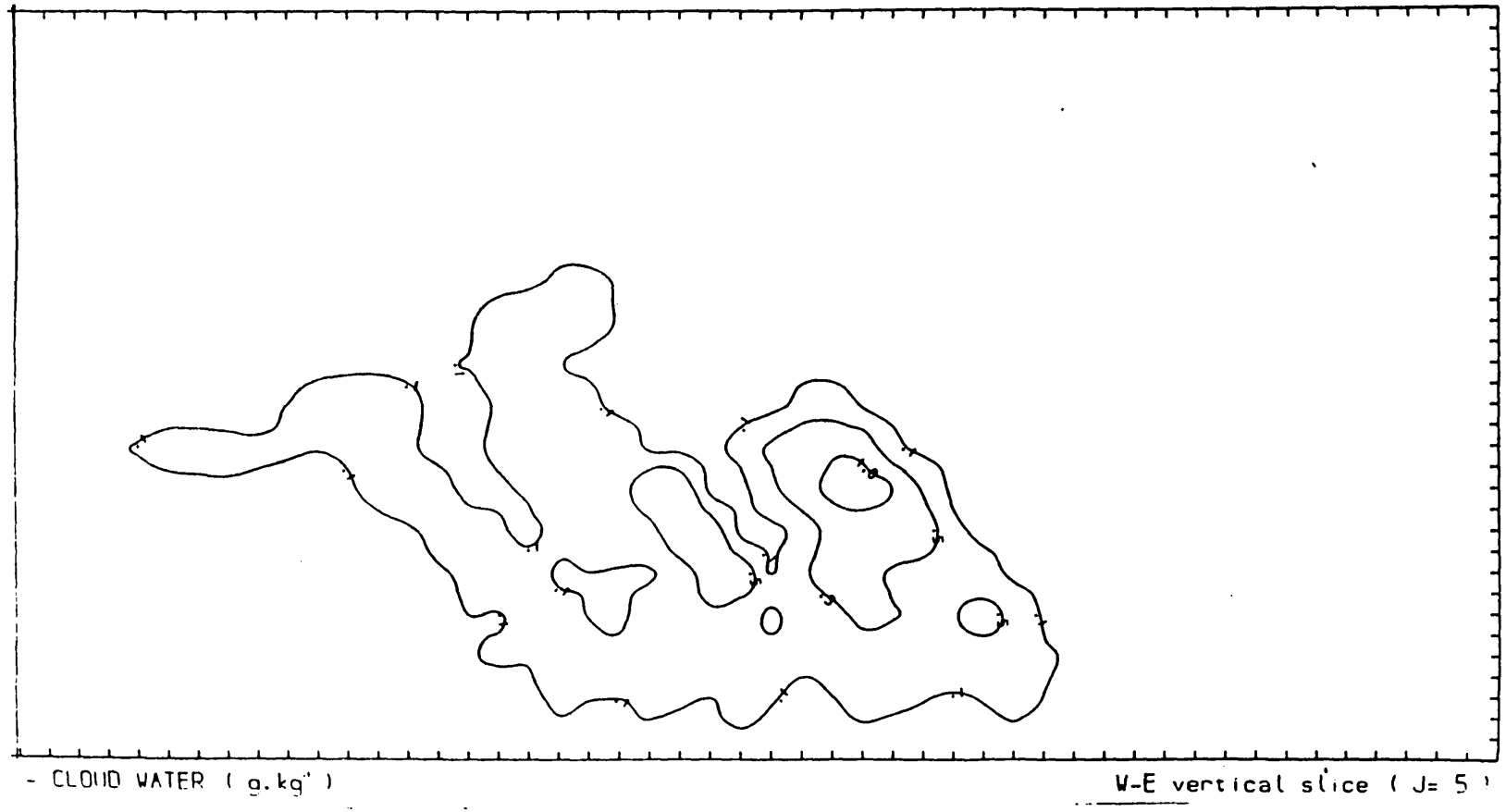
This orientation is further reinforced by the parallel mid-level jet which allows all rain from higher in the updraught to fall close to the front and behind it. The evaporatively driven downdraught probably keeps the pressure high behind the gust front and thus sustains it against being displaced north-eastwards by the ambient flow. The unforced run, BD44, showed that the lack of such a continuous cold air supply caused the existing surface outflow to be blown downwind and warmed by subsidence.

6.2.2 Band Development Stage

In the simulation's second hour the first signs of a band of co-existing cumulonimbi appear. Up until 60-80 minutes there was only one mature cell at any given time but as the gust front lengthened it became possible for simultaneous developments of convective cells at several positions along this convergence line (fig. 6.3). Development of clouds at the front starts with low-level dry forced ascent at favoured positions along the outflow boundary. These regions are probably critically dependent on the local downdraught strength behind the front which itself may be determined by the rainfall from mid-level westward moving updraught cores. These downdraughts originate at 2-3 km typically being elongated downshear and having a scale, determined by the rain area at that height, of about 2x5 km. The upper half of these descending cores is not all cooled below the environmental temperature by rain evaporation and is therefore driven by liquid drag. The acceleration provided by typical rain amounts is enough to produce a downdraught strength of 2 m/s in 100 s of contact with this rain. It is only in the lowest kilometre that the negative thermal buoyancy from evaporative cooling becomes the dominant force with the potential temperature being 1 K less than that of the ambient



6.3a Vertical velocity at 80 min. E-W slab mean (average taken over 10 km in N-S direction).



6.3b As fig. 6.3a for cloud water content.

air. In this layer the downdraught decelerates and diverges horizontally being approximately half the strength and twice the area at 950 mb compared to 900 mb. Below 950 mb this downdraught air is merged with the rest of the surface outflow and cannot be identified apart from its residual descent which forces surface divergence within the cold pool and can thus locally strengthen convergence at the pool's boundary if it is sufficiently close.

During the second hour the convection changes from individual weak clouds developing almost independently to an organised ensemble of strong cumulonimbi as the rainfall rates rise from 25 to 50 mm/hr. This intensification results from the reduction of the proportion of environmental air entrained into updraughts. The reason for this is the increased length of the gust front convergence which enables larger low-level updraught cores to develop in comparison with those in the first hour and these remain relatively unmixed in their interiors. These clouds grow to 8 km by 100 minutes being more able to penetrate the high shear layer since they have both a greater mass flux and more buoyancy. The low-level organisation into larger cores enables the mean lower tropospheric temperature in the clouds to rise as the total condensation starts to become significantly greater than evaporation.

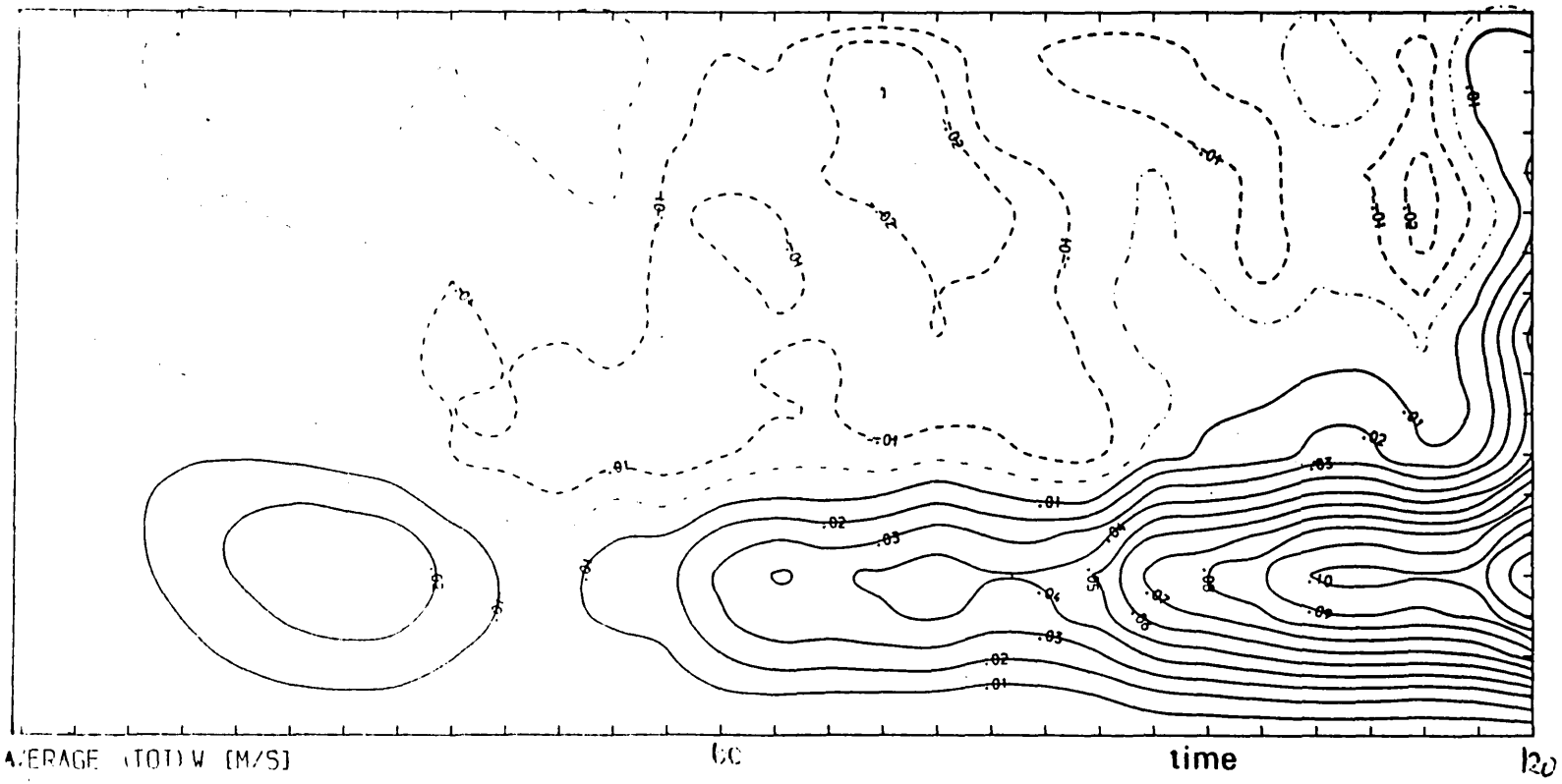
The large scale pressure field undergoes an important transformation in this phase of development probably in response to the increased net latent heating brought about by the organisation of convection. At 60 minutes the pressure gradient at the domain's southern boundary was almost negligible but by 120 minutes a mesoscale low pressure, associated with cloud heating, has a dynamical influence on the whole lower troposphere out to the southern boundary which is 10 km from the convergence front. Thus, domain scale convergence is generated by the cloud band with an average magnitude of 5×10^{-5} /s in the lowest 2 km, this being six times the externally forced value for this layer. Hence, the mass flux in updraughts is increased further and enhances the net condensation warming and surface low pressure and in this way the circulation amplifies in strength into the third hour.

6.2.3 Mature Stage

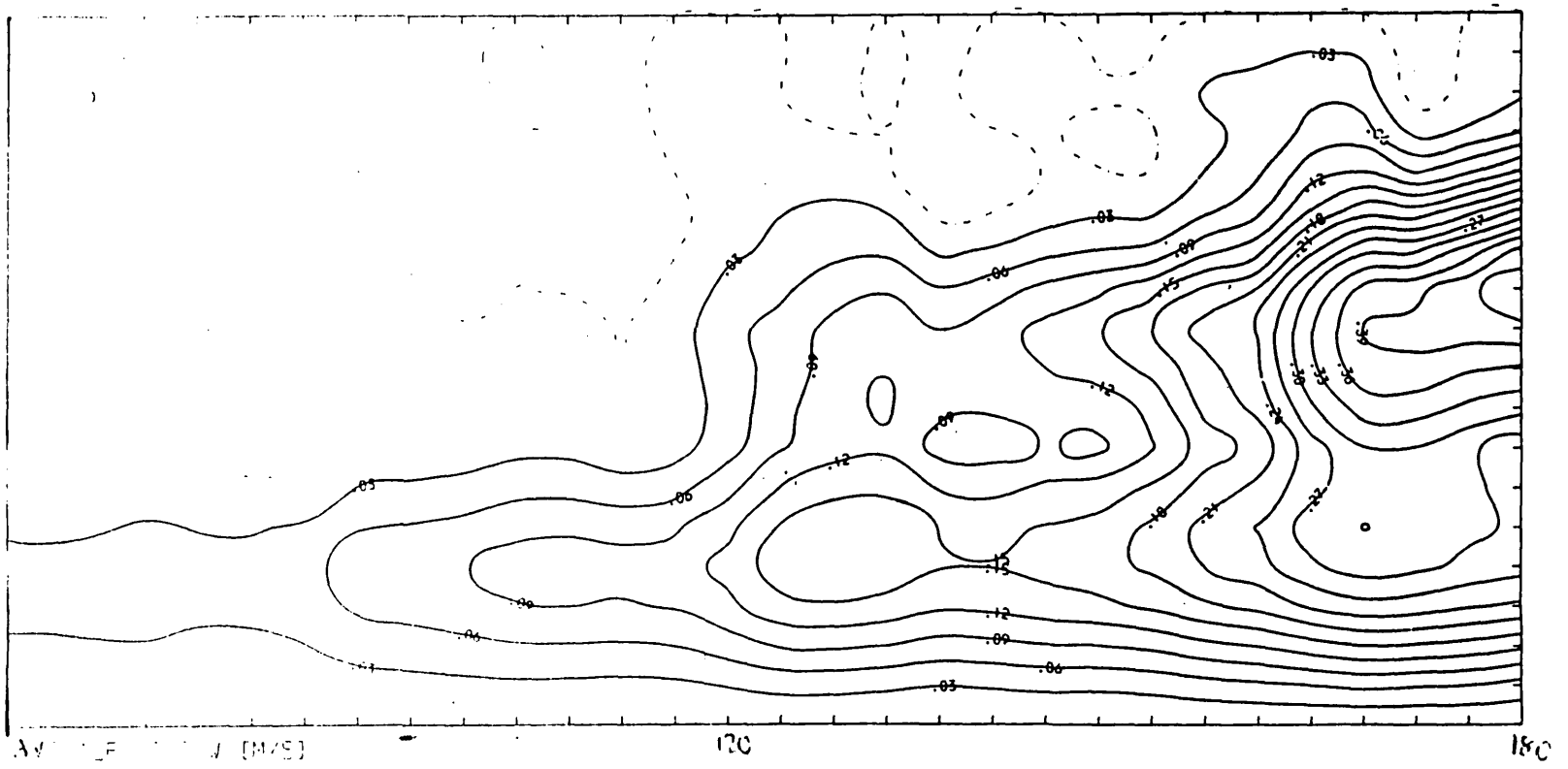
At 120 minutes the domain mean vertical velocity (fig. 6.4) shows a sudden marked development. Before this time, ascent was confined to the lower troposphere but was gradually strengthening. At about 2 hours into the simulation, upper tropospheric ascent appeared and intensified through the third hour. This upper maximum is at about 500 mb and is separated from the 800 mb maximum by a relative minimum at 650 mb, the jet level. Both the maxima increase steadily and rise 50 mb by the end of the simulation at 180 minutes. The upper maximum grows faster reaching the same magnitude as the lower maximum at 160 min and attaining a final peak value of 40 cm/s compared to 25 cm/s at 750 mb. The corresponding mean mass fluxes at these are almost equal and is 80 per cent at the relative minimum between them.

This mean structure implies either that re-acceleration occurs in updraughts which grow through the jet and mid-level convergence is forced by the resulting dynamic entrainment or that there are two separate populations of clouds, one with mid-level divergence and one with convergence up to 500 mb and upper tropospheric divergence.

Inspection of the model fields shows that neither of these two alternatives is completely true because, although there are two populations, there are also individual updraughts which show mid-level deceleration and re-acceleration, thus exhibiting characteristics of both populations. It is probable that this is a reflection of three updraught development stages contributing to the mean ascent profile. Typically, in the third hour, there may be five cores at various stages of growth. The first stage is a lower tropospheric updraught diverging and detraining at mid-levels but continuously intensifying until it has sufficient buoyancy and mass flux for a tower to develop through the shear layer without completely evaporating through detrainment mixing. Having grown into the less sheared environment above 500 mb conversion from CAPE to convective kinetic energy re-accelerates the updraught. The final stage is an upper tropospheric core gradually decaying from the base upwards. The time scale of this growth and decay is about 40 min.



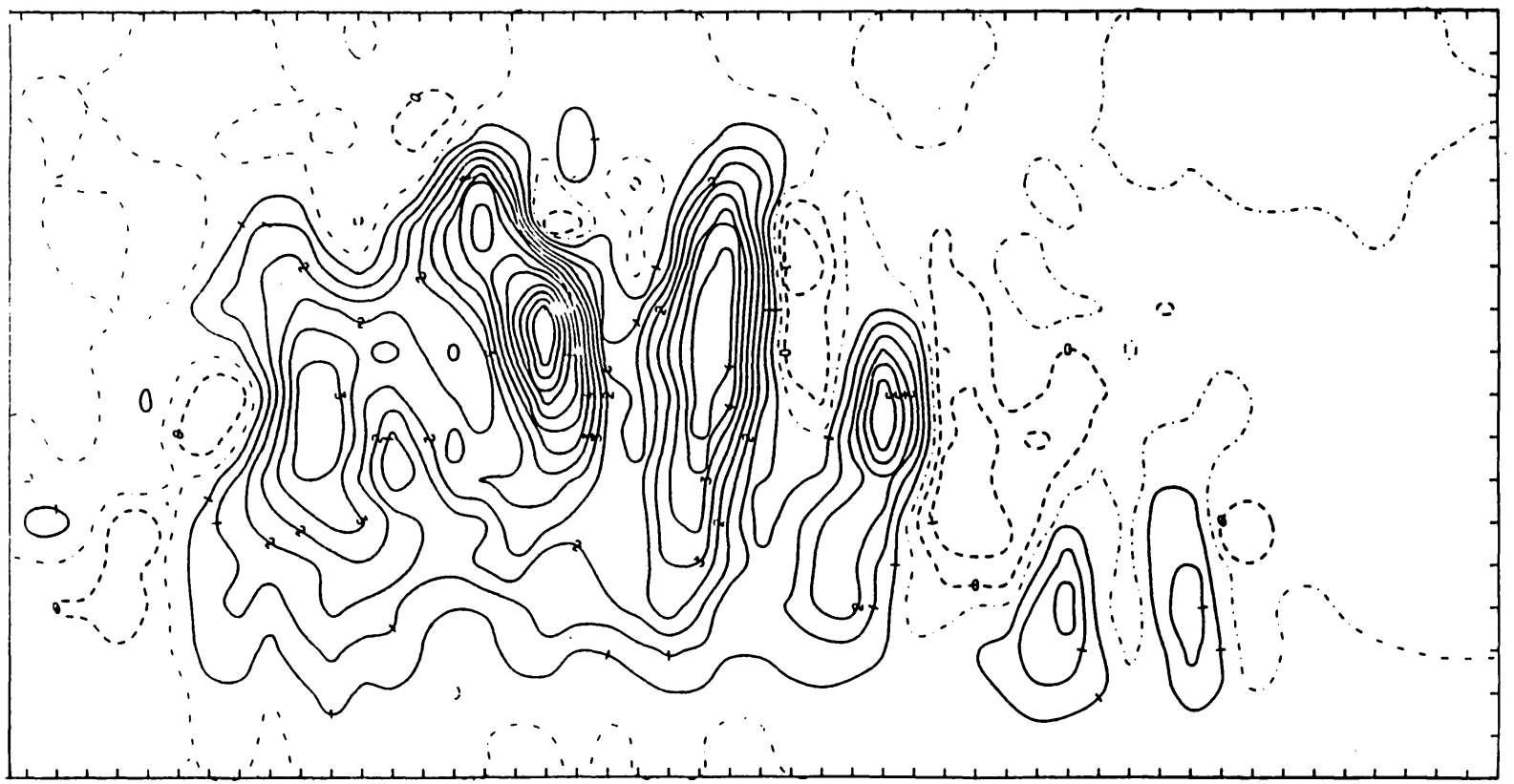
6.4a Pressure-time plot of domain mean vertical velocity (0-2 hrs).



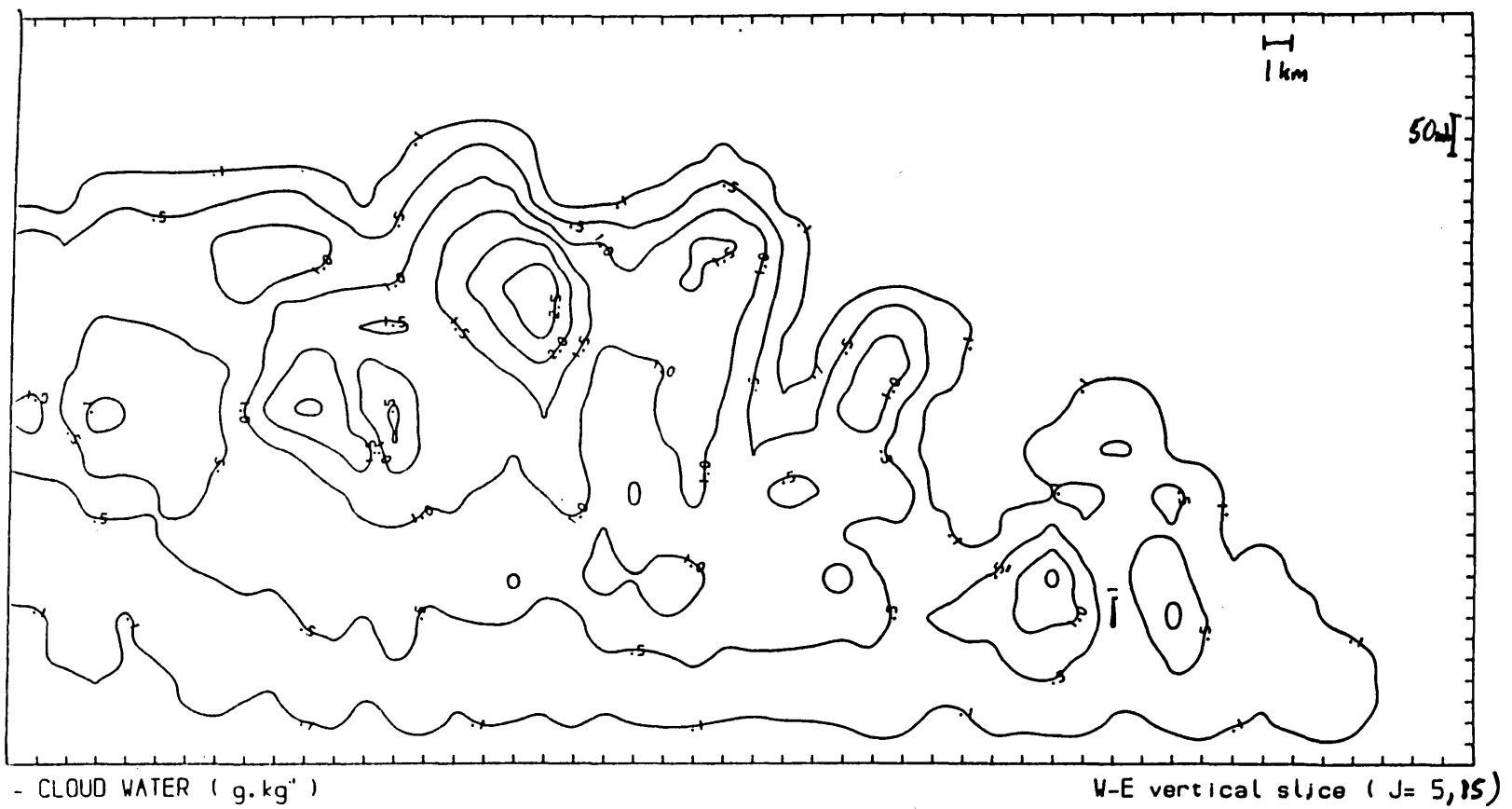
6.4b As fig. 6.4a but 1-3 hrs.

It is noticeable from the west-east sections of cloud and vertical velocity (fig. 6.5) that updraughts at the eastern end develop only as far as the first stage being incapable of overcoming the effects of the easterly jet. Those further west grow much higher and probably benefit from the moisture transport of the upwind clouds into the jet. In chapter 3 it was shown that mixing of jet air with one upstream cell's updraught may be sufficient to allow a downstream core to remain buoyant on mixing with the resulting jet air. This seems to happen and the alignment of the band along the jet axis is crucial to the development of high clouds such as those observed. As the number of cells upstream of a given cell increases, the jet humidity increases and its evaporating potential thus decreases enabling cores to remain buoyant. Aswell as moisture these upstream cells transport surface westerly momentum into the jet reducing its downstream strength so that the western cells grow in a slightly reduced shear and hence are subject to less dynamical pressure. It is noticeable in the horizontal flow at 675 mb (fig. 6.6) that to the south and north of the updraught band are regions of higher easterly momentum than the ambient inflow, being 16 m/s compared to 14 m/s. This is a consequence of the jet's diversion to the north and south and is similar to the acceleration past solid obstacles in other fluids.

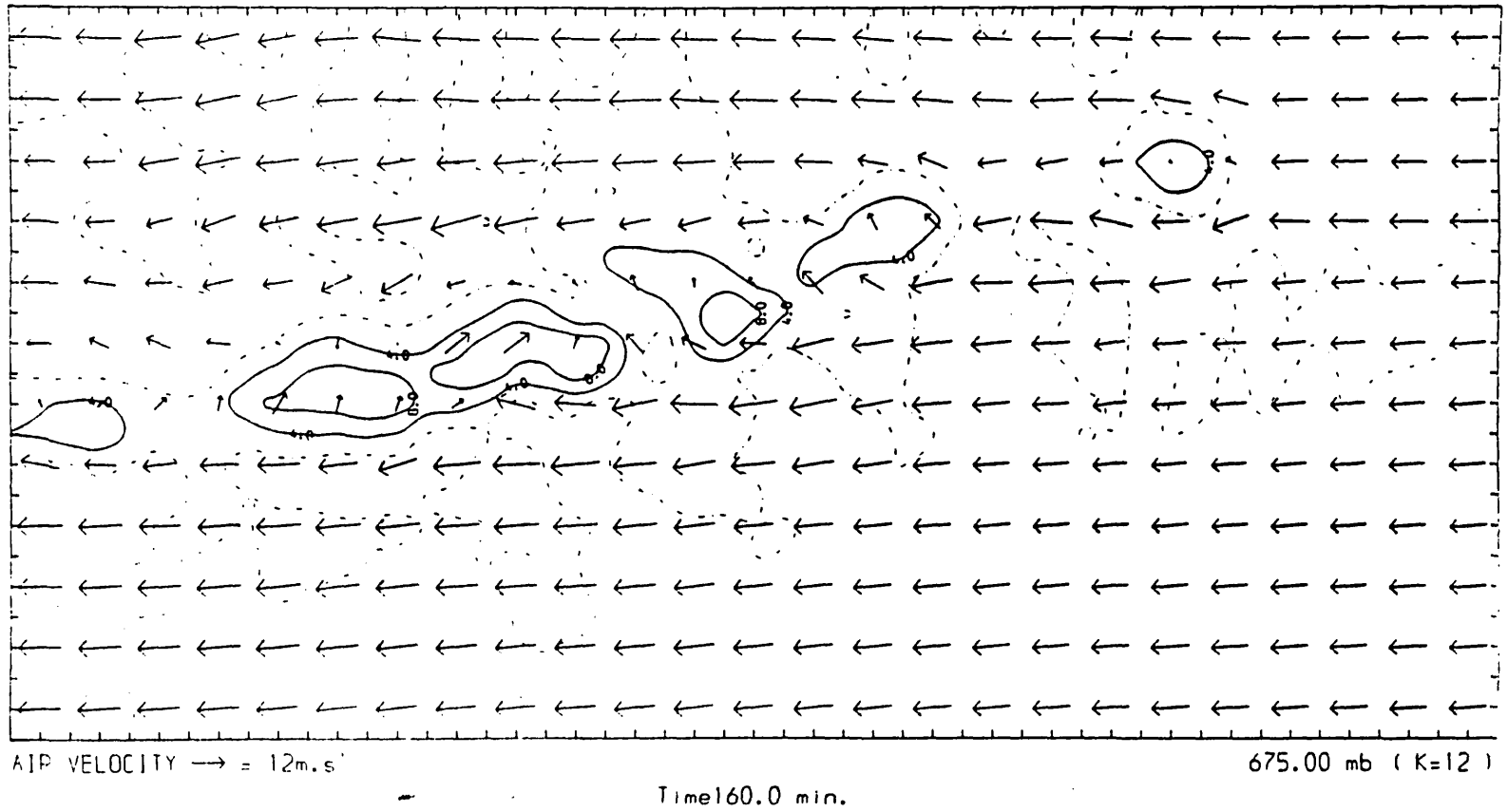
The suddenness of the development of the upper tropospheric ascent shown in the pressure-time section of vertical velocity (fig. 6.4) suggests a critical dependence of updraught development on the size of the mesoscale system. Below this critical size there are insufficient overall convergence and too few cells coexisting to form an updraught buoyant enough to counteract the shear. When the critical size is reached as the band lengthens and provides more of its own convergence, there may be two or more simultaneously active updraughts, the easternmost modifying the jet sufficiently for a significant mass flux through this level to occur further west. The less forced simulation, BD45, shows signs of a similarly rapid development in vertical mass flux at nearly three hours when its amplitude was similar to that of BD43 at two hours.



6.5a Vertical velocity at 160 min. E-W slab.



6.5b As 6.5a but for cloud water content



6.6 675mb wind with vertical velocity contours at 160 min.

The general trend in the third hour is for updraught cells to become larger and even merge at low levels. By 180 min, ascent up to 750 mb is almost in a continuous band 3-4 km wide and sloping northwards at approximately 45 degrees. It is only above this level that individual cells are clearly discernible as the updraughts accelerate to 20 m/s in separate cores between 450 and 550 mb. This horizontal convergence into narrower ascent regions occurs because of the vertical divergence forced by a buoyancy acceleration which increases with height as the core becomes relatively warmer with height through latent heating.

The surface rainfall grows from maxima of 50 mm/hr to 100 mm/hr by the end of the simulation. It is probable that the development has stopped intensifying by 160 min because the surface convergence remained constant thereafter. Thus, by 180 min, the mature stage of the band has been reached.

6.3 The Flow Structure of the Band

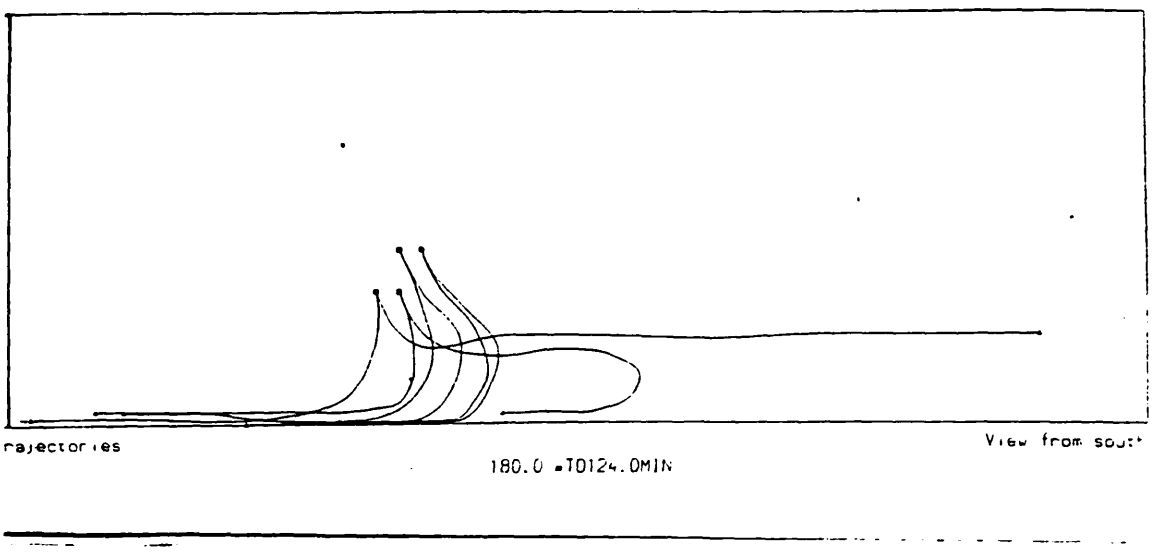
6.3.1 Model Trajectories

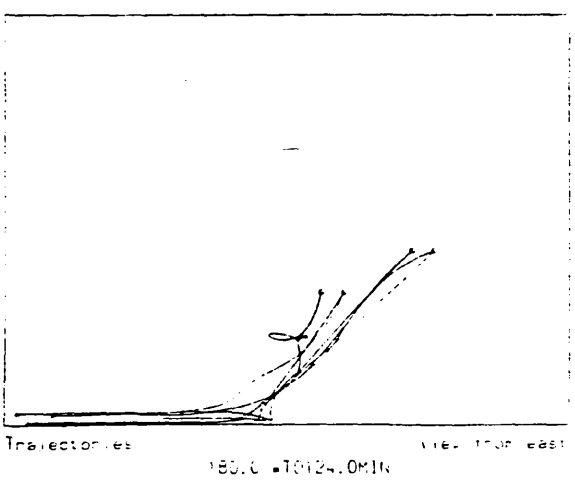
Trajectories of air parcels through the system were obtained from the simulation data dumped to tape at four minute intervals. These data were linearly interpolated to 30 sec intervals and the velocity fields thus obtained at each grid point were linearly interpolated to the parcel's position in the grid. This gives an estimate of the trajectory when the local velocity is continually time integrated to give a new set of coordinates each 30 secs. The four minute resolution is a limit set by tape storage requirements but is considered sufficient to reproduce trajectories with reasonable accuracy.

6.3.2 Updraught Trajectories and Structure

Tracing a parcel's motion back from an updraught core (fig. 6.7) shows that the origin of much of this air is in the lowest 2 km in the south-westerly inflow though some is entrained from the jet. Equal amounts seem to originate from above and below 900 mb. This shows the importance of entrainment mixing because the air around 850 mb is only marginally buoyant in the mid-troposphere. The maximum core temperatures are consistent with air originating in the lowest 500 m implying that the interior remains almost unmixed. Some sets of trajectories (fig. 6.8) show that there is a large volume of surface air detrained at jet level having risen in the low level general ascent but not converging into a mid-level core. Instead it is mixed with dry environmental air and loses its buoyancy. Trajectories from the middle of the inflow layer at 900 mb (fig. 6.9) rise in an updraught at 150-160 min to heights of around 275 mb where the outflow is primarily south-westwards. This air is directed by the Tropical Easterly Jet which has a strong northerly component above 300 mb. The divergence at the updraught top superimposed on this 7 m/s northerly component leads to a north to south variation between 3 and 11 m/s in the outflow's southward speed. Outflow below 300 mb is generally northwards and extends down to 450 mb. The ambient meridional wind is negligible at these heights but in outflow air it reaches 10 m/s, this being a significant northward acceleration of updraught air. The trajectories show a distinct northward slope with height in updraughts. This is greatest in the lower updraught where inflow ascends over the gust front and is accelerated towards the mesoscale low pressure centre below the anvil. The tilt decreases with height mainly as a result of the vertical acceleration in the core and the northward momentum is maintained by most of the ascending air. Upper tropospheric divergence above 500 mb causes the forward (southern) edge of the updraught to lose its positive meridional momentum and this air ascends almost vertically into the upper north-easterly flow.

In summary, the inflow to updraughts comes from the lowest 2 km though some is also entrained from the jet level. It rises over the gust front moving northwards and becoming more buoyant. At heights of

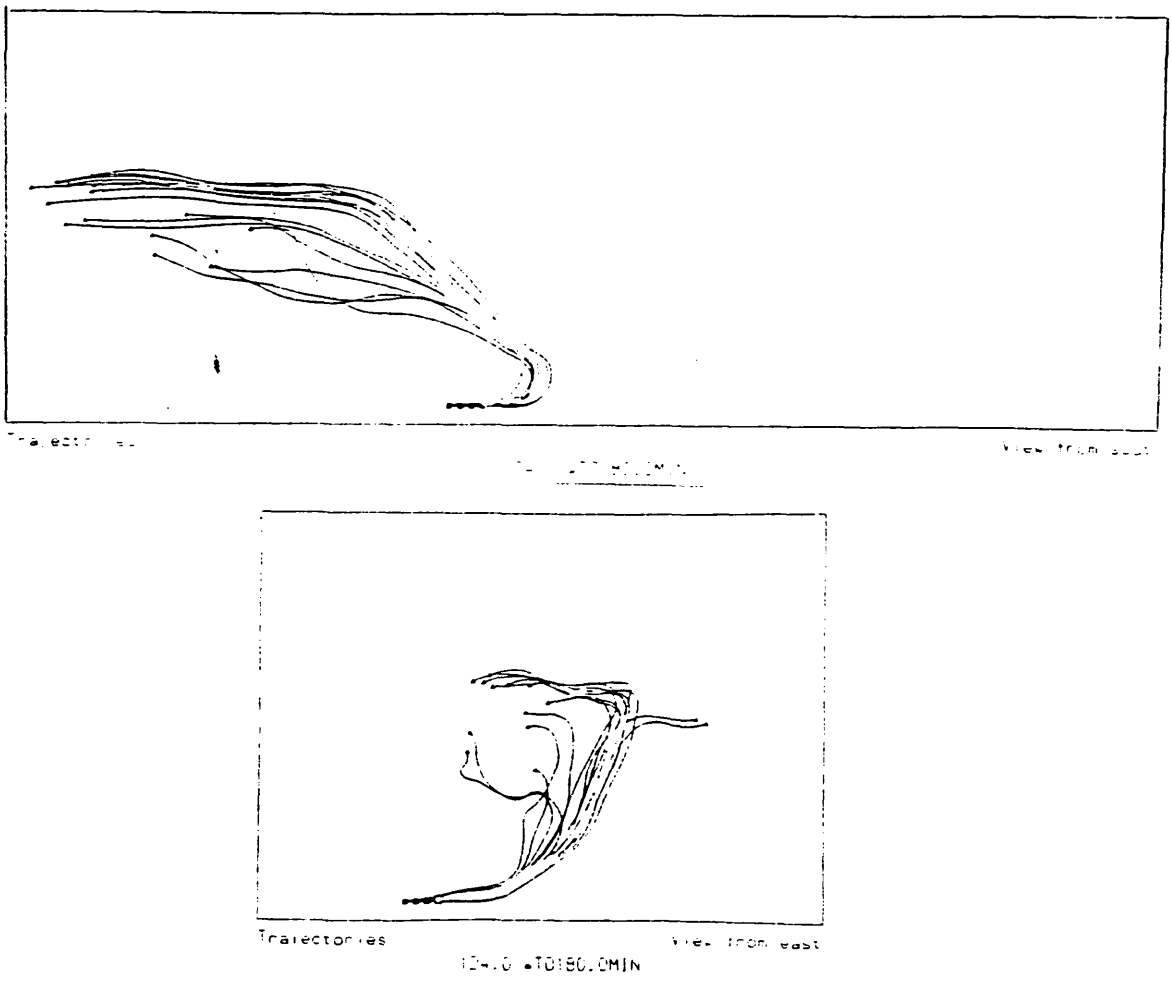




6.7 Reverse trajectories from an updraught, 180-124 min. NB all trajectory plots have a log (pressure) vertical scale.



6.8 16 inflow trajectories from 975 mb 124-180 min.



6.9 16 inflow trajectories from 900 mb 124-180 min.

2-3 km it is strongly accelerated into the low pressure region converging into a narrow core which ascends northwards and diverges above 500 mb. The rear updraught outflow air leaves the domain between 300 and 450 mb moving rapidly relative to the ambient meridional component. This outflow is unable to rise further because of the opposite direction of the overlying upper jet. The forward part of the outflow, however, is able to ascend into this jet where it diverges at 250 mb and is accelerated southwards.

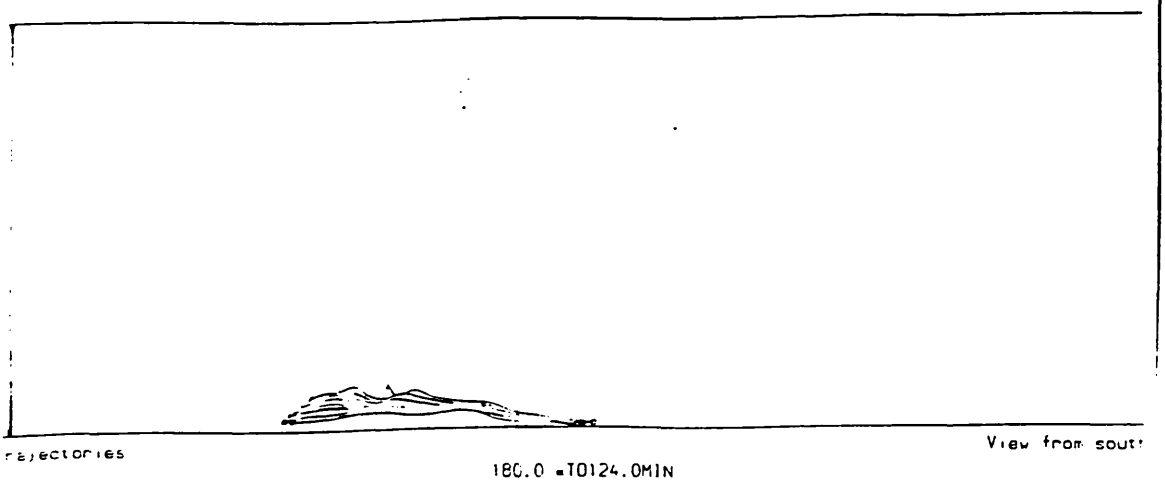
In the plane of the band's axis the trajectories show a distinct downshear (westward) slope with height above 750 mb as the updraught gains easterly momentum from the jet. It attains an easterly velocity of 10 m/s which it preserves above the jet thus transferring easterly momentum upwards. This component of outflow is all, therefore, to the west. The instantaneous updraught slope in the band's plane is negligible in comparison with the trajectory slope implying that these updraughts move steadily downshear remaining almost vertical. At the end of the simulation the updraughts have a strong westerly momentum even at the jet level. Since ascent takes place in an almost continuous east-west line rather than as separate cells, the low-level westerly flow is preserved by air ascending into the jet better than in the case of individual cells which are relatively unprotected from this rapid inflow current. In terms of vorticity tilting, a zonally elongated updraught in a strong zonal shear, such as occurs at the end of the simulation, will have a vertical vorticity component determined mostly by the tilting term. Analysis shows that this term is of sufficient magnitude to produce the observed maximum to the north and minimum to the south of the updraught in about 100 s which is short compared to the advective time scale because of the length of the updraught in the direction of motion.

6.3.3 Downdraught Trajectories and Structure

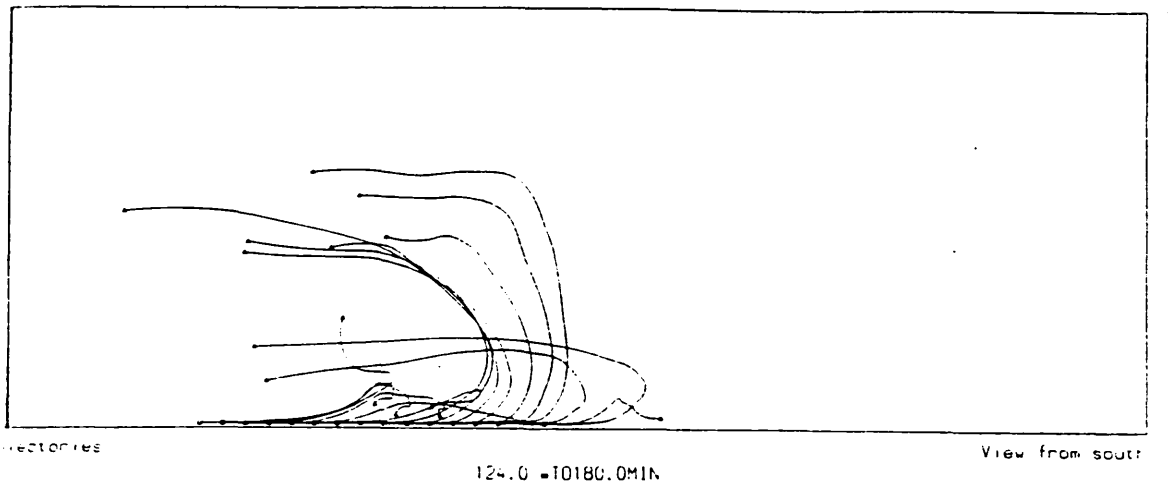
It is clear from the thermodynamic properties and the majority of trajectories (fig. 6.10) that most of the surface cold air originates in the lowest 2 km and is therefore initially identical to some of the air which forms updraughts. Trajectories from 975 mb (fig. 6.11) show that depending upon where along the band the inflow enters the system it may either converge into an ascending core or be forced down by rain drag and evaporative cooling.

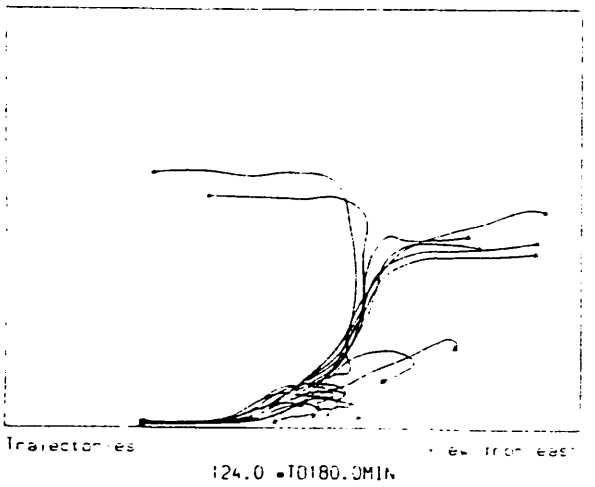
Downdraughts are rather less organised and weaker than updraughts and tend to be initiated by heavy rainfall from the northward sloping updraughts and the northern 300-500 mb anvil outflow. In the mature stage there is a 2-3 km wide line of descending air about 5 km north of the frontal ascending region and well-defined up to 2 km above which there are only local cores associated with the rain from individual updraughts. This almost mesoscale continuous downdraught has a typical descent rate of 2 m/s and is a consequence of the low-level merging of updraughts into a linear ascent band. Its temperature is, as in the developing stage, not significantly different from the ambient air between 1 and 2 km and negative thermal buoyancy is only achieved as it descends into the less statically stable region below 1 km. This shows that the evaporative cooling rate is only sufficient to lower the downdraught parcel temperature at the environmental lapse rate between 1 and 2 km. Thus, as the lapse rate and vertical velocity decrease towards the surface, this cooling rate overtakes and allows descending parcels to cool below their surroundings.

The gust front and dense outflow pool form a central part of the mesoscale organisation. As shown in fig. 6.12, the cold surface region is typically 2 K cooler and 2 g/kg drier than the mixed layer air below 500 m. This places its average level of origin around 850 mb from tephigram and moist static energy considerations. The horizontal motion within it is clearly divergent around the downdraught base and the intensification of rain in the third hour has a strong influence on this surface flow pattern. As the updraughts

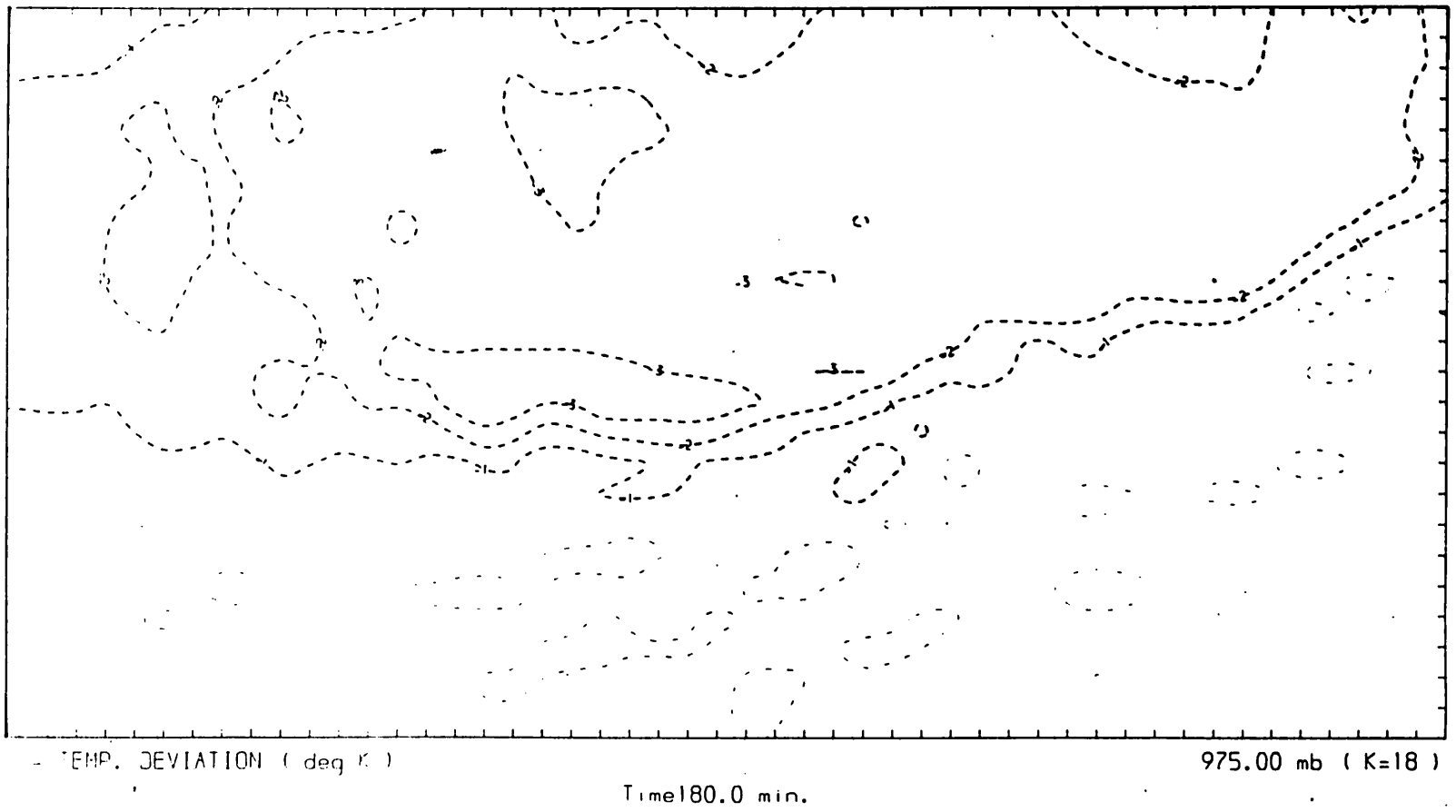


6.10 16 reverse trajectories from cold surface outflow 180-124 min.

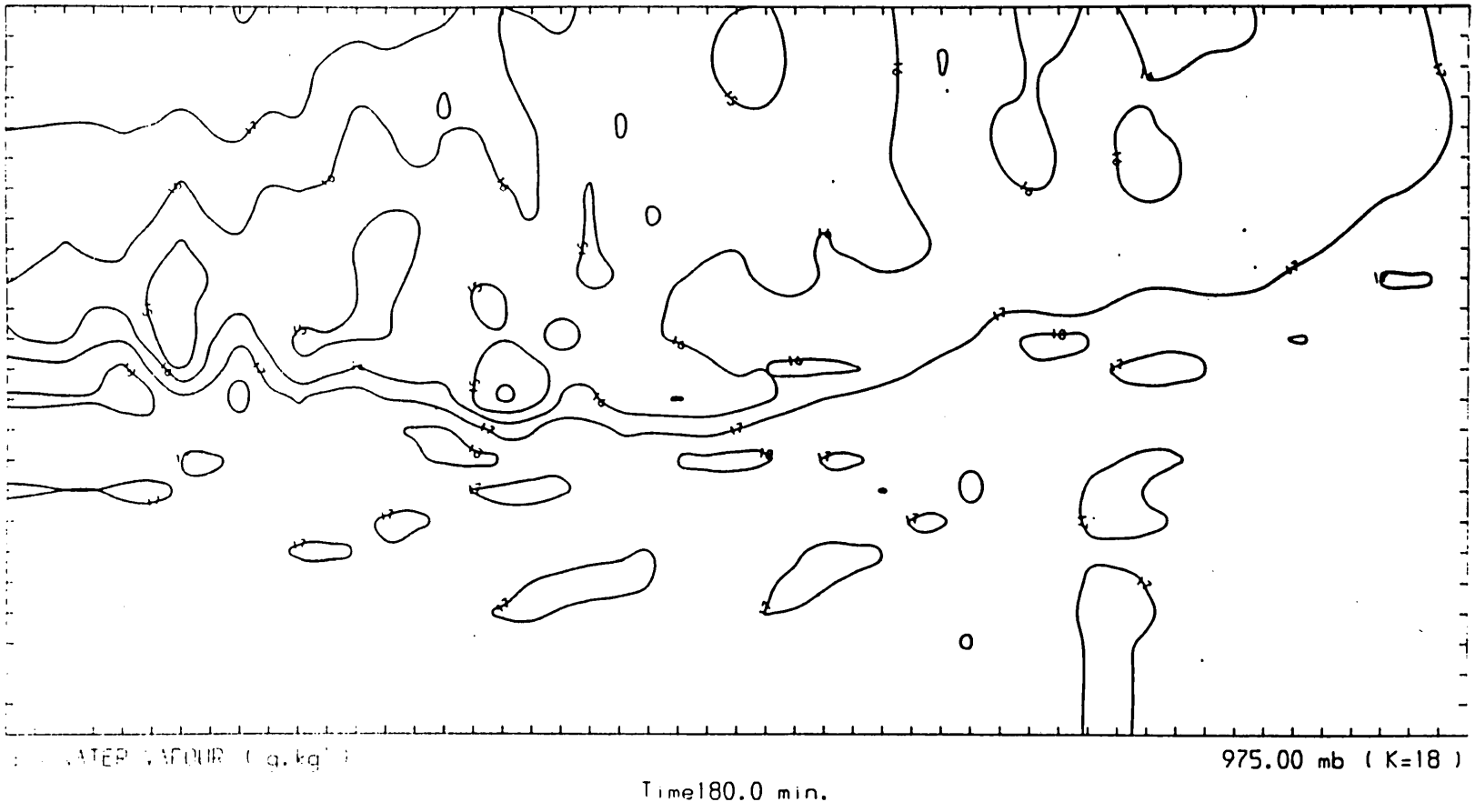




6.11 16 trajectories from 975 mb 124-180 min.



6.12a **Temperature deviation at 975 mb 180 min.**



6.12b As fig. 6.12a for moisture content.

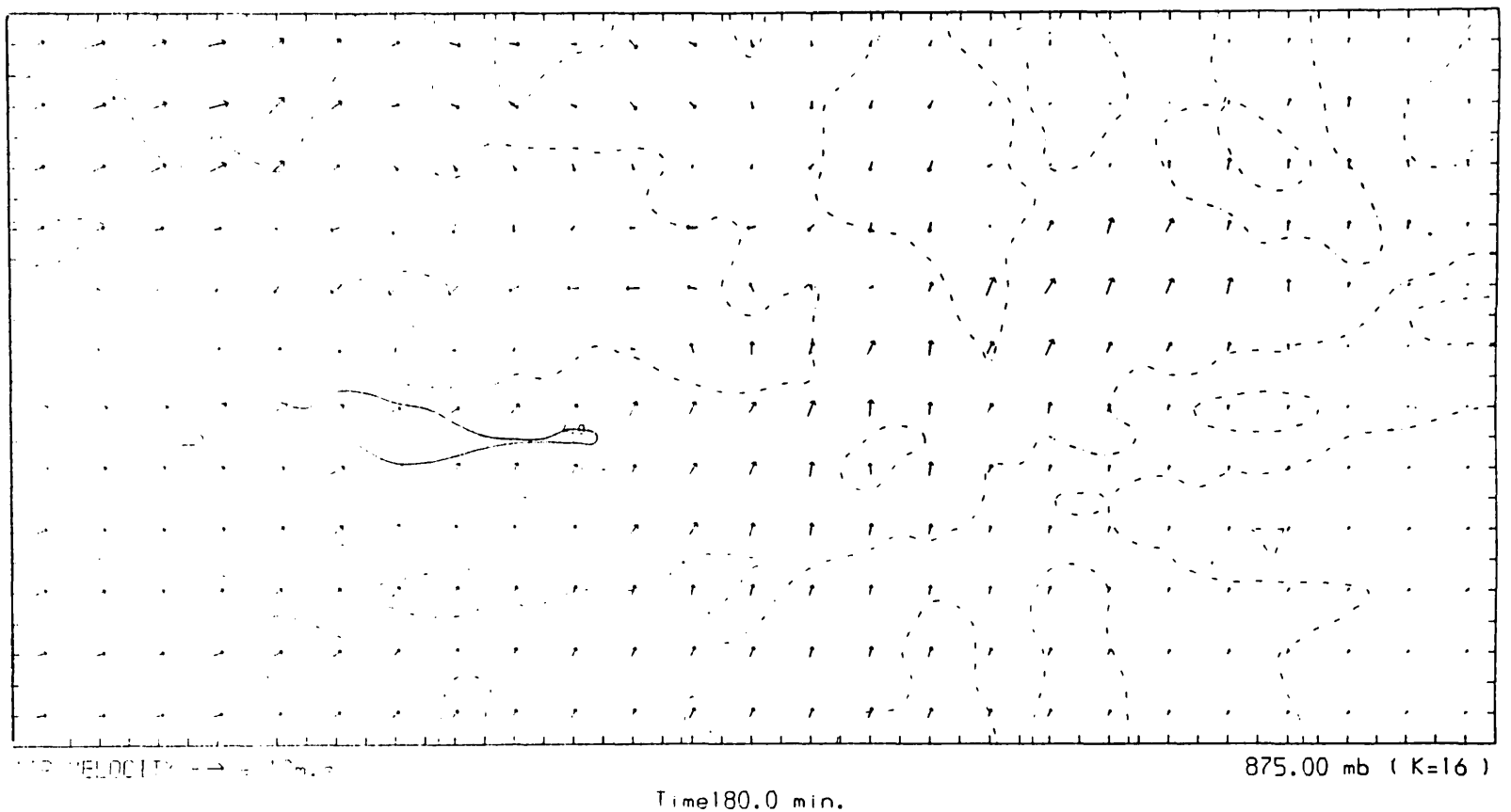
develop higher, the centre of heavy rainfall moves northwards away from the front, probably as a result of the northward updraught tilt. Consequently, the downdraught position which is closely linked to the rain area below 2 km also moves north and intensifies. Eventually at 140-160 min there is sufficient divergence produced at the surface by descent for some dense air to be forced southwards and by 180 min there is a 4 km wide band of cold dense air moving in the opposite meridional direction to the environmental inflow over a depth of 500-1000 m at up to 5 m/s. There is little evidence of ascent occurring in the cold air behind the front nor does the front itself move southwards faster than 1 m/s. Hence, a certain degree of mixing must take place at the head causing some cold air to ascend with the rest of the updraught. The horizontal resolution may cause more such mixing than is realistic because this is responsible for a 1 km wide line of surface air with properties somewhere between those of the two primary air masses. Nevertheless, despite this mixing, much of the ascending inflow remains undiluted into updraught cores and 20 reverse trajectories from two such cores shows none to have originated from the cold air.

Conversely to updraughts, the downdraught band transports easterly momentum into the lower westerlies to the extent that by 180 min there is an easterly stream moving at 4-5 m/s at 875 mb (fig. 6.13). The width of this descending stream is about 4 km and there is a high vertical vorticity, generated by tilting, at its boundaries with the ambient 3 m/s westerlies.

6.4 Comparison with Observed Convection

6.4.1 Comparison with GATE Observations

In the case of the 3rd September band, observations are restricted to radar sequences which give the three-dimensional development of the rain area. The most distinct features common to the simulation and the observed band are the alignment and merging of low-level rain areas. The width of the heavy rain area of 5-10 km is also similar but the rainfall in excess of 100 mm/hr in the model is



6.13 Velocity at 875 mb 180 min.

twice as intense as that measured by radar possibly as a consequence of cloud process parameterisations in the model such as those of accretion, coalescence and rain evaporation.

Typical updraught cores move west at approximately 6 m/s in the simulation, comparable with the observed 7-8 m/s. Cloud tops at 180 min were around 10 km and still growing and this is consistent with the observed heights at 2100, approximately 4 hours after the initial convection. Satellite pictures show outflow to the south-west consistent with the upper jet direction.

The time development of cloud heights follows that determined from radar at a similar rate, implying that the time scale of the simulated band's growth is realistic with a 2 cm/s forcing applied. Half this forcing results in this time scale being longer than that observed.

The simulation represents only part of the 250 km long band which developed on the 3rd Sept but this latter consisted of several convective regions initially independent but eventually merging. It is possible that the easternmost of these systems may have moistened the jet in the way the eastern cells of the simulation do. This would imply that the large scale alignment may largely be determined by a moist tongue of jet air favouring convective growth downstream from an existing system.

6.4.2 Comparison with 14 September Band Study

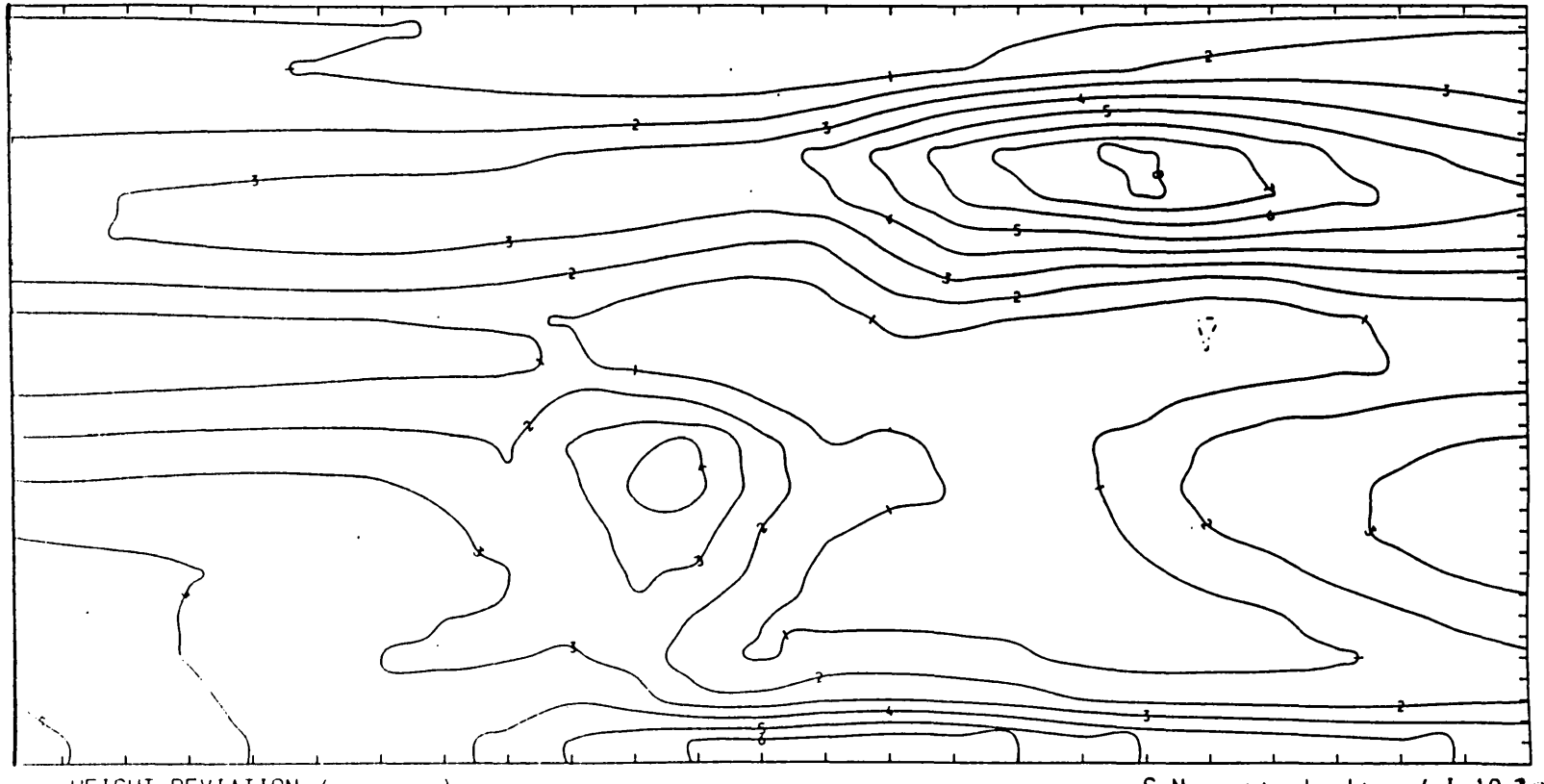
Zipser, Meitin and Lemone (1981) have made an observational study of another Phase III GATE band using aircraft data obtained at several elevations and times. This study shows several interesting features in common with the simulation presented in this thesis and so is useful in generalising the results.

The 14 Sept band developed in the north-south direction and in this sense is not typical of most GATE bands which are usually oriented near ENE-WSW. However, the wind profile shows that the

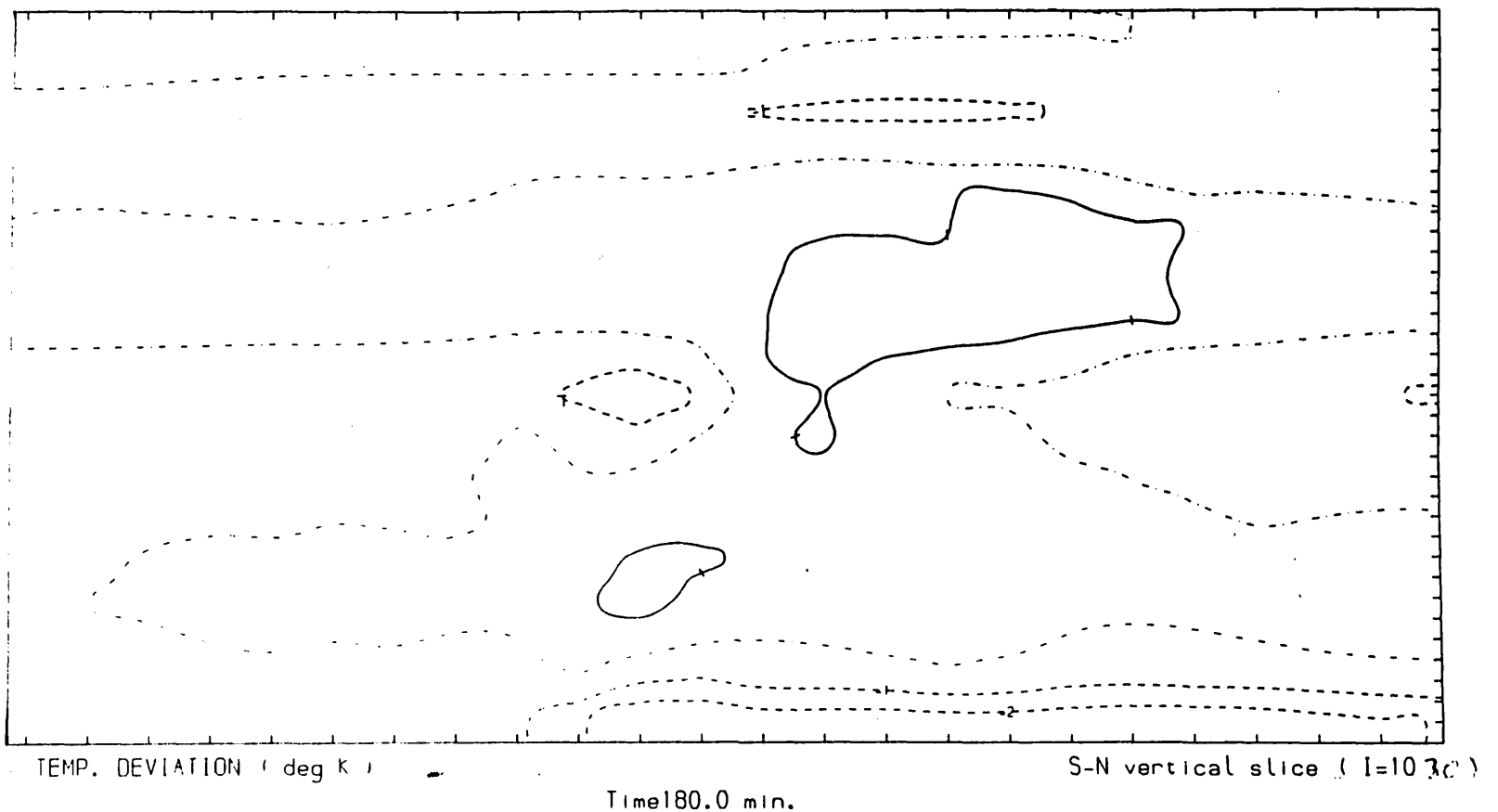
alignment is along the maximum lower mid-tropospheric shear vector, there being an almost negligible cross-band flow of 1-2 m/s throughout the lowest 5 km. However, the motion of the band eastwards enhances this inflow to 4 m/s in the relative frame. The shear in the wind component parallel to the band is almost uniformly 2 m/s/km up to 5 km with the maximum wind at the surface (10 m/s). Thus the environment is rather less sheared than in the 3rd Sept case. Also note that the shear direction is opposite to the wind direction in contrast to the 3rd Sept.

The lack of a strong surface wind perpendicular to the band may account for the eastward motion of the system because under these circumstances the gust front tends to move relative to the surface in a similar way to a density current head. The horizontal 20 km resolution of the aircraft data may be too coarse to show the surface outflow's minimum equivalent potential temperature which is measured to be only 3 K cooler than the environment compared to about 7 K in the simulated band. The maximum recorded updraught strength is also rather smaller being only 6 m/s compared to 20 m/s in some model cores. As a consequence of the cores being weaker, the rearward slope of the updraught is 1:3 which is much more pronounced than in the simulation where the updraught vertical velocity is of a similar magnitude to the mid-tropospheric rearward component of velocity. Both systems, however, show a distinct rearward acceleration of the ascending air. Lemone (1983) attributes this to the hydrostatic pressure variation across the 14 Sept band which arises through the rearward increase of warm anvil air above the surface outflow pool. The pressure and temperature fields in the 3 Sept simulation (fig. 6.14) show that a strong mesoscale low pressure to the rear (north) of the updraught is caused by a similarly warm anvil region above. It, therefore, seems that these mesoscale hydrostatic deviations primarily caused by the anvil are a major influence on the perpendicular momentum component to such bands.

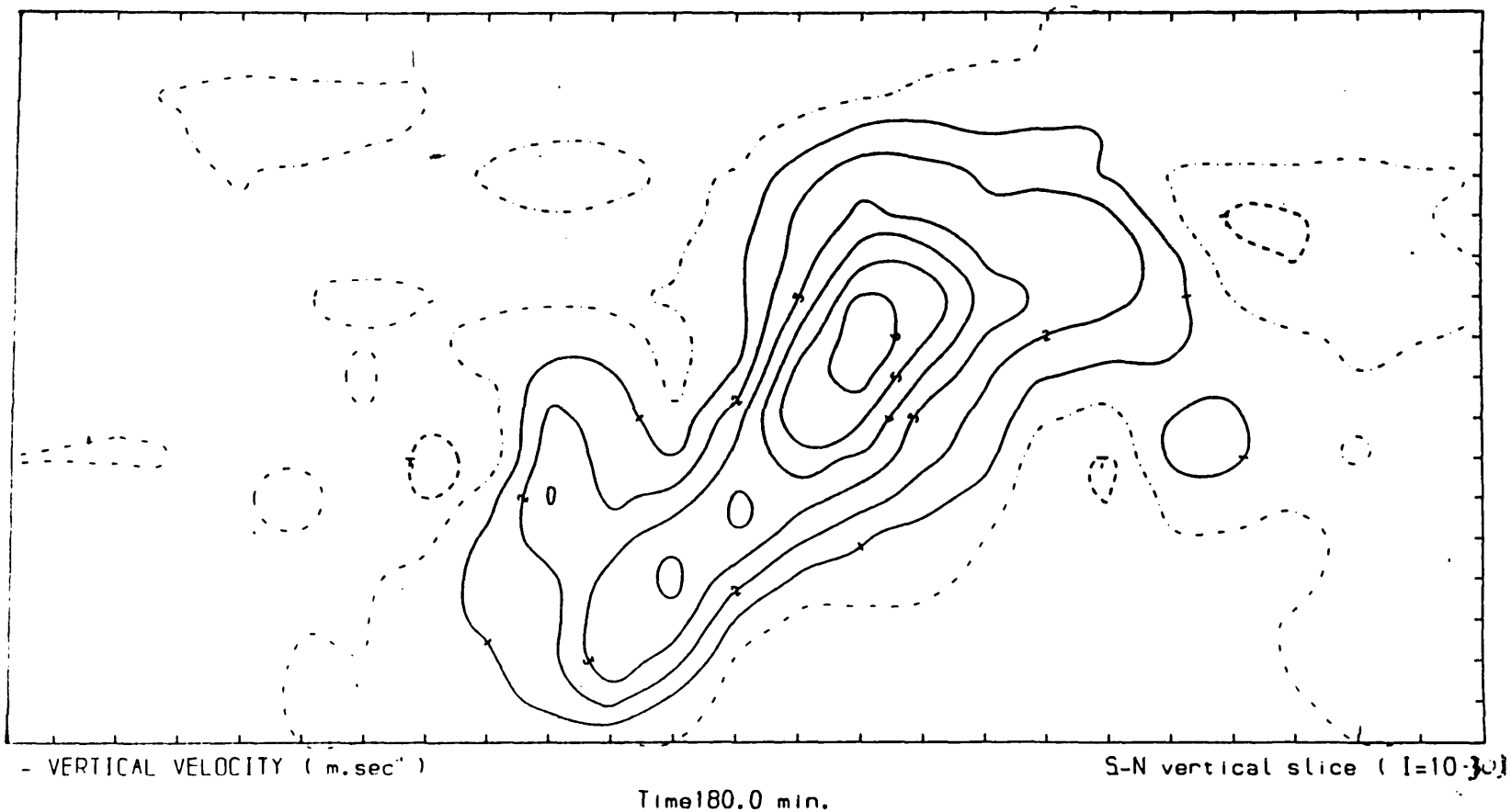
Another dynamical feature common to the 14 Sept band and the simulation is in the transport of the parallel momentum component. Zipser et al. (1981) find that there is a zone of high negative



6.14a Height (pressure) deviation at 180 min. N-S slab mean over 20 km.



6.14b As fig. 6.14a for temperature deviation.



6.14c As fig. 6.14a for vertical velocity.

vertical vorticity associated with the updraught region and account for its generation by vorticity tilting. The rear of the updraught has a small positive vorticity in comparison and this feature is different from the simulation where the vorticity couplet centres generated by tilting were almost equal in magnitude. This asymmetry in the 14 Sept case can be accounted for by the presence of a significant large scale vorticity component throughout the band's studied lifetime. The mean mid-tropospheric wind to the rear (west) of this north-south band is rather greater than that to its east thus resulting in an overall transverse shear in the parallel component of the wind. The simulation has no such background shear or vorticity. However, despite this difference, vorticity tilting is important in both cases because of the vertical shear parallel to the band which provides a source of vorticity available for tilting into the vertical.

Hence, vorticity tilting provides a downgradient vertical transport of parallel momentum (as discussed in chapter 3) and hydrostatic pressure gradients generate perpendicular momentum.

Radar pictures show that the 14 Sept band consisted of successive cells which were generated at the front and moved rearwards and downwind whereas the 3 Sept band simulation showed only a downwind cell motion and almost continuous ascent at the front. The difference arises mainly from the lack of a low-level shear component perpendicular to the band in the former case whereas one exists in the latter case to keep the ascent zone almost stationary relative to the surface convergence line. The stationarity of the observed 3 Sept band suggests that it too must have had a persistent ascent zone rather than successive impulses.

6.4.3 Comparison with Large Scale Convective Behaviour

All studies of E.Atlantic tropical convection and easterly waves show that this region is distinguished from other tropical regions by the delay in convective development into the upper troposphere. Typically, there is a two stage growth in the mean ascent profile as described by Frank (1978) (fig. 4.3), Ogura et al.(1979), Soong and Tao (1980) and McBride and Gray (1978) with convection initially confined to providing only mean lower tropospheric ascent.

The simulation shows, though on a rather faster time scale, that band growth also occurs in two comparable stages. The reason for the initial suppression in the simulation is clearly the shear in the lower half of the troposphere. It could be suggested that the large scale convective behaviour is also to some extent suppressed initially by this shear. This is especially consistent with the fact that the vertical shear is strongest ahead of easterly wave troughs where synoptic conditions are otherwise the most favourable for convective development in the E.Atlantic.

Downdraughts in the simulation also show properties consistent with large scale behaviour. The argument of Riehl and Malkus (1958) that shallow downdraughts in the lowest 2 km are necessary to account for the ITCZ energy budget (see chapter 4) seems to be supported by the prominence of these in the dynamics of band convection. This low-level overturning is required to enable the air between 1 and 2 km to come into contact with the ocean surface where sufficient heat and moisture can be supplied to make it convectively buoyant enough to rise in high hot towers. Because much of the converging air has insufficient CAPE to ascend immediately and unmodified into a convective core only this mechanism can reconcile the observed deep trade convergence layer with updraught activity in the ITCZ. Trajectories in the simulation and the thermodynamic properties of cold outflow air confirm that 850 mb is a typical level of downdraught origin. Surface fluxes of heat and moisture were not included in the model because of the comparatively long time scale but over the period of an easterly wave trough these are important as they convert cold

outflow into mixed oceanic boundary layer inflow for subsequent generations of clusters.

6.5 Mean Behaviour and Vertical Transport Properties of the Band

6.5.1 Introduction

One useful application of numerical simulations of convection is that of evaluating vertical transports of heat, moisture and momentum which are difficult quantities to determine from observations without an expensive network providing pre-storm and post-storm environmental soundings with a good time and space resolution.

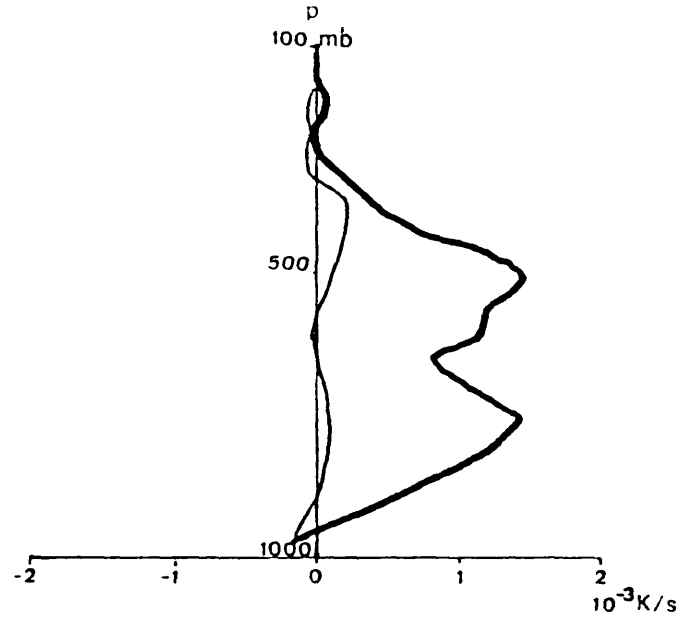
This knowledge is required for the parameterisation of convection in global models where the overall effects of clouds and clusters cannot be represented simply. In this section the band's large scale behaviour will be described in terms of vertical profiles of transports, rates of change and latent heating and drying. Particular attention is given to the determination of eddy fluxes and latent heating, these being a measure of the deviation of a global model grid box's true behaviour from transport by the mean fluxes determined from grid values.

The time dependent behaviour of these transports shows several features corresponding to the dynamical development of the band and serves as a useful comparison with the results presented earlier in this chapter.

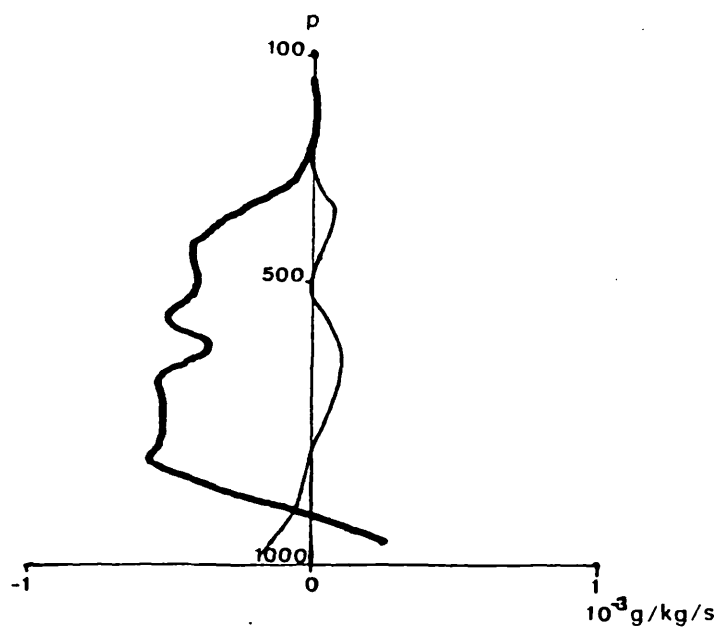
6.5.2 Mean Temperature Changes

Fig. 6.15 shows that there are levels of net heating at 350-550 mb and 700-900 mb where the domain mean temperature changes by 10^{-4}K/s and 0.5×10^{-4}K/s respectively. The pressure-time plots of mean temperature, cloud temperature and environmental temperature (where cloud is defined by cloud water content greater than 0.1 g/kg) (fig. 6.17) show that the mean profile has more overall similarity with that of the cloud-free region. This suggests that much of the

6.15

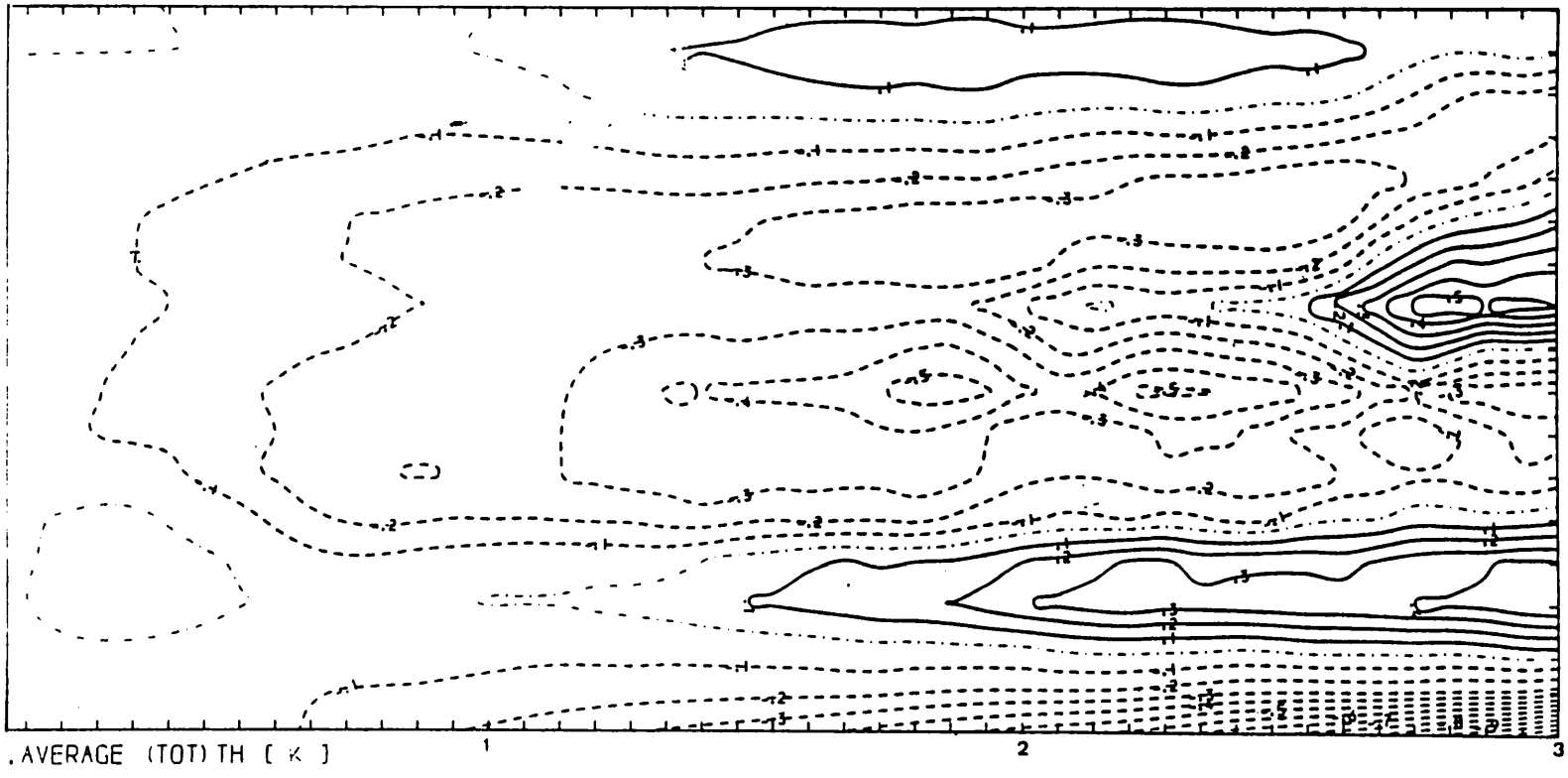


6.16

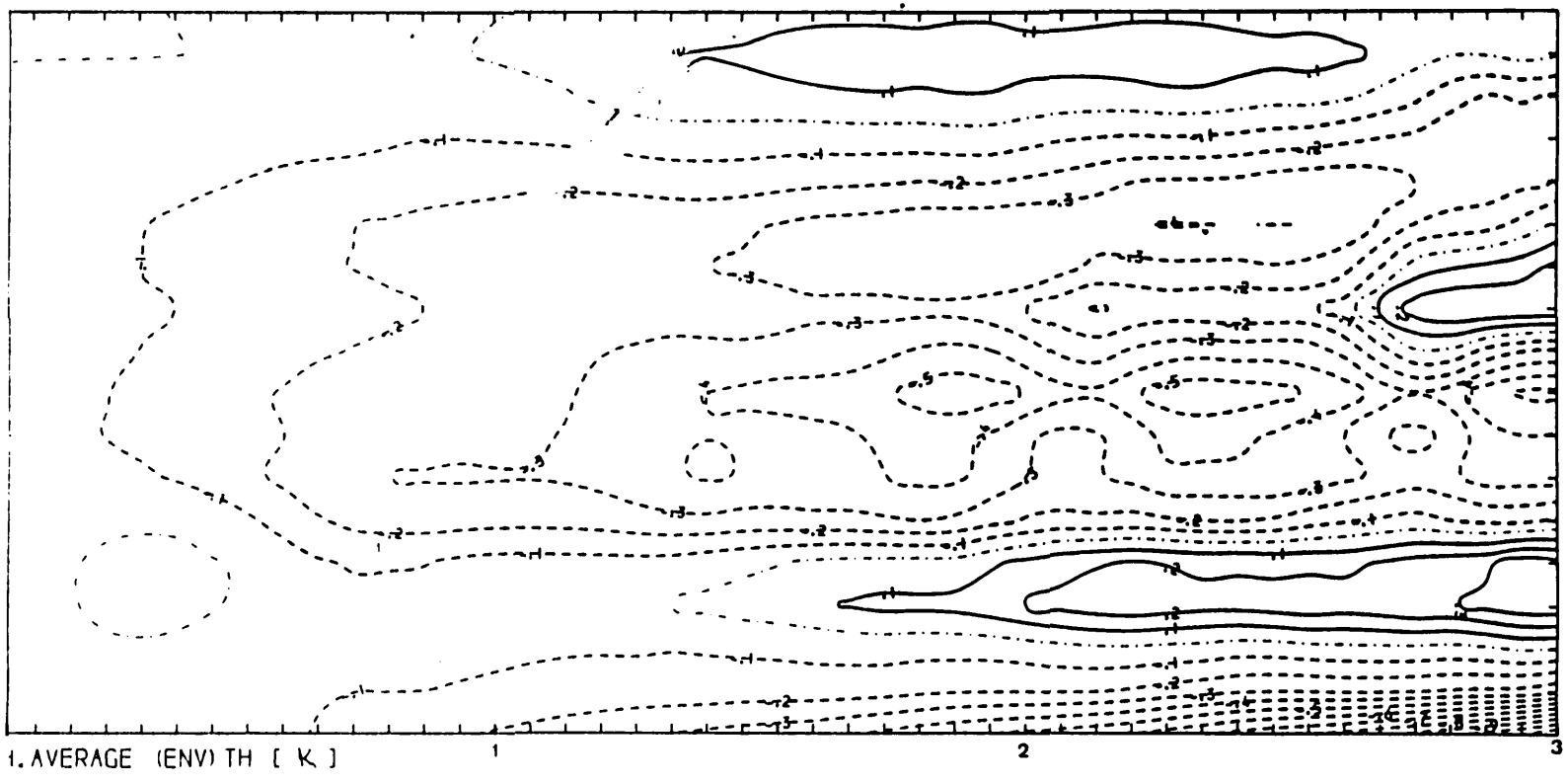


6.15 Horizontal mean rate of change of potential temperature (thin) and latent + subgrid scale heating (thick). Time average for 120-180 min.

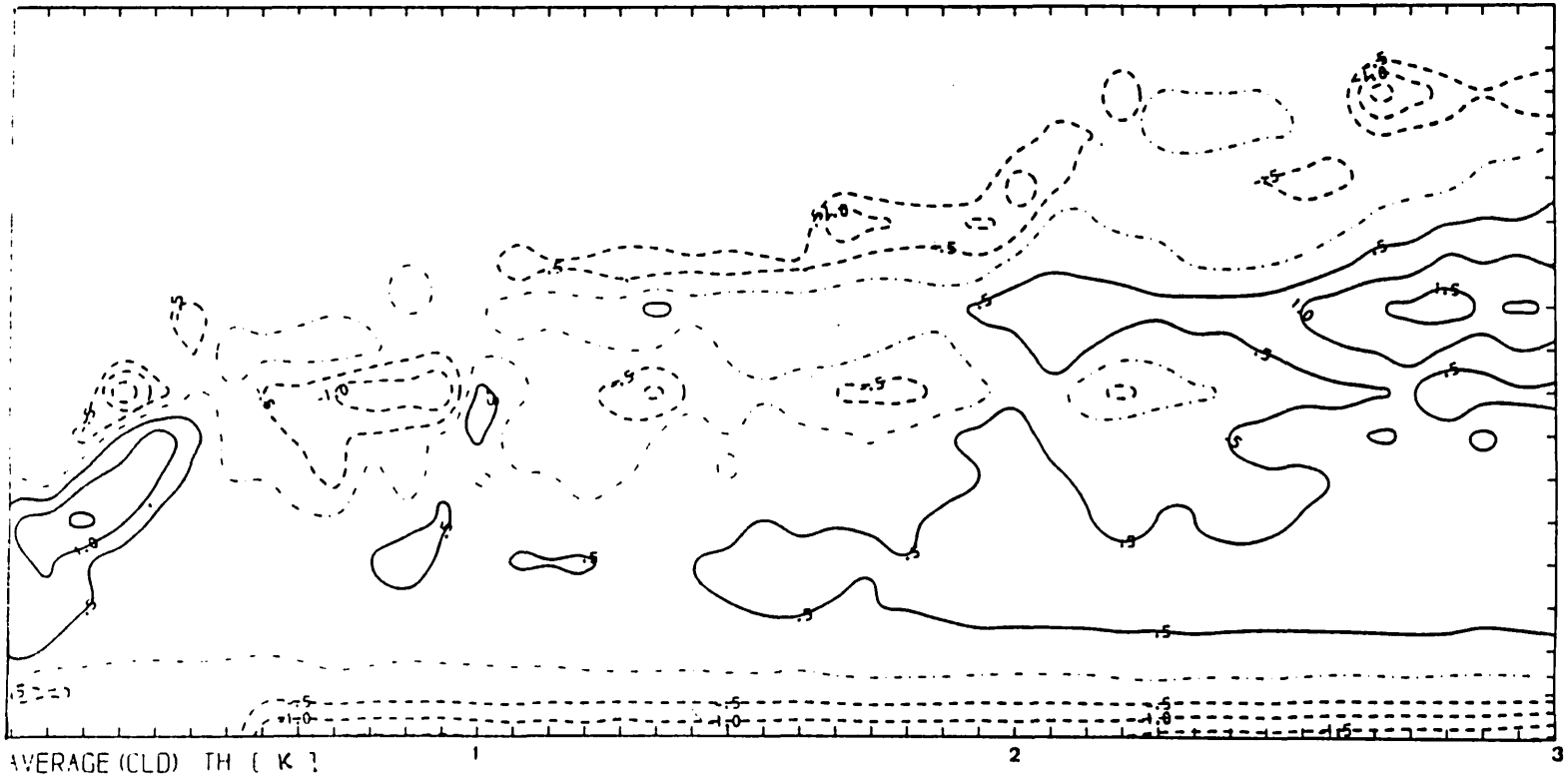
6.16 As fig. 6.15 for water vapour content and condensational + subgrid scale moistening.



6.17a Pressure-time plot of domain mean temperature deviation (0-3 hrs).



6.17b Pressure-time plot as fig. 6.17a for only cloud-free regions.



6.17c As fig. 6.17a for cloud.

mean warming is due to subsidence in the environment and hence supports the conclusions of Fraedrich (1973) and Yanai et al.(1973).

In the case of the model domain, the contribution of subsidence can be quantified by comparing the environmental warming rate with that of the whole domain. It is found that nearly 80 per cent is environmental, little being contributed by the warming of cloudy air in the lower troposphere. The upper maximum is also mainly subsidence warming with a smaller contribution from the spread of cloudy outflow.

The relative minimum in the warming at 650 mb results from the large amount of detrainment at the jet level. Here clouds evaporate and initially cool the environment but during the second hour a steady state is reached and the mean temperature remains constant thereafter. The balance at this level is between detrainment evaporative cooling and subsidence warming. Below and above this detrainment level, subsidence warming is not counteracted and provides net warming. Immediately above the upper warming layer at 200-300 mb is another detrainment cooling layer but this is comparatively weak. In the lowest 100 mb there is a gradual cooling of 10^{-4} K/s due to the spread of unsaturated cold downdraught outflow air.

6.5.3 Mean Moisture Content Changes

As seen in fig. 6.16, there are two maxima in the moistening rate at levels of 400 and 650 mb with magnitudes of 10^{-4} g/kg/s. The lower maximum corresponds to the jet detrainment level and approximately coincides with the heating minimum, being the result of evaporation. The 400 mb moistening is the effect of cloud top outflow, being almost entirely a consequence of the increase in cloud water vapour rather than environmental water vapour. This indicates that little evaporation occurs in this higher outflow probably because of its large volume and the low saturated mixing ratio at these altitudes.

As with heating, the lower troposphere is dominated by environmental processes. Below 750 mb subsidence drying becomes more important than detrainment moistening in the environment and from 850

mb downwards the domain drying rate is positive as a result of both environmental subsidence and downdraught transport.

The lack of net moistening at 500 mb may be explained by an equilibrium between cloud growth at this level and subsidence drying in the surroundings. This is supported by the environment's pressure-time moisture plot (fig. 6.18) which shows drying at 500 mb towards the end of the simulation while cloud volume increases and the cloud area mean moisture remains constant, i.e.total cloud moisture increases.

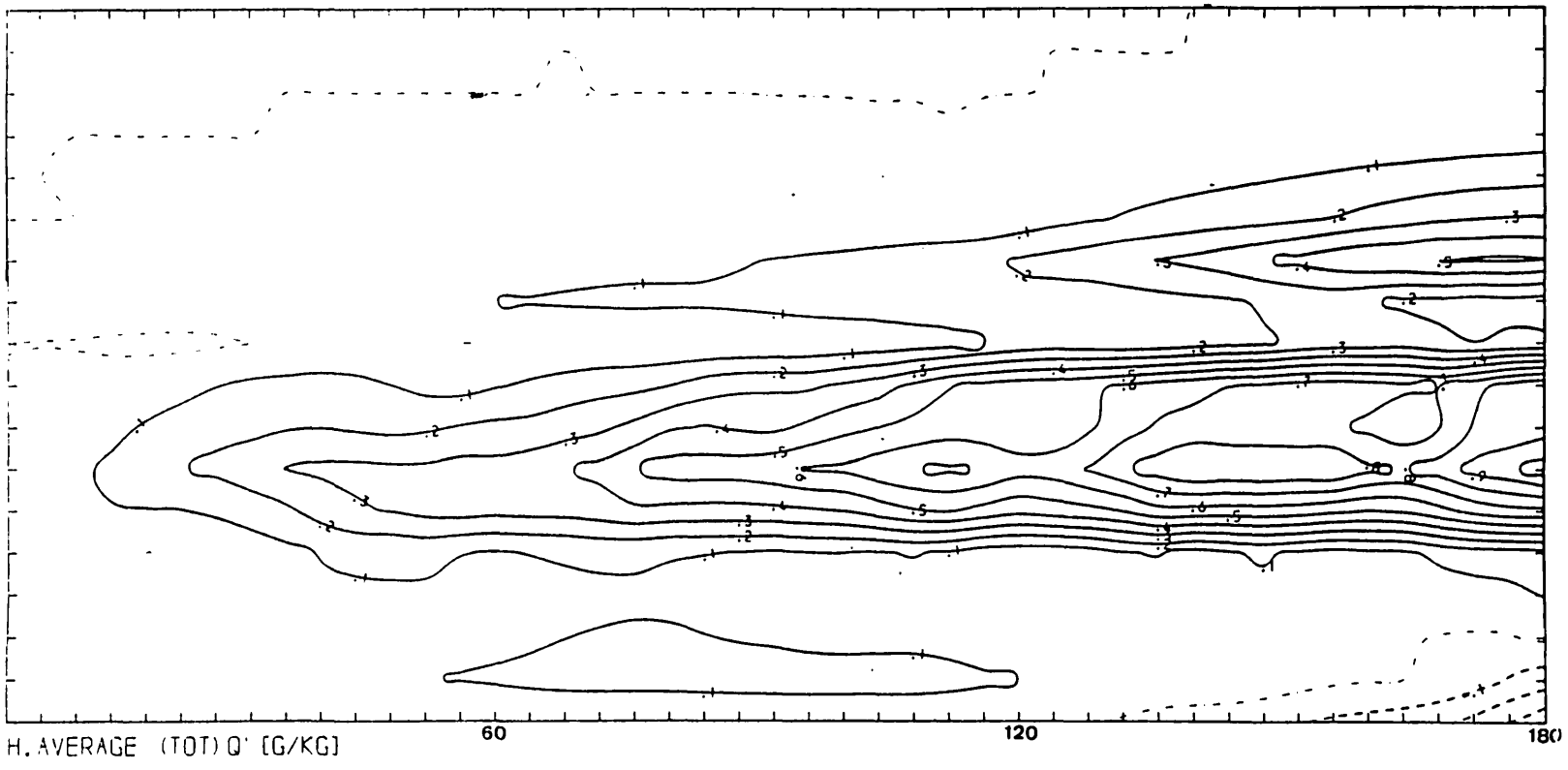
In summary, the mean rates of change of temperature and moisture are dominated by the effects of subsidence, detrainment and upper and surface outflows.

Subsidence causes warming and drying above, below and in the jet where detrained cloud air cools and moistens. Cloudy outflow warms and moistens the upper layers as evaporation at this height is rather limited in its effect. The low-level unsaturated downdraught outflow provides a net cooling and drying in the surface layer.

6.5.4 Latent Heating Profile

Evaluation of the net resolved fluxes at each grid level makes it possible to determine the combined effect of latent heating and subgrid scale mixing. The latter is comparatively unimportant as can be seen from the similarity of the heat source and moisture sink profiles thus calculated. Note that the heat source (fig. 6.15) should be multiplied by $c_p\pi/L$, which is a function of pressure, to be directly comparable with the moisture sink (fig. 6.16).

The profiles show a relative minimum in latent heating at 650 mb which is clearly the result of enhanced evaporation at that level. Nevertheless, the net effect in all but the lowest 50 mb and possibly at cloud top is that of condensation. The rate of latent heating is far greater than the observed change in temperature demonstrating the steadiness of mean saturated ascent in the domain. In this sense, the



6.18 As fig. 6.17a for moisture content deviation.

band can be seen as having mean properties similar to a steady flow with saturated ascent and unsaturated descent. Even in the development stages, the local time derivatives are much smaller than the Lagrangian (substantial) derivatives.

The positions of latent heating maxima and minima correspond very closely with those of net mass flux. This would be expected because, in a quasi-steady state, the greater the mass of ascending air, the more condensation is required to convert the water vapour into liquid to avoid a net local humidity increase. The latent heating profile is a reflection of the saturated moisture flux convergence, which in turn is dominated by the vertical advection of q_s, which is itself highly dependent on the cloud mass flux.

Alternatively, an approximation for steady updraughts is:-

$$Q = w\,T\,\gamma \qquad \text{(Eq. 6.1)}$$

γ: wet adiabatic lapse rate, $d\phi_w/dz$.
γ and T are smooth functions of height. Therefore, it is expected that maxima and minima in Q(z) should correspond approximately to those in w(z) as long as the cloud mass flux dominates the domain mean vertical mass flux.

6.6 Vertical Transport Properties and Apparent Heat and Moisture Sources

6.6.1 Apparent Heat and Moisture Sources

If the heat and moisture equations are decomposed into horizontal mean and eddy parts and area-averaged over the domain, they become:-

$$\left(\frac{D\bar{\theta}}{Dt}\right)_{\substack{large\\scale}} \equiv \frac{\partial\bar{\theta}}{\partial t} + \bar{u}\frac{\partial\bar{\theta}}{\partial x} + \bar{v}\frac{\partial\bar{\theta}}{\partial y} + \bar{\omega}\frac{\partial\bar{\theta}}{\partial p} \qquad \text{(Eq. 6.2)}$$

$$= \frac{\bar{Q}}{\pi} - \frac{\partial}{\partial x}\overline{u\theta'} - \frac{\partial}{\partial y}\overline{v\theta'} - \frac{\partial}{\partial p}\overline{\omega'\theta'} + \bar{D}_\theta$$

$$\left(\frac{D\bar{q}}{Dt}\right)_{ls} \equiv \frac{\partial \bar{q}}{\partial t} + \bar{u}\frac{\partial \bar{q}}{\partial x} + \bar{v}\frac{\partial \bar{q}}{\partial y} + \bar{\omega}\frac{\partial \bar{q}}{\partial p} \qquad \text{(Eq. 6.3)}$$

$$= -\frac{c_p \bar{Q}}{L} - \frac{\partial}{\partial x}\overline{uq'} - \frac{\partial}{\partial y}\overline{vq'} - \frac{\partial}{\partial p}\overline{\omega' q'} + \bar{D}_q$$

$$Q \equiv T D\phi/Dt \quad ; \quad \phi = \ln\theta \quad ; \quad \pi = T/\theta = \left(\frac{P}{1000_{mb}}\right)^{R/c_p}$$

- where Q (=TDϕ/Dt) is the latent heating rate and D is subgrid scale smoothing.

Radiative cooling is not included in the simulations' equations. These follow Yanai, Esbensen and Chu (1973) and Soong and Ogura (1980). The terms on the left hand side represent the change expected in the mean from area-averaged velocities and gradients. The right hand side shows that in addition to latent heating, horizontal and vertical eddy flux convergence and subgrid scale smoothing can contribute to the mean change. In practice, it is found that, provided the height of a grid level is small enough compared to the domain's length, mean horizontal eddy flux convergence is negligible compared to the vertical eddy term.

The apparent heat source, Q_1, and moisture sink, Q_2, are therefore defined as follows:-

$$\frac{Q_1}{\pi} \equiv -\frac{\partial}{\partial p}\overline{\omega'\theta'} + \frac{\bar{Q}}{\pi} + \bar{D}_\theta \qquad \text{(Eq. 6.4)}$$

$$\frac{c_p Q_2}{L} \equiv \frac{\partial}{\partial p}\overline{\omega' q'} + \frac{c_p \bar{Q}}{L} - \bar{D}_q \qquad \text{(Eq. 6.5)}$$

It can be seen that the presence of eddies and smoothing (which is comparatively small) effectively decouples the heat and moisture equations in the large scale mean and their apparent sources are no longer simply related by latent heating because of these smaller scale transports. Determining the apparent heat source is not sufficient to define the apparent moisture sink.

The simulation results can be used to determine the vertical profiles of these eddy transports and hence to evaluate the role of clouds in re-distributing heat and moisture in an atmospheric column. First, the time mean behaviour in the third hour of the simulation will be analysed. Later, the time development is considered because even in the maturing stage after two hours there is a gradual evolution of the overall properties.

6.6.2 Mean Transports in the Mature Stage

The horizontally averaged vertical flux convergence was divided into a mean component and vertical eddy component. The total was split thus:-

(Eq. 6.6)

$$\overline{\nabla . \underline{v}\phi} = \overline{\underline{v}} . \overline{\nabla \phi} + \overline{\frac{\partial}{\partial x} u\phi'} + \overline{\frac{\partial}{\partial y} v\phi'} + \overline{\frac{\partial}{\partial p} \omega'\phi'}$$

(1) (2) (3) (4)

(1) + (2) + (3) = mean flux divergence

(4) = eddy vertical flux divergence

Of the terms in the mean, the largest is the mean vertical advection (1) and all the smaller terms were absorbed into this except for (4) which is the term required in the evaluation of apparent sources and sinks.

Having determined these quantities at each of the 18 model levels at 4 min intervals, the results were time-averaged between 120 and 180 min to leave only the essential features.

6.6.3 Heat Transport Properties

The profile of Q_1 (fig. 6.19) is very similar to that of latent heating (fig. 6.15) because in the case of heat transports, the eddy term is relatively small throughout the troposphere. The eddy flux divergence of heat is positive between 650 and 900 mb and negative between 250 and 550 mb. This is the result of updraught transports of buoyant air from the lower troposphere to the outflow layer. There is also some structure in the profile at jet level indicating that heat is transported into the 600 mb region, probably by medium clouds and out of the 500-550 mb layer by upper cores which entrain moistened jet air. The eddy detrainment of heat and jet level re-entrainment is a real feature of the simulation because it shows in a one hour mean profile of eddy heat flux convergence aswell as in an independent band simulation with a smaller domain.

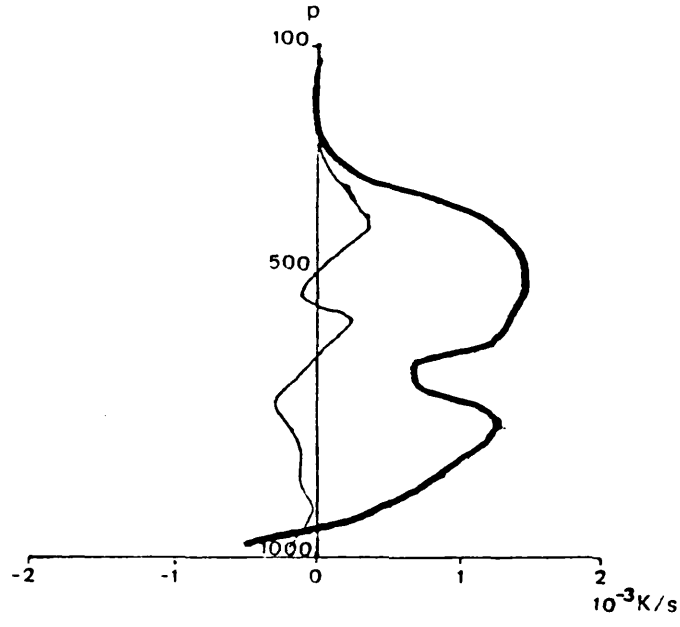
In terms of eddy flux, which is the vertical integral of eddy flux divergence, this shows a minimum at 550 mb of $\partial\theta/\partial t$ which is the combined effect of updraughts being cooled and slowed by evaporation. The noticeable gravity wave generation at this level confirms that much of the rising air at these heights is made negatively buoyant by cloud evaporation, thus reducing the mean eddy correlation.

The net effect of eddies on the apparent heat source is to slightly reduce the lower actual heat source and increase the upper heat source producing a net maximum in Q_1 at about 450 mb.

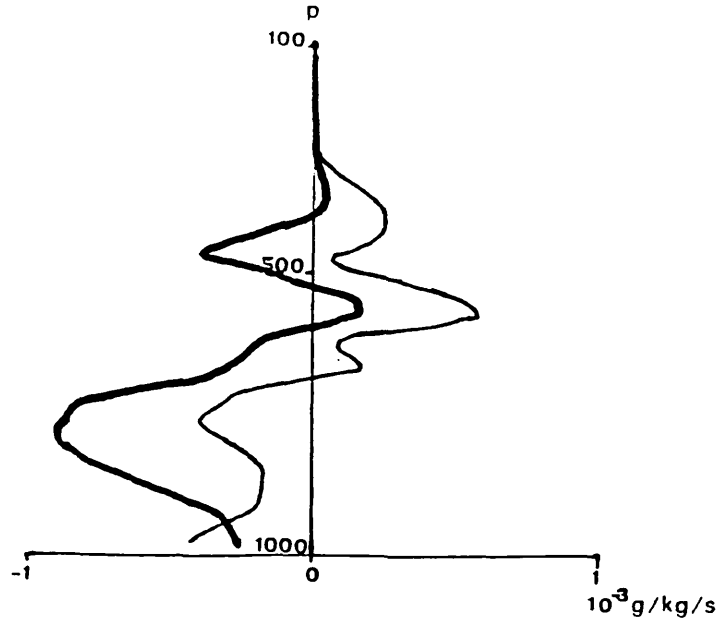
6.6.4 Moisture Transport Properties

The apparent moisture sink, Q_2 (fig. 6.20), is a maximum in the lower troposphere where, conversely to the heat source, eddies reinforce the condensational sink by transporting moisture out of this layer and oppose the upper level sink such that the net maximum in Q_2 is at about 800 mb.

Also in contrast to heat, the eddy moisture flux divergence is almost the size of the condensation term (fig. 6.16) so that Q_2 is



6.19 Q_1 (thick) and eddy flux convergence of heat (thin). 120-180 min.



6.20-Q_2 (thick). and eddy flux convergence of moisture (thin). 120-180 min.

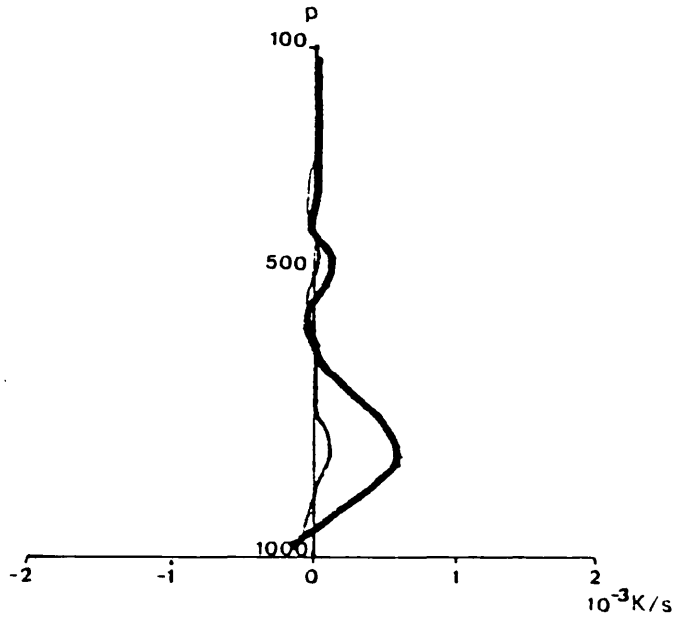
rather different from Q. Eddy divergence has two maxima corresponding to the drying effect of downdraughts at the surface and updraughts in the lower troposphere. Mean moisture convergence supplies water vapour at about the rate that it is removed by the combined effects of condensation and updraught transports.

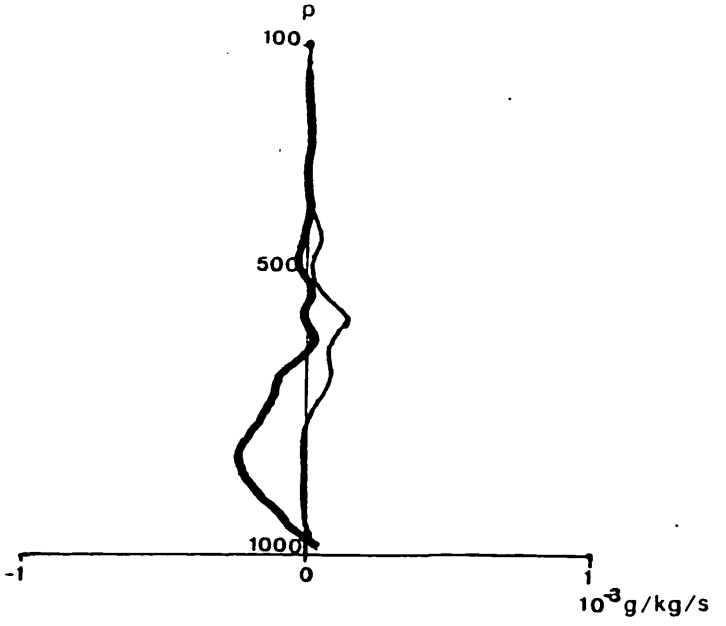
The complicated profiles of the eddy and mean moisture transport terms in the middle and upper troposphere are a consequence of the non-monotonic moisture gradient at these heights(fig. 3.7). There are reverses in the mean gradients at 550 and 400 mb where the moisture content observed increased with height. It would be expected, therefore, that the eddy moisture flux convergence should dominate over mean vertical advection at these heights since there is a net transport of water vapour into these levels despite the negative local vertical gradient. Between these levels it is the mean moisture convergence which is more important.

6.7 Time Development of Mean Heating and Moistening Profiles

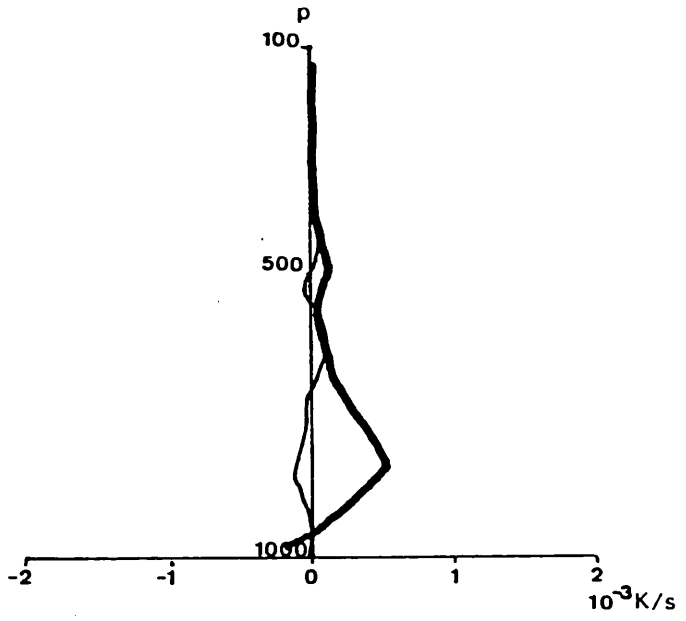
The above results describe the mean band behaviour in the third hour of the simulation. If the same profiles are calculated for the second hour, an indication is given of the time development. Note that up until the third hour there was no net mass flux above the jet (see fig. 6.4) although isolated weak cores did reach these levels. The net latent heating (fig. 6.21) shows that net condensation only exists up to 650 mb and the domain averaged latent heating rate is only about 30-40 per cent of that in the third hour because of both the reduced size and activity of the cloud area.

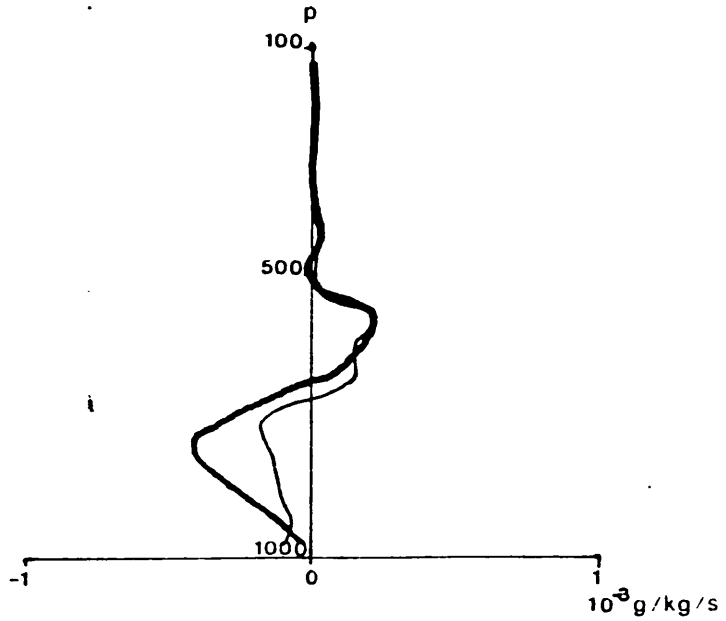
Heat and moisture are transported by eddies (short updraughts) from the lower to mid-troposphere (fig. 6.22) with net moistening occurring between 550 and 700 mb. More detailed data show that it is only after 100 min that net condensation occurs above the jet and eddies start to transport heat and moisture into upper levels. This upper condensation maximum grows throughout the third hour (fig. 6.15) and by 180 min is greater than the lower maximum being similar to the net mass flux development. It is interesting to compare these results





6.21 As 6.15 and 6.16 for 60-120 min.





6.22 As 6.19 and 6.20 for 60-120 min.

with those presented by Soong and Tao (1980) for a GATE cluster. They find a similar bi-modal structure in Q_1 and Q_2 with the upper maximum in Q_1 eventually becoming predominant 12 hours after initial formation. The maximum in Q_2 remains in the lower troposphere despite the upper development.

Thompson et al. and Frank (1983) present respectively an easterly wave and ITCZ composite of Q_1 and Q_2 showing, similarly, that in the mature stages of wave-related ITCZ convection the maximum of Q_1 is at about 500-600 mb and that in Q_2 is at 800-850 mb in agreement with the model results. As has been explained, this difference in the profiles of apparent heat and moisture sources comes from the upper tropospheric reinforcement of latent heating by heat flux eddies and the lower tropospheric drying being added to by moisture flux eddies. The absolute values of Q_1 and Q_2 in the simulation are actually 3-4 times those of Soong and Tao (1980) and ten times those of Thompson et al. and Frank and this corresponds to the increased sizes of domain considered in the latter studies. The model domain has an unrepresentative ratio of cloud to environment but the qualitative similarities in the results show that the structure of the Q_1 and Q_2 profiles are primarily determined by cloud processes and the immediate environment's response.

6.8 Moist Static Energy

Subtraction of Q_2 from Q_1 eliminates latent heating and leaves the eddy flux convergence of moist static energy, h, defined by:-

$$h = c_p T + gz + Lq \qquad \text{(Eq. 6.7)}$$

$$Q_2 - Q_1 = -\frac{\partial}{\partial p}\overline{\omega' h'} + \text{subgrid scale terms} \qquad \text{(Eq. 6.8)}$$

This is a useful quantity because it is almost conserved by unmixed air parcels. This follows from:-

$$dh = c_p dT + g dz + L dq \qquad \text{(Eq. 6.9)}$$

compared to:-

$$TdS = -Ldq = c_p dT - dp/\rho \quad \text{2nd Law of Thermodynamics} \qquad \text{(Eq. 6.10)}$$

where $dp/\rho = -gdz$, the hydrostaic approximation is made.

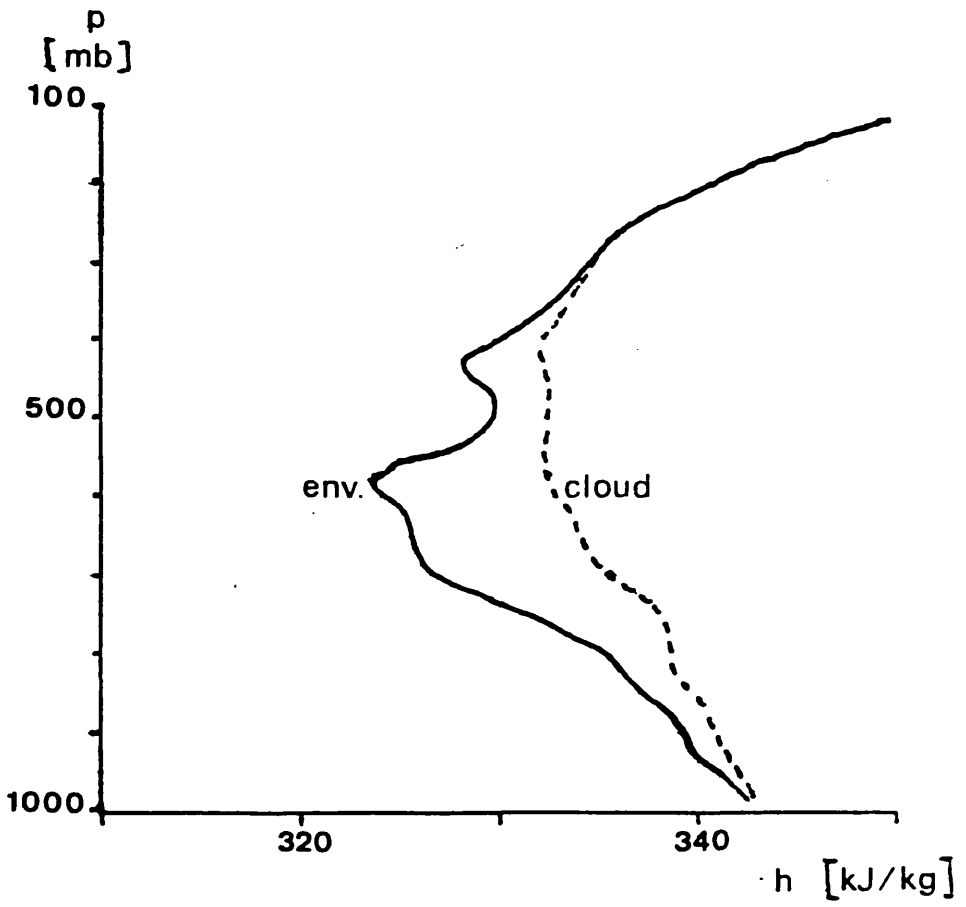
The moist static energy profile (fig. 6.23) has a minimum at 600 mb. Comparison with the value in cloudy air at 180 minutes shows that the updraughts transport h to 400 mb but with a significant degree of entrainment as is demonstrated by the variation of h with height in clouds.

The pressure-time plot of moist static energy (fig. 6.24) shows a gradual decrease below 850 mb due to the downward transport of air into this layer and overall increases around 675 and 425 mb due mainly to jet level detrainment of updraughts in the former case and cloud top outflow in the latter. Thompson et al. also show a low-level apparent sink of moist static energy below 800 mb in the E.Atlantic. In the simulation the upper apparent source is split because of the fluctuations in the environment's moisture profile but generally agrees with that found from the easterly wave composite analysis by Thompson et al. being at around 500 mb.

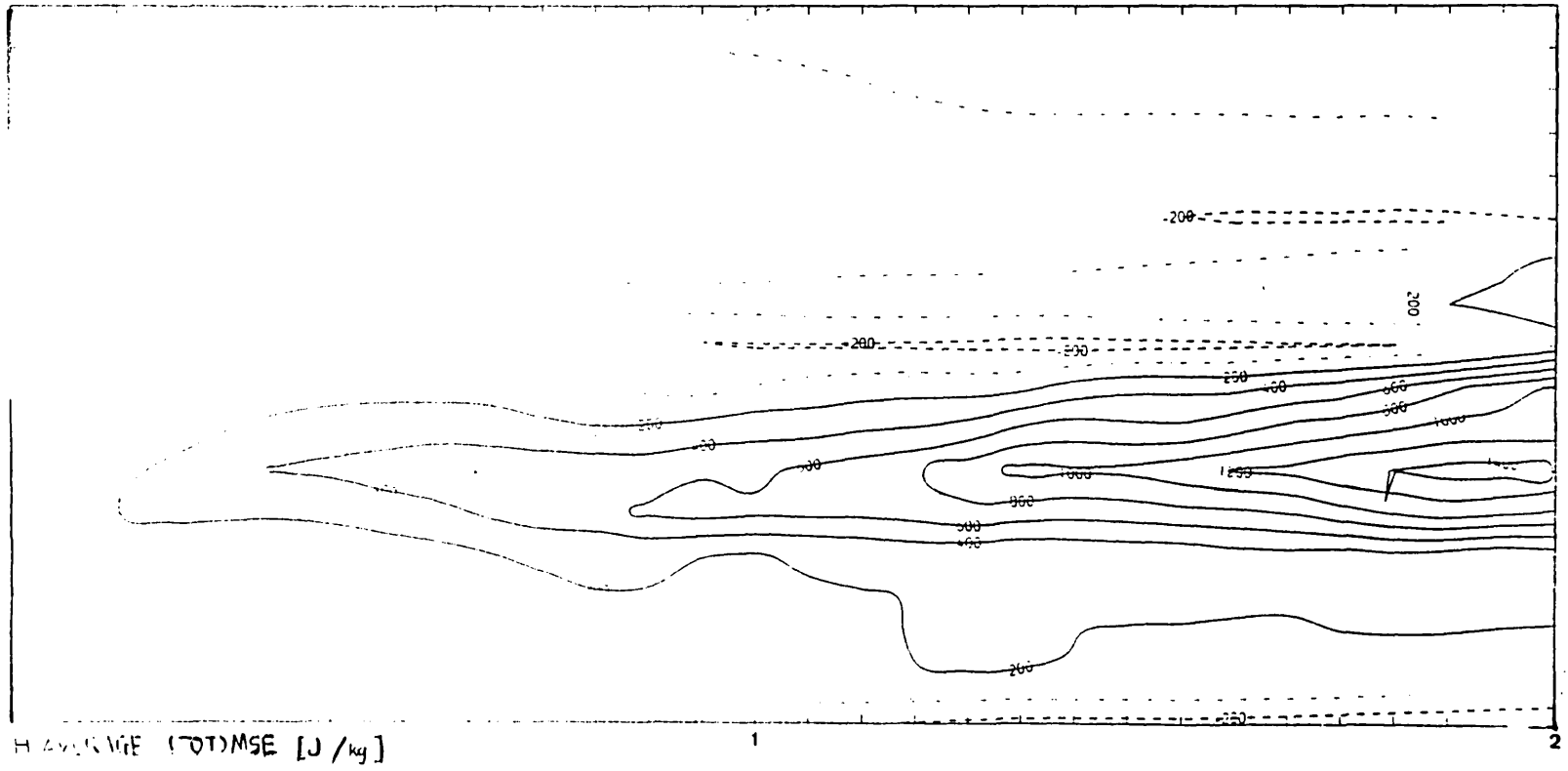
6.9 Summary of Mean Transport Properties

The simulated band is in a quasi-steady state; latent heating and drying being almost cancelled by ascent cooling and moistening. The effects of compensating subsidence are important in the heat and moisture balances and countered by those of mid-level detrainment. The upper and surface cloud outflows also have a considerable effect on the net change in temperature and moisture profiles.

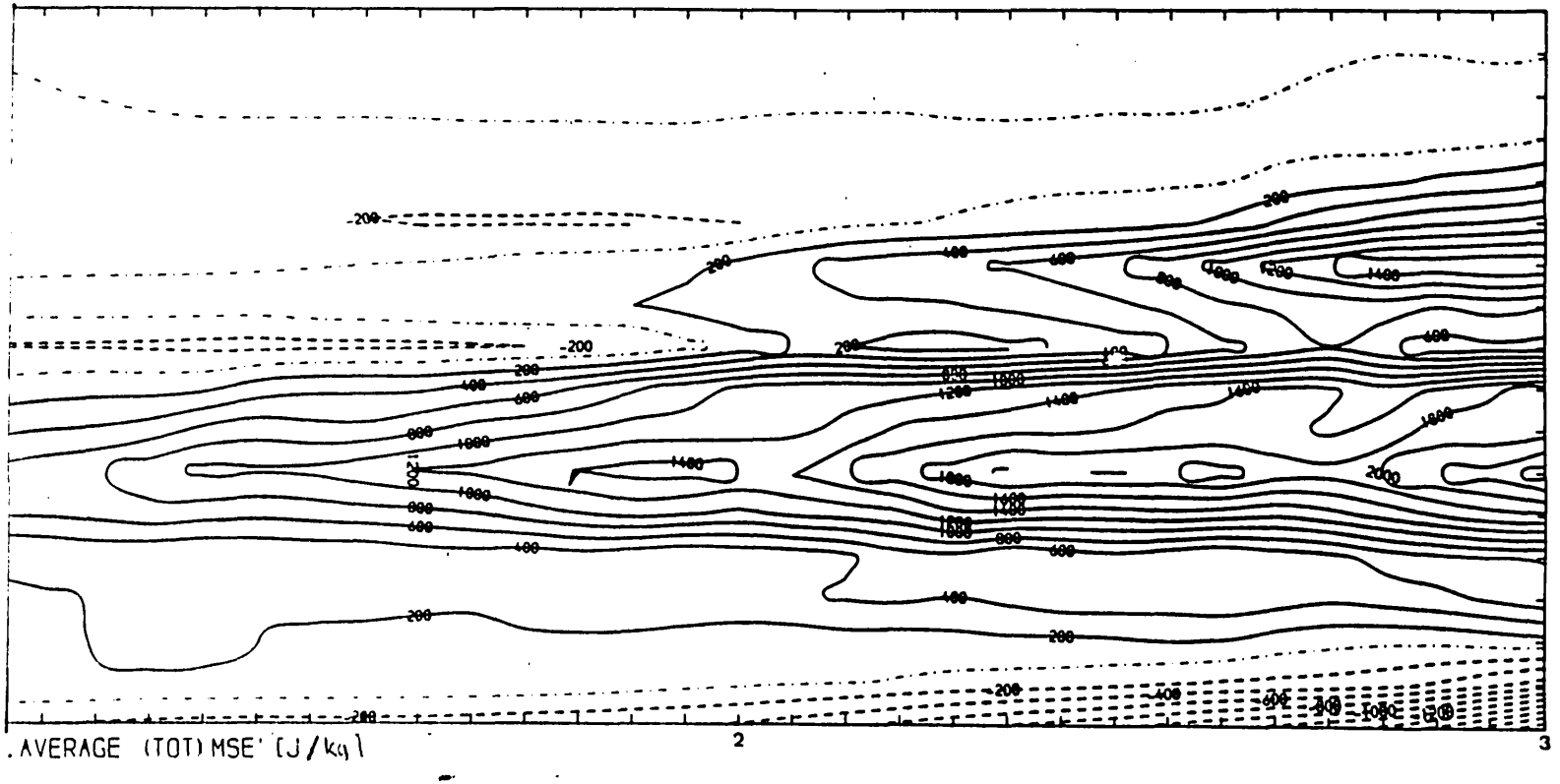
Mean convergence provides low-level moisture and its condensation produces heat which is transported by eddies to mid and upper levels. The eddy moisture fluxes are of a similar magnitude to the condensational term in Q_2 whereas Q_1 is primarily latent heating. This was also found by Ogura (1982) extending Soong and Tao's work.



6.23 Moist static energy profile (environment and cloud at 180 min.).



6.24a Pressure-time plot of domain mean moist static energy deviation (0-2 hrs).



6.24b As fig. 6.24a for 1-3 hrs.

Yanai et al.(1973) proposed that the overall lower tropospheric drying effect of deep clouds, produced by updraught transports and compensating subsidence, is probably counteracted by moisture supplied by smaller clouds in the region which are thus necessary for the maintenance of deep convection. This study confirms that mid-level moistening is the result of such cloud detrainment but most of the moisture is supplied by large scale convergence at lower levels.

CHAPTER 7
CONCLUSION

7.1 Large Scale Ascent and Tropical Band Convection

This numerical study has demonstrated the necessity of imposing the effects of large scale motion on a cloud model domain when attempting to simulate ITCZ convection. Background forcings have been shown to have a critical role in the development of mesoscale bands commonly observed in the GATE area. Hadley cell and easterly wave convergence may both contribute to the 1-2 cm/s lower tropospheric ascent which observational studies indicate to exist before any deep convection.

In this thesis, the associated convergence/divergence profile was taken as a background state on the domain scale with cloud motions superimposed and having no feedback effect on the specified divergence profile. This is a reasonable assumption in view of the long time scale of easterly waves and ITCZ convergence compared to that of the simulation. The spatial scale of this imposed motion was also taken to be large in comparison with the domain's and thus it provided a uniform ascent across this region. Observations support the specification of horizontal convergence in only the meridional direction through $\partial v/\partial y$.

It was found that without any imposed ascent, the shear below the easterly jet overcame convection and only weak clouds were able to survive producing rather less rain than was observed. The shear decelerated updraughts which thus mixed with environmental air in sufficient quantities to lead to evaporative cooling and loss of buoyancy. This happened despite the large CAPE in the thermodynamic sounding which would allow buoyant unmixed ascent up to 200-250 mb in the absence of shear. Increasing the resolution from 100 to 50 mb alone showed it was insufficient to just have a more realistic mixing rate; the lower updraughts themselves were not energetic enough.

The addition of mesoscale fluxes to the scalar fields provided

simulations in which continuous growth was possible throughout the three hours. There were found to be two primary reasons for this enhanced activity, namely ascent cooling and moisture convergence. Destabilisation at 700-800 mb enables updraughts to become more buoyant relative to an environment with lifting imposed. Lifting opposes the warming effect of compensating subsidence providing more CAPE than would exist without such background ascent. In larger scale terms, this can be seen as an opposition to compensating subsidence by trade wind or easterly wave induced convergence; i.e. an ITCZ environment is less liable to subsidence than one not subjected to such larger scale motions.

Instead of the imposed ascent having the effect of cooling the atmosphere by up to 0.4 K/hr, the mean cloud-free air's temperature remained steady until after one hour when net subsidence started. This is shown by the increasing environmental temperature and dryness between 650 and 850 mb.

During the whole development, the cloud's compensating subsidence is almost exactly enough to balance the imposed ascent. This implies that all the available potential energy generated by lifting is immediately converted into convective kinetic energy. Hence, cloud activity is forced to increase at a rate dependent on the potential energy supplied by this steady ascent.

The second effect of surface convergence is that of moisture supply. This slightly lowers the lifting condensation level and increases the potential buoyancy of low-level air allowing updraughts to become warmer.

Forcing therefore not only maintains the convection against decay but also enables it to grow until eventually organisation takes over. At this stage, about two hours into the simulation, the mesoscale pressure field generated by latent heating causes the mean convergence and vertical mass flux to become five to ten times greater than that imposed. The effects of forcing remain important because there is still a significant reduction in environmental subsidence which is

slightly smaller in magnitude than domain-averaged ascent (i.e.10-20 cm/s). There is also evidence that the final intensity reached by the convection may be determined by the degree of forcing.

7.2 Summary of Simulated Band Structure

The numerically simulated convection grew in three hours from a 4 km initial perturbation to a 40 km east-west band of cumulonimbi. This had a well-defined front between downdraught outflow air and surface boundary layer inflow. The outflow occupied only the lowest 500 m of the domain and was 2 K cooler than the ambient air but was prevented from propagating southwards by the surface southerly component of 5 m/s. The surface meridional shear and lack of meridional wind in the lower and mid-troposphere enabled the developing cells to remain close to the front thus sustaining it with a continuous downdraught supply.

In the mature stage, ascent took place almost uniformly along the front and individual updraught cores were not easily distinguishable below 2 km. This lower ascent band had a distinct northward slope and there was a significant rearward acceleration in much of the updraught air probably influenced by a mesoscale pressure gradient in the band. The slope was important in allowing rain to fall behind the ascending zone driving downdraughts through liquid loading and rain evaporation; these being equally important forces. Much of the downdraught reaching the surface originated around 850 mb indicating a shallow rain-driven circulation.

Cloud top outflow was strongly influenced by the north-easterly upper jet. Most cloud spread northwards as a warm anvil underneath the jet but a large volume was also entrained by this jet and carried south-westwards.

The band also showed an east-west structure, cloud development at the western end being rather stronger than that further east. This was a direct result of the effect of the dry sheared environment on convection in the lowest 4 km. Eastern updraughts were suppressed by

the shear and detrained completely in the jet. This moistened the 600-700 mb layer and enabled clouds to grow further west with less evaporation and hence less loss of buoyancy. In the case of the simulation, the alignment parallel to the easterly jet was vital to cloud growth because it enabled downwind cells to benefit from the moisture transports of the easternmost updraughts.

The zonal momentum component appeared to be quasi-conserved by updraughts and downdraughts in the highly sheared layer producing linear couplets of high vorticity at these cores' boundaries. Trajectories showed most updraught air to be accelerated eastwards by the 600 mb jet and retain this momentum into the upper outflow. The instantaneous updraught structure showed them not to be significantly tilted in the east-west plane but moving westwards at about 6 m/s, comparable with the observed rain area motion.

From the domain scale viewpoint, the primary time-dependent changes in the horizontal mean heat and moisture profiles come from four almost equally important processes.

(1) Environmental subsidence throughout the mid-troposphere - warming and drying.

(2) Detrainment of cloud primarily at jet level, some at cloud top - cooling and moistening.

(3) Cloud top and anvil outflow - warming and moistening.

(4) Downdraught outflow in the boundary layer - cooling and drying.

The last two are probably only important in the cloud development phase which was the part simulated. Later the anvil and cold pool will cease to grow and then will no longer contribute as much to the mean time-dependent behaviour. The subsidence and detrainment, however, are continuous processes while clouds persist and are therefore more likely to be important in long-term budgets.

The apparent heat source and moisture sink are found respectively in the upper mid-troposphere and lower troposphere, consistent with observations. This was explainable in terms of the upper tropospheric heating and lower tropospheric drying by eddy transports adding to the latent heating and drying provided by net condensation which occurs throughout the troposphere (except in the boundary layer). These eddies are primarily the effect of deep updraughts in the mature band.

7.3 Environmental Conditions Favourable for Stationary Band Development

The commonness of these convective features shows that in the GATE region there can be few coincidences required for their formation. They must depend only on regularly observed occurrences and should not be very sensitive to slight differences in the wind or thermodynamic profile.

Easterly waves are responsible for most of the changes in the basic wind profile and the part of the wave between the ridge and trough is the commonest position for band development. It is in this phase that the easterly wave transports easterly momentum at 700 mb southwards into the GATE area thus increasing the zonal shear below 700 mb to typically 6 m/s/km, almost double its time mean value. The surface westerly monsoonal flow remains nearly constant.

In addition, enhanced surface convergence occurs in the south-westerlies ahead of the wave trough and mid-level divergence takes place as a dynamical consequence of air overtaking the wave. This produces conditions favourable for convection by providing wave-induced mean ascent in the lower troposphere which adds to the constant background Hadley convergence. Hence the trade inversion is eroded and deep convection made possible.

The low-level zonal shear, surface northerly shear and conditionally unstable environment with forced ascent are thus all natural consequences of easterly wave dynamics and seem also to be the major requirements for band development. The zonal shear component

determines alignment through cell motion and protection provided by upwind cells' transports into the dry jet. The meridional shear allows relative stationarity between the updraughts and the gust front.

The ENE-WSW alignment of nearly all GATE bands is consistent with the jet direction (and lower tropospheric shear direction) ahead of easterly wave troughs and most are found around wave category 3±2 (where 4 denotes trough, 8 denotes ridge). Aswell as forming in the southerly surface flow around 7 N there seems to be another preferred latitude at 10 N, the ITCZ surface confluence line, and it is quite usual, as shown by Chen and Ogura (1982), for co-existing bands to be seen in the GATE area at both these latitudes.

7.4 Conclusion and Further Work

The purposes of this study were firstly to develop a better understanding of the processes involved and environmental conditions required for a particular, but typical, observed case of tropical band convection and secondly to verify the ability of the Imperial College Cloud Model to reproduce these systems numerically.

Probably the most interesting modelling result was the sensitivity of convection to background low-level convergence despite the relatively small upward motion associated with this compared to that in updraughts. These numerical results can be interpreted in physical terms and thus the arguments presented for mechanisms should also be applicable to the real tropical atmosphere. This is verified by observations which indicate a sensitivity of convective activity to synoptic scale convergence and show overall similarity with the model band in scale, alignment, stationarity and time development.

There are several ways in which this work can be extended. Firstly, from the numerical modelling viewpoint, domain size or vertical resolution could be increased to reduce numerical inaccuracies which can arise from boundaries and dispersion. It would be hoped and expected that the results obtained in this research do

not depend too much on these purely numerical effects since little activity occurs near boundaries until the end of the third hour and the vertical scale of ascending cells seems to be sufficiently resolved, though it is possible that the surface cold pool may not be. An increase in domain size would also enable the simulation to be extended to a fourth hour or further making it possible to study the beginning of the decay phase.

The analysis of the results obtained so far could also be continued by studying the mean and eddy momentum transfers and time dependence. It has been demonstrated that the components parallel to and perpendicular to the band have diverse behaviours, the latter being more strongly influenced by pressure gradients in the band. So far little quantitative work has been done on momentum budgets in mesoscale tropical systems and parameterisation schemes require more knowledge than at present is available.

Sensitivity tests are needed to demonstrate that the numerically simulated band is not an untypical instance and to find out what range of environmental conditions can support such systems. Changes can be made to the jet strength and meridional surface shear, both of which are important to the dynamics of band convection. The low-level shear is particularly interesting as observations indicate that this component increases rapidly equatorwards and sensitivity of convection to this shear may help to determine the latitude at which bands are formed. The study of the effects of different imposed ascent rates could be extended as at present only three profiles have been compared in their influence (2 cm/s, 1cm/s and no ascent). The initial sounding may also be a critical factor and tests could be done with other thermodynamic profiles representative of the GATE area.

It may be possible to impose forcing by other methods such as through boundary conditions on the pressure field and this could also be a direction for further investigation.

Another direction is to study GATE observational data at the times of other bands and find similarities, possibly simulating other

instances and obtaining a more general description of these occurrences. By finding features common to most bands it would become easier to predict the synoptic situations in which this mode of convection is favoured.

A simplified two-dimensional mathematical model of the Moncrieff and Miller (1976) type could be compared with the transverse section of the band, particularly with regard to momentum transports and the effect of the hydrostatic pressure field on the updraught air.

The number of suggestions, outlined above, for furthering this work demonstrates that this thesis is not a complete study but hopefully the results presented can serve as a basis for future research into this important and interesting topic.

REFERENCES

Beebe, R.G. and F.C. Bates, 1955: A mechanism for assisting in the release of convective instability. MWR 83 1.

Betts, A.K., 1982: Cloud thermodynamic models in saturation point coordinates. JAS 39 2182.

Burpee, R.W., 1972: The origin and structure of easterly waves in the lower troposphere of North Africa. JAS 29 77.

Chang, S.W. and H.D. Orville, 1973: Large-scale convergence in a numerical cloud model. JAS 30 947.

Charney, J.G. and M.E. Stern, 1962: On the stability of internal baroclinic jets in a rotating atmosphere. JAS 19 159.

Chen, Y.-L. and Y. Ogura, 1982: Modulation of convective activity by large-scale flow patterns observed in GATE. JAS 39 1261.

Chen, C.-H. and H.D. Orville, 1980: Effects of mesoscale convergence on cloud convection. JAM 19 256.

Chong, M. and J. Testud, 1983: Three-dimensional wind field analysis from cloud Doppler radar data. JCAM 22 1227.

Clark, T.L., 1979: Numerical simulation with a three-dimensional cloud model: Lateral boundary condition experiments and multi-cellular severe storm simulations. JAS 36 2191.

Estoque, M.A. and M. Douglas, 1978: Structure of the intertropical convergence zone over the GATE area. Tellus 30 55.

Fraedrich, K., 1973: On the parameterisation of cumulus convection by lateral mixing and compensating subsidence. JAS 30 408.

Frank, W.M., 1978: The life-cycle of GATE convective systems. JAS 35 1256.

Frank, W.M., 1983: The structure and energetics of the east Atlantic intertropical convergence zone. JAS 40 1916.

Harlow, F.H. and J.E. Welch, 1965: Numerical calculation of time-dependent viscous incompressible flow of fluid with free surfaces. Phys. Fluids 8 2182.

Houze, R.A. and C.-P. Cheng, 1977: Radar characteristics of tropical convection observed during GATE: mean properties and trends over the summer season. MWR 105 965.

Kessler, E., 1969: On the distribution and continuity of water substance in atmospheric circulation. Met. Monog. No.32 AMS 84.

Klemp, J.B. and R.B. Wilhelmson, 1978: The simulation of three-dimensional convective storm dynamics. JAS 35 1070.

Kreitzberg, C.W. and D.J. Perkey, 1977: Release of potential instability: Part II. The mechanism of convective/mesoscale interaction. JAS 34 1569.

Kung, E.C. and H.A. Burgdorf, 1978: Maintenance of kinetic energy in large-scale tropical disturbances over the eastern Atlantic. QJ 104 393.

Kuo, H.L., 1949: Dynamical instability of two-dimensional non-divergent flow in a barotropic atmosphere. JM 6 105.

Lemone, M.A., 1983: Momentum transport by a line of cumulus. JAS 40 1815.

Lin, C.C., 1945: On the stability of two-dimensional parallel flows.

Q. Appl. Math. 3 117.
Ludlam, F.H., 1980: Clouds and storms. Penn State.
Mansfield, D.A., 1977: Squall lines observed during GATE. QJ 103 569.
McBride J.L. and W.M. Gray, 1978: Mass divergence in tropical weather systems. Part II: Large-scale controls on convection. QJ 106 517.
Miller, M.J., 1974: On the use of pressure as vertical co-ordinate in modelling convection. QJ 100 155.
Miller, M.J., 1978: The Hampstead storm: A numerical simulation of a quasi-stationary cumulonimbus system. QJ 104 413.
Moncrieff, M.W. and M.J. Miller, 1976: The dynamics and simulation of tropical cumulonimbus and squall lines. QJ 102 373.
Newton, C.W. and H.R. Newton, 1959: Dynamical interaction between large convective clouds and environment with vertical shear. JM 16 483.
Norquist, D.C., E.E. Recker and R.J. Reed, 1977: The energetics of African wave disturbances as observed during Phase III of GATE. MWR 105 334.
O'Brien, J.J., 1970: Alternative solutions to the classical vertical velocity problem. JAM 9 197.
Ogura, Y., 1982: A modelling study of mesoscale convective systems. Proc. Symp. Mesoscale Modelling, Norman, Oklahoma, 1982.
Ogura, Y., Y.-L. Chen, J. Russell and S.-T. Soong, 1979: On the formation of organised convective systems observed over the eastern Atlantic. MWR 107 426.
Pearson, R.A. and S. O'Connor, 1977: A numerical dynamical instability. MWR 105 301.
Potter, D., 1973: Computational Physics. Wiley.
Reed, R.J., D.C. Norquist and E.E. Recker, 1977: The structure and properties of African wave disturbances as observed during Phase III of GATE. MWR 105 317.
Reeves, R.W., C.F. Ropelewski and M.D. Hudlow, 1977: Relationships between large-scale motion and convective precipitation during GATE. MWR 107 1154.
Rennick, M.A., 1976: The generation of African waves. JAS 33 1955.
Riehl, H., 1954: Tropical Meteorology. McGraw-Hill.
Riehl, H. and S.J. Malkus, 1958: On the heat balance in the equatorial trough zone. Geophysica 6 503.
Schlesinger, R.E., 1982: Effects of mesoscale lifting, precipitation and boundary layer shear on severe storm dynamics in a three-dimensional numerical modelling study. Preprints, 12th Conf. Severe Local Storms, San Antonio, Texas. AMS 536.
Simpson, J., G. Van Helvoirt and M. McCumber, 1982: Three-dimensional simulations of cumulus congestus clouds on GATE day 261. JAS 39 126.
Soong, S.-T. and Y. Ogura, 1980: Response of trade-wind cumuli to large scale processes. JAS 37 2035.
Soong, S.-T. and W.-K. Tao, 1980: Response of deep tropical cumulus clouds to mesoscale processes. JAS 37 2016.
Thompson, R.M., S.W. Payne, E.E. Recker and R.J. Reed, 1979: Structure and properties of synoptic-scale wave disturbances in the Intertropical Convergence Zone of the eastern Atlantic. JAS 36 53.

Thorpe, A.J. and M.J. Miller, 1978: Numerical simulations showing the role of the downdraught in cumulonimbus motion and splitting. QJ 104 873.

Tripoli, G.J. and W.R. Cotton, 1980: A numerical investigation of several factors contributing to the observed variable intensity of deep convection over south Florida. JAM 19 1037.

Weisman, M.L. and J.B. Klemp, 1982: The dependence of numerically simulated convective storms on the vertical wind shear and buoyancy. MWR 110 504.

Yanai, M., S. Esbensen and J.-H. Chu, 1973: Determination of the bulk properties of tropical cloud clusters from large-scale heat and moisture budgets. JAS 30 611.

Zipser, E.J., R.J. Meitin and M.A. Lemone, 1981: Mesoscale motion fields associated with a slowly moving GATE convective band. JAS 38 1725.

ACKNOWLEDGEMENTS

I would like to thank my supervisor, Dr.M.W.Moncrieff and Dr.M.J.Miller for their guidance in this research and Mr.A.G.Seaton for programming. I am also grateful for the financial support of the NERC through a Research Assistantship.